

Fitness consequences of pollen movement and its dependence on spatiotemporal  
isolation: Field studies in *Echinacea angustifolia*

A DISSERTATION  
SUBMITTED TO THE FACULTY OF THE  
UNIVERSITY OF MINNESOTA  
BY

Amy Waananen

IN PARTIAL FULFILLMENT OF THE REQUIREMENTS  
FOR THE DEGREE OF  
DOCTOR OF PHILOSOPHY

Dr. Ruth G. Shaw, Advisor

June 2023

© Copyright by Amy Waananen, 2023

## ACKNOWLEDGMENTS

I appreciate the many individuals who supported me in the development of this dissertation. First, I thank my advisor, Ruth Shaw, for her advice, encouragement, and wordsmithing, which clarified both my writing and thinking. My advisory committee, Diane Larson, Daniel Cariveau, and Allison Shaw, also offered thoughtful input at many stages of this work. Diane and Dan co-advised me during the early stages of my PhD while my ideas for this thesis began to take shape. The freedom to follow ideas and my curiosity throughout my degree has made this a more rewarding journey.

I am grateful to my sources of funding, especially the Bell Museum of Natural History and the Ecology, Evolution, and Behavior graduate program, which supported several years of my field research. I also received funding from Prairie Biotic, Inc., the American Museum of Natural History, the Crosby and Huempfer family endowments to the College of Biological Sciences, the Nature Conservancy, the American Society of Naturalists, the Society for Study of Evolution, and the Botanical Society of America. My work relied upon research infrastructure at my field sites and a wealth of data that would not exist without the support of the National Science Foundation provided to the Echinacea Project, led by Ruth Shaw and Stuart Wagenius.

I feel fortunate to have been a member of Team Echinacea and have worked alongside this community throughout my time in graduate school. In particular, Stuart Wagenius and Jennifer Ison have served as mentors, sources of advice, and inspiration to me for many years. I do not think it is much of an exaggeration to say they taught me everything I know. Thank you to my collaborators within Team Echinacea, who improved the manuscripts that I present here in many ways: Lea Richardson, Scott Nordstrom, Jared Beck, Riley Thoen, Erin Eichenberger, Amy Dykstra, and Gretel Kiefer. Thank you to Dwight and Jean Wagenius for opening your home to make this research possible and for offering me a place to stay during one of my more chaotic field seasons. Thank you to the plants and bees in that corner of Douglas County, who taught me about resilience.

It is humbling to consider the many hands and hours that led to the results that I present here. Mia Stevens, Alex Carroll, Lindsey Paulsen, and Michael LaScaleia were responsible for coordinating much of the team's data collection and compilation between 2018 and 2022. Numerous members of Team Echinacea, including both the summer field crews and the volunteers from the Chicago Botanic Garden, made thousands of observations of flower phenology and seed counts to make this work possible. Anna Manson helped me with molecular lab work; Em Daily, Mike G, Jenny Foster, Jennifer Ison, and Mia Stevens patiently answered my many questions about how to do it.

I am grateful to have been part of the Ecology, Evolution, and Behavior graduate program community. Thank you especially to graduate program coordinators—neal jahren, Kate Barry, Lisa Wiggins—and Directors of Graduate Studies—Ruth Shaw and Elizabeth Borer—who made jumping through each hoop on the way to this degree not so bad. I am also thankful to the administrative staff in the College of Biological Sciences for logistical support. I benefitted from the friendship and advice of many at UMN, especially my cohort. Thank you to current members of the Shaw Lab—Rachel Pain, Anna Peschel, Wes Braker—for stimulating conversations and for reading and re-reading my drafts of these chapters. Thank you to other groups on campus, including the Cariveau Native Bee Lab—I am especially grateful for the friendship and support of Julia Brokaw—and Theory Group, for welcoming me in your spaces and for stimulating discussions over the years.

Thank you to my friends and family, especially my parents, Susan and Kurt Waananen, who taught me to be curious, to value my education, and to work hard. I am also owe a debt of gratitude to my siblings, Mark and Lisa, the Gullicksons, who became family to me while during my time in graduate school, my friends, Betsy Vomacka and Rachel Lee, and my dog Gooseberry, who was not much help in the field but made up for it in other ways. Finally, thank you to Matthew Gullickson who was by my side in every dimension of this work. I could never have finished this dissertation without your love and support.

*For my parents.*

## ABSTRACT

Habitat destruction leads to not only local extinction, but often increases isolation within and among the populations that remain. Plants, being sessile, are susceptible to reproductive failure due to isolation from mates, which can further compromise population persistence. However, persistence depends not only on the production of offspring but also on their survival. Furthermore, the isolation between two plants may correspond to patterns of genetic differentiation, such as relatedness or local adaptation, which can influence the fitness of their offspring. Here, I study how plants' isolation from potential mates links to both their reproductive rates and offspring fitness. I focus on *Echinacea angustifolia*, a bee-pollinated perennial forb of the North American tallgrass prairie, which has lost 96-99% of its extent over the past 180 years. I expand upon previous work by considering isolation not only in space (distance to prospective mates) but also in time (overlap in flowering time). In Chapter 1, using ten-year dataset of reproductive success, I found that both spatial isolation and flowering asynchrony reduce reproductive outcomes to a similar degree. In Chapter 2, I assessed how distance between parental plants and their asynchrony of flowering influence the fitness of their offspring, revealing that offspring fitness increases with distance between parents and the difference in their flowering time. In Chapter 3, I evaluated whether isolation from mates has consequences for reproductive fitness after accounting for the precarious transitions between seedling emergence and survival to adulthood. While mate density increased seedling emergence, it had no effect on offspring survival, so its fitness benefits eroded over time. Together these chapters provide an integrative understanding of how pollen movement patterns influence plant fitness, which can inform conservation and management in fragmented landscapes.

## Table of Contents

Acknowledgements.....	i
Dedication.....	iii
Abstract.....	iv
Table of Contents.....	v
List of Tables.....	vii
List of Figures.....	viii
Author Contributions.....	xi
Introduction.....	1
Chapter 1: Variation in reproductive fitness among individual plants depends on the spatial proximity of prospective mates and the timing of their reproduction	
Synopsis.....	6
Introduction.....	7
Materials and methods.....	10
Results.....	19
Discussion.....	22
Acknowledgements.....	26
Illustrations.....	28
Bibliography.....	33
Chapter 2: Flowering asynchrony moderates fitness effects of outcrossing distance in fragmented populations of an herbaceous forb	
Synopsis.....	37
Introduction.....	38
Materials and methods.....	41
Results.....	50
Discussion.....	52
Acknowledgements.....	59

Illustrations .....	61
Bibliography .....	67
Chapter 3: High juvenile mortality overwhelms benefits of mate density for reproductive fitness	
Synopsis .....	73
Introduction.....	74
Materials and methods .....	76
Results.....	82
Discussion.....	83
Acknowledgements.....	88
Illustrations .....	89
Bibliography .....	94
Appendices.....	97
A. Reproductive asynchrony and optimal outcrossing distance model .....	97
B. Chapter 1 Supplemental Tables and Figures.....	109
C. Chapter 2 Supplemental Tables and Figures.....	118
D. Chapter 2 Supplemental Analysis .....	122
E. Chapter 3 Supplemental Tables and Figures .....	126
F. Details of Mating Potential Calculations.....	132
G. Chapter 3 Demographic Stochasticity Simulations .....	135



## List of Tables

### Chapter 1

Table 1. Model selection for seed set predicted as a function of distance to 4 <sup>th</sup> nearest neighbor, flowering synchrony, date of flowering, and population census size.....	28
Table 2. Model selection for style persistence predicted as a function of distance to 4 <sup>th</sup> nearest neighbor, flowering synchrony, date of flowering, and population census size ...	30

### Chapter 2

Table 1. Model selection results for models of interparent asynchrony and interparent distance separately .....	62
Table 2. Results from likelihood ratio tests comparing nested models .....	63
Table 3. Summary of terms in final model .....	63

### Chapter 3

Table 1. Candidate aster model summaries .....	89
Table 2. Model comparisons based on likelihood ratio tests .....	90

### Appendix D: Chapter 2 Supplemental Tables

Table S1. Model selection results for models of interparent asynchrony and interparent distance separately for offspring 2014-2022.....	122
Table S2. Results from likelihood ratio tests comparing nested models for offspring 2014-2022 .....	123
Table S3. Summary of terms in final model for offspring 2014-2022 .....	123

### Appendix E: Chapter 3 Supplemental Tables

Table 1. Results of AIC analysis for competing models using Akaike weights.....	126
---	-----

## List of Figures

### Chapter 1

Figure 1. Relationships between reproductive success and predictors of interest .....	29
Figure 2. Scale dependence of the relationship between seed set and spatial isolation when considering all individuals .....	31
Figure 3. Assessment of variation in scale of isolation influencing seed set among separate subsets of the data .....	32

### Chapter 2

Figure 1. Map of the study area .....	61
Figure 2. Effect plot for interparent distance and offspring fitness .....	64
Figure 3. Predicted fitness contours across interparent distances and asynchronies .....	65
Figure 4. Correlation of interparent asynchrony with parents' start date of flowering .....	66

### Chapter 3

Figure 1. Graphical model for aster analysis of offspring emergence and survival .....	89
Figure 2. Predicted offspring count per mating bout at emergence and in year eight .....	91
Figure 3. Predicted offspring count per mating bout at emergence and after eight years by cohort and site .....	92
Figure 4. Output from model investigating final offspring count as a function of a maternal plant's emergence advantage and the chance of juvenile survival and simulation model results .....	93

### Appendix A:

#### Reproductive Asynchrony and Optimal Outcrossing Distance Conceptual Model

Figure 1. Distance to individuals 1-3 <sup>rd</sup> nearest flowering neighbors by flowering date....	98
Figure 2. Heterosis scenarios .....	102
Figure 3. Local adaptation scenario .....	103
Figure 4. Intermediate optimal outcrossing distance scenario .....	104

Figure 5. Pollen dispersal distance declining more or less quickly with distance .....	105
Figure 6. Threshold in mating distance scenario .....	106
Figure 7. Non-monotonic patterns of pollen dispersal with distance scenario .....	107

#### Appendix B: Chapter 1 Supplemental Figures

Figure S1. Summary of seed set observations by site and year .....	110
Figure S2. Summary of style persistence observations by site and year .....	111
Figure S3. Example of x-ray image of achenes used to assess seed set .....	112
Figure S4. Residuals vs. fitted values of the full model for style persistence .....	113
Figure S5. Generalized additive models (dashed) compared to fit from the full model..	114
Figure S6. The correlation between seed set and style persistence .....	115
Figure S7. Scale dependence of the relationship between seed set and spatial isolation when considering all individuals .....	115
Figure S8. Scale dependence of the relationship between seed set and spatial isolation when considering different subsets of individuals .....	116
Figure S9. Distributions of distance to 4th nearest neighbor by population size .....	117

#### Appendix C: Chapter 2 Supplemental Figures

Figure S1. Aster graphical model for the analysis .....	118
Figure S2. Distributions of predictor variables and offspring fitness .....	119
Figure S3. Variation in start date and interparent asynchrony among parental source populations .....	120
Figure S4. Achene position in relation to interparent asynchrony .....	121

#### Appendix D: Chapter 2 Supplemental Analysis

Figure S1. Predicted cumulative head count as a function of the interaction between interparent distance and interparent asynchrony in 2014-2022 .....	124
Figure S2. Predicted fitness contours across the range of observed interparent distances and asynchronies for 2014-2017 .....	125

Appendix E: Chapter 3 Supplemental Figures

Figure S1. Log<sub>10</sub> of distances (m) between a maternal plant and its 1<sup>st</sup> through 7<sup>th</sup> nearest neighbors across all sites and years in the study.....127

Figure S2. Effect sizes of model coefficients from the best performing aster model.....128

Figure S3. Correlation between a maternal plant’s number of seedlings and its number of offspring at eight years.....129

Figure S4. Predicted offspring count at emergence and after eight years by year of emergence .....130

Figure S5. Predicted offspring count at emergence and after eight years by site.....131

Appendix F: Mating Potential Calculations

Figure S1. Relationship between a neighbor’s distance to a focal plant and its contribution to the focal plant’s mating potential for  $\gamma = 1/13.3$ . .....132

## **DESCRIPTION OF AUTHOR CONTRIBUTIONS**

I acknowledge others' contributions to the work presented in this dissertation in detail following each chapter and briefly here. All of the work presented here was possible due to funding obtained by S. Wagenius and R. Shaw to the Echinacea Project through the National Science Foundation.

CHAPTER 1: A. Waananen contributed to data collection, designed the analysis, analyzed the data, and wrote the manuscript. All authors contributed to data collection and designing the research questions. S. Wagenius secured funding to address the specific aims of this study. J. Beck and R. Shaw contributed to the design of the analysis and manuscript revisions and R. Shaw contributed to manuscript revisions.

CHAPTER 2: A. Waananen contributed to data collection of offspring fitness, designed the analysis, analyzed the data, and wrote the manuscript. S. Wagenius and J. Ison led the initial studies and design of the experimental plots upon which this study builds. R. Shaw provided input to these studies and helped plant the experimental plots. All authors contributed to data collection, the design of the analysis, and manuscript revisions.

CHAPTER 3: A. Waananen contributed to data collection and compilation, designed the analysis, and drafted the manuscript. R. Shaw, A. Dykstra, and S. Wagenius designed the overarching study. L. Richardson, S. Nordstrom, R. Thoen, E. Eichenberger and G. Kiefer collected data and contributed to data compilation. All authors, especially L. Richardson and S. Nordstrom, contributed to manuscript revisions.

## INTRODUCTION

The Anthropocene has ushered in an era of isolation. Due to habitat loss and fragmentation, populations of many plant species are more isolated than ever before. Isolation can initiate a spiral of population decline by reducing genetic variation and hindering mate finding, both of which elevate the risk of local extinction. Pollinators could potentially delay or prevent this cycle of decline by transporting pollen among isolated plant populations. However, isolation might reduce the chances that a pollinator visits a plant. Furthermore, distance between two plants could influence the fitness of their offspring positively or negatively depending on the existence and cause(s) of genetic divergence. The questions guiding my research are (1) how does the isolation of individual plants influence patterns of pollen movement and (2) what are the consequences of those patterns for the fitness of plants in fragmented habitats?

Pollen movement distance is at the center of a conflict between theorized selective pressures on bees and plants. Bees collect pollen from flowers mostly to feed offspring developing within their nests. Incidentally, they often bring pollen grains into contact with pollen-receptive surfaces of a flower, leading to fertilization. Many flowering plants have evolved myriad adaptations to improve the chances that this transaction takes place. However, flight is energetically costly and exposes bees to predators and other dangers. With each foraging bout, bees navigate a complex spatial problem that rewards minimizing distance traveled and maximizing resources gained. In general, bees will venture from their nests only as far as necessary, to distances dependent on the density of floral resources in the area. For plants, on the other hand, pollination serves two critical functions—reproduction and dispersal. Reproduction passes an individual's genes into the next generation. Dispersal may also be important, especially in fragmented habitats, where long-distance pollen movement could allow individuals to escape inbreeding or track shifting climates and thus increase offspring viability. Thus, while bees benefit from flying short distances, a plant benefits from bees carrying pollen between plants separated by long distances.

Empirical studies of bees and understanding based on optimal foraging theory indicate that flowering density influences pollinator-mediated pollen movement patterns. Time represents a key, but underexplored, dimension of flowering density. Plant populations rarely bloom in perfect synchrony. Staggered flowering among individuals during the growing season reduces the density of plants flowering on any given day and influences which pairs are likely to mate. If bee foraging distances respond to floral density, then asynchronous flowering might increase long-distance pollen movements. I develop this reasoning further in Appendix A. Based on this, I hypothesized that plant reproduction would decrease with an individual's spatial isolation (distance to prospective mates) and flowering asynchrony (degree of overlap in timing of flowering with prospective mates) and that pollen movement distances would increase. I expected that if populations were genetically impoverished, increased pollen dispersal distance would lead to increased offspring fitness.

For each of my chapters, I focus on the narrow-leaved purple coneflower, *Echinacea angustifolia*. Native to North American tallgrass prairie, *E. angustifolia* thrives on the upland "high and dry" soils in the rolling topography of prairie habitat west of the Mississippi River. Its range reaches across central North America, extending to the west to the beginning of the drier mixed and shortgrass prairie of the Great Plains, north to the Manitoba and Saskatchewan and south to Texas. *E. angustifolia* was historically widespread throughout areas of suitable habitat in this region. However, extensive land-use change in the region since European settlement beginning in the 1800s has resulted in dramatic loss of tallgrass prairie habitat, including 99% of Minnesota's original seven million hectares. Today, *E. angustifolia* populations persist largely in remnant patches of prairie in the margins of agricultural landscapes. Beginning in 1996, Stuart Wagenius established a study area focusing on the ecology and evolution of natural populations of *E. angustifolia* within Solem Township in western Minnesota. The work that I present here builds on this system.

In my first chapter, I investigate how the interplay between spatial isolation, flowering asynchrony, population size, and time of season influence mating success. I compiled a ten-year dataset of reproductive success, timing of flowering, and spatial isolation of populations of *Echinacea angustifolia*, using data collected across thirty-one populations during field seasons dating back to 1996. After analyzing the relationships between spatial isolation, flowering asynchrony, and reproductive success, I found that spatially isolated plants and asynchronously flowering individuals experienced lower rates of pollination and produced fewer seeds. This offers an important corroboration of previous results, which have largely focused on large populations, and extends the scope of inference to small patches. Surprisingly, we found that individuals' distance to intermediate neighbors (i.e., 3<sup>rd</sup> through 8<sup>th</sup> nearest flowering conspecifics) predicted reproductive success better than distance to individuals' closest or more distant neighbors, regardless of the time of season and across populations varying in size by an order of magnitude. In addition, we found that spatial isolation modified the effects of flowering asynchrony on reproductive success; synchrony improved reproductive outcomes most when spatial isolation was low, but if spatial isolation was high, synchrony had little effect. Similarly, reproductive success declined with spatial isolation, but it declined more in small populations than large ones.

In my second chapter, I test the assumption that offspring viability corresponds to pollen dispersal distance. I also test a novel hypothesis that temporal dispersal distance, or mating between more or less synchronous individuals, affects offspring viability. To do so, I analyzed the survival and reproduction of the offspring of plants collected as seeds from populations across my study area and grown together in an experimental plot. Using molecular markers, my collaborator Dr. Jennifer Ison and I identified the parental plants for each offspring. Using this pedigree and source population data for the parental plants, I identified the distance between the parental plants of each offspring. I used a long-term dataset of timing of flowering in the plot to calculate inter-parent asynchrony. I then related offspring survival and reproduction to inter-parent distance and asynchrony. I found that offspring survival and reproduction increased with the distance between



parental source populations, supporting the idea that pollen movement distance improves offspring viability. Interestingly, the effect of interparent asynchrony on offspring viability depended on whether the maternal plant or the paternal plant flowered first: the *direction* of parental asynchrony. Offspring were highest fitness when maternal plants flowered later than the paternal plant. This description of a previously unexamined relationship presents opportunities for a new area of inquiry and the development of theory to explain these results.

In my third chapter, I investigate whether the reproductive consequences of isolation from mates in terms of both quantity (number of offspring produced) and quality (number that survive to adulthood) are long lasting. This chapter also tests the assumption that seed count represents a reliable proxy for a plant's success in passing its genes onto the next generation. The number of offspring several years old may relate only weakly to the number of seeds initially contributing to the cohort if offspring survival decreases with mate density. To clarify the demographic consequences of mate density I used a long-term dataset of flowering and juvenile demography to investigate how an individual's distance from potential mates influenced the number of offspring it produced (quantity) and that survived over 8 years (quality). I found that spatial isolation reduced the maternal plants' number of seedlings that emerged, but had no effect on the survival of those seedlings. Because of both low seedling emergence and high juvenile mortality, the final differences in maternal progeny counts were consistent with demographic stochasticity at the maternal plant level. From a conservation perspective, this offers insight to the demographic consequences of isolation from mates. Will plants produce more offspring, potentially increasing a population's rate of increase, if they are less isolated from mates? Here, we find the answer is yes, but that the benefits of mate density diminish over time.

I hope that these results will help to disentangle the mechanisms leading to persistence (or not) in fragmented landscapes and offer insight to the development of conservation strategies. While previous work has focused on the reproductive

consequences of density measured at the population level (i.e., population size), my first chapter demonstrates how the heterogeneity in individuals' isolation over space and time within and among populations leads to variation in reproductive rates. Furthermore, spatial isolation alone would have led to misleading predictions about the reproductive potential of plants in fragmented populations. The management implications of these findings include informing planting density and the consideration of actions that could reduce temporal isolation. At the same time, my second chapter shows that the reproductive benefits of mate density may come at a cost to offspring fitness when considering mating within and among these isolated populations. Finally, my third chapter shows that individuals produce so few seeds that survive to adulthood that the fitness effects of mate density over the long term are largely overwhelmed by stochastic processes of juvenile survival. Management actions to increase density of mates, outcrossing, and the density of seeds being recruited in each generation—such as supplementing a population with regionally sourced seeds—could address these concerns and promote persistence even amid highly fragmented landscapes.

## CHAPTER 1

Variation in reproductive fitness among individual plants depends on the spatial proximity of prospective mates and the timing of their reproduction

### SYNOPSIS

The density of individuals is often associated with their ability to find mates. However, typical population-level approaches for assessing density ignore that the mechanisms of mate finding depend on both the spatial arrangement of individuals and the relative timing of their reproductive activity. In animal-pollinated plants, variation in the spatial scale at which pollinators respond to floral resource availability across a season may further complicate the influence of isolation in space and time on mate finding. Identifying the mechanisms that underlie mate-finding Allee effects would improve our understanding of persistence amid habitat loss, which often increases isolation. In a ten-year study of the herbaceous perennial *Echinacea angustifolia* across 31 populations, we evaluated individual plant's spatial location, flowering phenology, and reproductive success. We investigated how isolation in space and time related to two measures of reproductive success: style persistence (N = 5354), which indexes pollination success, and seed set (N = 983), which encompasses pollination and post-pollination processes. We found that individuals' reproductive success consistently increased with flowering synchrony and population size. Seed set declined with spatial isolation, but the negative association was stronger in small populations. Distance to intermediate neighbors (3-8<sup>th</sup> nearest) predicted reproductive success better than distance to close (1<sup>st</sup>-2<sup>nd</sup>) or far (8-30<sup>th</sup>) neighbors and, surprisingly, this was consistent across the season and a wide range of population sizes. Seed set and style persistence both declined across the season, suggesting that reproductive outcomes are, to some extent, decoupled from individuals' temporal isolation from mates. Our findings reveal how mate-finding Allee effects in fragmented populations can arise from interactions between pollinator behavior, spatiotemporal mate availability, seasonal context, and population size.

## INTRODUCTION

Mate finding plays a fundamental role in both ecological and evolutionary processes, especially where habitat loss has reduced population sizes and mate availability. Impediments to mate finding can depress individuals' reproductive fitness and subsequent population growth rates, which is called a 'mate-finding Allee effect' (Gascoigne et al. 2009). Empirical studies of constraints on mate finding primarily investigate the role of spatial isolation in population-level mate-finding success (e.g., Abrahamczyk 2022). However, focus on population-level spatial density presents two problems. First, it neglects how variation in the spatial location of individuals within a patch contributes to fitness differences among individuals (e.g., Groom 1998; Wagenius 2006). Second, it ignores temporal variation in mate availability, which may individually influence fitness or interact with spatial isolation from mates in complex ways (Calabrese et al. 2004; Fagan et al. 2010). Focusing only on density at the population level could lead to overly optimistic predictions of mating success and obscure the individual-based mechanisms that underlie mate-finding Allee effects.

Addressing the influence of isolation in both space and time on mating may be especially important for understanding implications of habitat loss in animal-pollinated plants. Pollinators respond sensitively to the distribution of floral resource availability and mediate mate finding (Ogilvie and Forrest 2017). For example, bees must travel further between plants in environments with low floral density (Levin and Kerster 1969; Osborne et al. 2008), incurring costs in energy expenditure, exposure to risk, and future offspring production (Zurbuchen et al. 2010; Nooten and Rehan 2019). More spatially isolated plants tend to receive fewer visits and produce fewer seeds (Kunin 1997; Wagenius 2006; Ison and Wagenius 2014). At the same time, flowering is usually far from uniformly distributed in time (Elzinga et al. 2007), instead often varying dramatically both within and across seasons (Waananen et al. 2018). Flowering asynchronously with potential mates can also translate to reduced reproductive success (Ison and Wagenius 2014). While a few recent studies have investigated the effects of

both spatial and temporal dimensions of isolation on reproductive success, these efforts have mostly taken place within large populations (Wagenius et al. 2020; Alonso-López et al. 2022; Richardson and Wagenius 2022). Thus, inferences about the effect of isolation on reproductive success to smaller populations, where mate finding may be most constrained, remain limited.

The effects of spatial isolation on mate finding may depend on synchrony of flowering in animal-pollinated plants (Calabrese et al. 2004). For instance, regardless of the spatial proximity of conspecifics, a plant that blooms too early or too late may be reproductively isolated. For plants that are more distant from potential mates, the chance of encountering a mate might depend on a higher degree of reproductive synchrony to be likely to find a mate. In this way, temporal isolation might exacerbate the effects of spatial isolation. On the other hand, reproductive asynchrony could mitigate competition for pollinators among plants in dense patches (Elzinga et al. 2007). Interplay between isolation in space and time could be consequential. Theory predicts that when the effects of isolation in space are amplified by isolation in time, this could accelerate the formation of spatial genetic structure (Peters and Weis 2019), contribute to dramatic patterns of synchronized reproduction (i.e., masting; Bogdziewicz et al. 2020), and support the formation of range limits (Sánchez-Castro et al. 2022). If isolation in space reduced the effect of isolation in time, or vice versa, then these outcomes could be less likely.

Individual isolation might have disparate consequences for mating depending on the local abundance of conspecifics, or the population size. Small and fragmented populations may have lower genetic diversity. In self-incompatible species, mating incompatibility between individuals that share alleles at a self-recognition locus (i.e., S-Allee effects; Wagenius et al. 2007) can reduce mate-finding success. On one hand, if mate incompatibility rates are high, individuals in small populations may be less sensitive to the effects of isolation because these population-level genetic mechanisms would reduce individuals' reproductive success regardless of their individual degrees of isolation. On the other hand, patterns of mating incompatibility between individuals

could depend on their degree of isolation. For example, in many plants, seed dispersal is limited and individuals' near neighbors tend to be close relatives and therefore genetically incompatible mates. As a result, higher rates of reproductive failure in small populations due to mating incompatibility could be exacerbated for isolated individuals. In other words, the effect of isolation could be more negative in small populations than in large ones. Similarly, the spatial scale of isolation that influences individual reproductive success may depend on population size. In particular, proximity to a broader set of potential mates beyond immediate neighbors, which may likely be relatives and incompatible especially in genetically impoverished small populations, could be most critical for reproductive success in small populations.

Many studies have documented variation in reproductive success within flowering seasons. Further, the relationship between reproductive success and plant isolation could also vary within a season. Seasonal declines in reproductive success are widespread in Angiosperms (Munguía-Rosas et al. 2011) due to mechanisms including shifts in abiotic conditions, such as drought, as well as seasonal declines in pollinator visitation. Pollinators might be less likely to visit isolated plants at different times across the season. For instance, plant species might compete for pollinators during periods of overlap in flowering (Bolmgren et al. 2003; Elzinga et al. 2007). A recent study supports this notion; Yourstone et al. (2023) found that, contrary to the findings of small-scale or laboratory studies, bumblebees showed little fidelity to particular species within foraging bouts and individual floral preferences did not persist across a season. When multiple species of floral resources are available, generalist pollinators may instead switch between plant species according to their density (Hayes and Grüter 2023) or the novelty of the resource (i.e., either “neophilia” or “neophobia”; Forrest and Thomson 2009; Muller et al. 2010). Similarly, bees' increase of flight distances might depend on the time of the season, shifting only when few other floral resources are available and not when there are alternatives (Ogilvie and Forrest 2017). As a result, the relationship between reproductive success and isolation and its spatial scale may vary across a season.

We investigated patterns of individual-level isolation and reproductive success across 31 natural populations of *Echinacea angustifolia* over ten years (1996-1999, 2014-2020). In our system, *E. angustifolia* grows in patchy populations varying in size. Individuals also vary in their degree of spatial isolation within and among populations, with documented consequences for reproductive success (Wagenius 2006). Increased reproductive success following spring fires are associated with both increased flowering synchrony and reduced spatial isolation (Wagenius et al. 2020). Furthermore, previous work in this system has shown that mate availability, rather than resource availability, limits reproduction (Wagenius 2004; Wagenius and Lyon 2010). We hypothesized that: (H1) spatial isolation and flowering asynchrony amplify each other's negative effect on reproductive success and (H2) that population size and time of season modify the effects of spatial and temporal isolation on reproductive success. Finally, we predicted that (H3) the spatial scale of reproductive isolation varies among populations of differing sizes and across the flowering season.

## MATERIALS AND METHODS

### Study Area and Organism

Our study area consists of 6400 ha in western Minnesota, USA, centered near 45° 849' N, 95° 843' W. This region is part of the North American tallgrass prairie. In Minnesota, less than 1% of the original extent of tallgrass prairie remains intact (Samson and Knopf 1994); instead, agricultural use, especially for corn and soybeans, dominates the contemporary landscape. We studied natural populations of the narrow-leaved purple coneflower, *Echinacea angustifolia* (Asteraceae), persisting in remnant patches of prairie located along roadside and railroad rights of way, private property, and wildlife protected areas. Although *E. angustifolia* is widespread in the remaining tallgrass prairie habitat, its populations are often small and fragmented. *Echinacea angustifolia*'s non-clonal growth habit makes it straightforward to identify individuals, necessary for estimating census sizes. Because of *E. angustifolia*'s self-incompatible mating system, receipt of self-pollen

and pollen from close relatives will not yield successful fertilization. As a result, reproduction is sensitive to reductions in population size associated with habitat loss, which may increase the likelihood of mating with relatives, as well as isolation from mates (Wagenius et al. 2007). A diverse assemblage of solitary native bees, mostly small-bodied generalists, mediate pollination of *E. angustifolia* (Wagenius and Lyon 2010). Based on both expectations based on bees' body size (Greenleaf et al. 2007) and pollen dispersal studies from large populations, pollination most often occurs between highly proximate plants (e.g., 16 m; Page et al. 2019) and rarely up to several hundred meters (Ison et al. 2014). Previous studies have found that early flowering plants tend to receive more visits from pollinators and higher quality visits (i.e., receive more conspecific pollen per visit) than those that flower at peak or late in the season (Ison et al. 2018), resulting in greater reproductive success for early-flowering plants (Ison and Wagenius 2014). *Echinacea* flower heads (capitula) consist of many (typically 70-200) uniovulate florets. Each floret produces an achene—a dry, indehiscent fruit derived from a single ovule—regardless of whether the ovule develops a seed.

#### Data Collection Overview

We studied 31 populations of *E. angustifolia* between 1996-1999 and 2014-2020. For each flowering individual in these populations, we measured its spatial isolation, flowering synchrony. We collected data on reproductive success from all (style persistence) or a random sample (seed set) of individuals. In some years, we did not survey every population or small populations did include any flowering individuals; summaries of the number of individuals for which we had complete data on spatial isolation, flowering phenology, and reproductive success in each population and year are located in Supplemental Materials (Figure S1, Figure S2). The spatial data and corresponding records of reproductive success from 1996-1999 were previously reported in a study of scale-dependence of reproductive failure (Wagenius 2006). Our expanded dataset here allows us to test more hypotheses including the roles of flowering synchrony, population size, and date of flowering in mediating reproductive success.



## Spatial Isolation

In each population, we searched for and mapped all reproductive individuals using survey-grade GPS equipment that is precise up to  $< 1$  cm. We calculated the Euclidian distance between each individual and its 1<sup>st</sup>-30<sup>th</sup> nearest conspecific neighbors that were flowering within the same year. In populations with fewer than 30 individuals, we calculated the distances to individuals in adjacent populations. For our analyses of H1 and H2 ('Effects of distance, synchrony, population size, and date of flowering on reproductive success'), we estimated spatial isolation as an individual's distance to their fourth nearest neighbor ( $k = 4$ ), based on the findings of Wagenius (2006) that distance to  $k = 3$ -7<sup>th</sup> nearest neighbors best predicted reproductive success in our study populations. The populations included in our study represent the majority of *E. angustifolia* in the area, but there are some unmapped populations. These were inaccessible for a variety of reasons including being on private property or being too large for us to feasibly census. Because all but one population had at least four individuals flowering in each year, and because distances were log-transformed, the instances in which an unmapped plant may have been a plants' true 4<sup>th</sup> nearest are rare and will have little effect on our inferences.

## Flowering Phenology

We defined an individual's flowering period as the days that it produced pollen. To determine individuals' start and end dates of flowering, we visited each individual at least once every three days, prior to flowering and until it ceased shedding pollen, recording its flowering status during each visit. Florets of *E. angustifolia*'s composite flowering head develop regularly in roughly concentric rows beginning at the bottom of the flowering head. Each floret opens first as an anther tube, which persists for one day (Wagenius 2004). On the following day, style branches emerge through anther tube. When styles receive compatible pollen, they shrivel within a day. Otherwise, styles persist until they senesce due to wear and age, typically after seven days. We use these characteristics to assign start dates of flowering, even when we did not visit plants every

day: flower heads that only have anthers present must be on their first day of flowering and flower heads presenting one row of styles and one row of anthers must be on their second day of flowering. On their third day of flowering, individuals have two rows of emergent styles, some of which may have shriveled and may no longer be visible. This also allows us to determine end date of flowering for individuals that we observed presenting anthers, but no immature florets. For all other individuals, we determined a two-day range of possible end dates of flowering. For analysis, we used the earliest date in this range.

### Style Persistence

The regular progression of flowering in *E. angustifolia* also allows us to quantify a measure of reproductive success: style persistence, which estimates the average number of days that a plant's styles are receptive to pollen and as such is an index of pollination (Wagenius 2004). Because styles that receive compatible pollen shrivel within 24 hours, longer style persistence indicates that pollination has not occurred, although styles may also disappear due to herbivory or to senescence after about week. Each time that we visited a head to record its flowering status, we also noted how many rows of styles were more than 50% persistent. When a head had fewer than 11 immature florets, we did not record style persistence, because rows become difficult to identify near the apex of the cone-shaped flower head. To calculate style persistence, we averaged the number of days that a row of styles persisted for each individual within a year.

### Seed Set

To assess another measure of reproductive success, we estimated individuals' seed set. Each year, we harvested seedheads from a randomly selected sample of the flowering plants in each population. The number of plants sampled varied across sites and years (Figure S1); in general, we aimed to sample one seedhead from each of five plants in small populations and from 10-15 plants in larger populations. If individuals had more than one seedhead, we randomly selected which seedhead to collect. If an

individual had dropped more than 50% of its seeds prior to harvest or if the seedhead was missing (e.g., due to herbivory or landowner mowing), we randomly chose a replacement from the same population. To assess seed set, we evaluated whether a sample of achenes from each seed head we collected contained a seed, or embryo. The precise number of achenes sampled from each head varied. Typically, we aimed to sample 30-45 achenes per head. We occasionally assessed fewer than 30 achenes; for instance, when a head had fewer than 30 achenes, in which case we assessed all of them. We sometimes sampled more than 45 achenes (115 of 983 observations); in all cases, we either (1) selected achenes randomly or (2) assessed all achenes. In either case, we excluded from sampling achenes that would be uninformative to assessments of reproductive success (i.e., were too damaged to assess or derived from the sterile ray florets).

For samples from 1996-1999, we determined whether an achene contained a seed based on mass; we counted achenes that weighed  $> 0.2$  mg as full (Wagenius 2004). For samples from the years 2014-2020, we evaluated seed set by x-raying seeds using a Faxitron MX-20 for 10 seconds at 18 kV. Pollinated achenes appear brightly lit on x-ray images and are easily distinguished from achenes that do not contain embryos (Figure S1). Occasionally, it was ambiguous whether an achene contained an embryo. For instance, embryos occasionally appeared small and undeveloped on x-ray images. In these cases, we removed the ambiguous achene from our sample and calculated seed set based on the remaining achenes.

#### Seed Set *versus* Style Persistence

Why assess two measures of reproductive success? Seed set and style persistence offer complementary metrics of reproduction. Seed set relates directly to reproductive output, while style persistence reflects the rate at which pollination occurs. As such, seed set relates inversely to style persistence. When styles persist longer, reflecting poor pollination, we observe lower seed set (Wagenius 2004). Because it is possible to evaluate style persistence rapidly and non-destructively in the field, we assessed style

persistence for a larger sample of individuals and their florets than would have been possible for seed set. Furthermore, seed set and style persistence, though related, are not redundant; in particular, seed set encompasses the outcomes of both pollination and post-pollination processes that influence seed production such as disease and resource allocation. Thus, assessing both measures allows us to assess the distinct dependences of pollination, separate from post-pollination processes, and ultimate reproductive success on our predictors.

Analysis for H1 and H2: Effects of distance, synchrony, population size, and date of flowering on reproductive success

To test H1 and H2, we used mixed effects models to represent reproductive success, assessed as both seed set and style persistence, as a function of spatial isolation, flowering synchrony, start date of flowering, the census size of their population, and two-way interactions between these factors. Distance to neighbors relates inversely to the local density of flowering conspecifics. We measured start date of flowering as the difference between an individual's start date and the median start date of the population (i.e., the number of days after the median start date that an individual began flowering). We calculated individual's flowering synchrony as the mean overlap in days flowering between an individual and all others flowering within the same site and year. Synchrony ranges between 0 (no overlap) and 1 (complete overlap) (Augspurger 1983). Finally, we estimated census size using the flowering records from the populations over the past 10 years by compiling all coordinates of tagged plants. We considered points within 10 cm of one another to represent a single plant. We used R version 4.2.2 (R Core Team 2022) for all statistical analyses.

*Seed Set* – To model seed set, a measure of the number of fruits that contained a seed ('successes') given the number of fruits that we sampled ('trials'), we used a generalized linear mixed model. Our full model included eight fixed-effects terms: (1) spatial isolation (distance to 4<sup>th</sup> nearest neighbor), (2) asynchrony, (3) population size,

and (4) start date of flowering. We also included terms for interactions between (5) spatial isolation and synchrony, (6) spatial isolation and population size, (7) spatial isolation and start date of flowering, and (8) synchrony and start date of flowering. We also included random effects for site and year.

To ensure appropriate fit of our model of seed set, we used likelihood ratio tests and model diagnostics from the R package ‘DHARMA’ (Hartig 2022) to compare a set of candidate models including all predictors and random effects; we include the full details of this in Appendix B and a brief summary here. An assessment of an initial binomial model of seed set (i.e.,  $Y = \text{Binomial}(n,p)$  where  $Y$  - a fruit contains a seed,  $n$  = number of fruits sampled, and  $p$  = probability that a fruit contains a seed) indicated strong zero-inflation and overdispersion. We determined that a zero-inflated (ZI) beta-binomial model represented the data better than alternative zero-inflated binomial or beta-binomial models. Thus, we used a ZI beta-binomial model implemented in the R package ‘glmmTMB’ for our analyses of seed set (Brooks et al. 2017).

While not commonly used in the ecological literature, a ZI beta-binomial model has a few key attributes that suit our seed set data well. The beta-binomial accommodates greater-than-binomial dispersion through its compound structure: a beta distribution with parameters  $\alpha$  and  $\beta$  defines the probability of success  $p$  in binomial model. ZI models include a component that specifically models the likelihood of observing a zero in excess of the process in the conditional component of the model. These models assume that excess zeros are due to structural causes (Blasco-Moreno et al. 2019), for example, if a plant had zero seeds because it flowered under conditions such that it could receive no visit from pollinators. Because we did not have distinct hypotheses for the probability of a plant producing zero seeds versus a fraction of all possible seeds, we included all predictors in both the ZI and conditional, i.e., beta-binomial, components of the model.

We used backwards model selection to test our hypotheses H1 and H2 regarding the relationships between the model predictors and seed set, using likelihood ratio tests

with a p-value threshold  $< 0.05$  to compare the reduced and full models. First, we tested models that dropped interaction terms in the ZI portion of the full model. We determined if removing the term significantly reduced model fit. Then, we established a new reference model, retaining only the interactions that significantly improved model fit. We then repeated the process with the interactions in the beta-binomial component of the model and then with the main effects of the model in both the ZI and beta-binomial components to determine a final model that included all retained terms.

To visualize the relationships of synchrony, spatial isolation, population size, and timing of flowering with seed set estimated by the final model, we used the function ‘ggpredict’ from the R package ‘ggeffects’ (Lüdtke et al. 2020) to calculate predicted values for our best-performing model for seed set without conditioning on the random effects. Specifically, we made predictions across the range of each variable while holding each other variable constant at its mean value in the observed data. For interactions, we held one value constant and generated predictions based on two or three values of the interacting variable, holding all other variables constant at their mean observed values. Predictions were conditioned on both the zero-inflated and beta-binomial portions of the model; specifically, predictions returned the expected value from the beta-binomial model multiplied by  $1-p$  from the binomial, zero-inflation component (Brooks et al. 2017, p. 391).

*Style Persistence* – To analyze H1 and H2 using style persistence as our measure of reproductive success, we used the same random effects, predictors, and backwards model selection process as for seed set, described above, but with linear mixed models. We used the ‘lme4’ R package (Bates et al. 2015) to construct models. Style persistence has a lower bound of one because styles persist for at least one day before shriveling. This led to a bound in the residuals compared to the model fitted values, which assumed a simple linear response (Figure S2). We used generalized additive models to assess visually whether there were non-linear patterns in the relationships between the predictors of interest and style persistence and did not observe any (Figure S3).

Furthermore, the random effects were not of primary interest, and the modest heteroscedascity we observed was not a major concern for our inferences about the fixed effects in the model.

To visualize the model predictions of our style persistence model, we used the ‘bootMer’ function from ‘lme4’ to generate bootstrap model predictions and 95% confidence intervals for hypothetical individuals representing the range of each variable and interaction of interest while each other variable was assigned to its mean value in the data.

### Analysis for H3: Scale Dependence of Reproductive Success

*Overall Spatial Scale Dependence* - Next, we evaluated the scale at which isolation influences reproductive success (H3), measured as seed set and style persistence by modifying the final models identified for seed set and for style persistence in the previous step of the analysis to represent spatial isolation at a range of scales. Specifically, instead of representing spatial isolation as distance to the  $k = 4^{\text{th}}$  nearest neighbor, we fit thirty separate models with distance to each of  $k = 1-30^{\text{th}}$  nearest neighbors; the first model represented spatial isolation as distance to the first nearest neighbor ( $k = 1$ ), the second to the second nearest neighbor, and so on. To assess model performance at each spatial scale, we plotted the model AIC against the corresponding rank in proximity of the neighbor  $k$  to which we measured distance to represent spatial isolation in the model.

*Spatial scale dependence by population size* - To investigate how scale-dependence varied among populations of differing sizes, we used the ‘cut2’ function in the R package ‘Hmisc’ (Harrell and Dupont 2023) to divide observations of both seed set and style persistence into population size categories (small, medium, large) with roughly equal numbers of observations. As such, each category did not represent equivalent intervals of population sizes. Because our sampling differed for collecting data on style persistence and seed set, the exact boundaries for these categories also differed between

the style persistence and seed set analyses of scale dependence. ‘Small’ represented individuals from populations with census size 4 to 272 for seed set and 4 to 372 for style persistence; ‘middle’ represented 304 to 709 for seed set and 513 to 893 for style persistence. Finally, ‘large’ represented individuals from populations with census size 794 to 2108 for seed set and 1080 to 2108 for style persistence.

Our goal was to repeat the process of fitting models with considering spatial isolation as distance to each of  $k = 1-30^{\text{th}}$  nearest neighbors separately to the ‘small,’ ‘medium,’ and ‘large’ subsets of the observations. Because population census size was implicit in the definition of these respective datasets, we omitted terms including population size from the final seed set and style persistence models identified in model selection. Because our final model of style persistence that we determined in evaluating H1 and H2 only included spatial isolation as a term modifying the effect of population size (results below), we included spatial isolation as its own term when considering subsets of the population based on population size. Again, we assessed trends in model performance visually by plotting AIC in relation to  $k$ .

*Spatial scale dependence by time of season* - We repeated this procedure based on start date of flowering, dividing both the seed set and style persistence datasets into thirds based on start date of flowering (‘early,’ ‘peak,’ and ‘late’ thirds). In this case, when we fit a separate model to represent spatial isolation based on distance to individuals’  $k = 1-30^{\text{th}}$  nearest neighbor to separate subsets of the data, we omitted terms related to start date of flowering from set of models. The category ‘early’ represented individuals with start dates -14 to -1 days after median for seed set and -19 to -2 for style persistence; ‘peak’ represented -1 to 3 for seed set and -1 to 2 for style persistence. Finally, ‘late’ represented plants starting flowering 3 to 35 days after the population median for seed set and 3 to 27 days for style persistence.

## RESULTS



H1 and H2: Effects of distance, synchrony, population size, and date of flowering on reproductive success

*Seed Set* – In total, we observed seed set of 983 individuals. Predicted seed set of individuals increased consistently with synchrony and these increases varied markedly with isolation of individuals (H1; Figure 1A). From the least to most synchronous individuals, seed set tripled, from 6% to 33%, among spatially isolated plants ( $\text{Dist}_{k4} = 100$  m), but increased only modestly, from 30% to 44%, among plants in clusters ( $\text{Dist}_{k4} = 1$  m). Predicted seed set of spatially isolated plants nearly doubled depending on whether the population was large (Predicted Seed Set = 21%, Pop Size = 1000) or small (Predicted Seed Set = 12%, Pop. Size = 10) (H2; Figure 1B). In contrast, wide confidence intervals (95% CI: Small [0.22., 0.68], Large [0.19, 0.62]) indicated weak support that seed set was contingent upon population size when individuals were in dense clusters ( $\text{Dist}_{k4} = 1$  m).

Regardless of population size or individual's degree of flowering synchrony or spatial isolation, predicted seed set declined substantially with individual's start date of flowering (H2; Figure 1C), from a predicted 31% at the onset of the season to 7% at the end. Flowering synchrony and population size influenced the probability an effective pollination event occurred, as evidenced by their presence in the ZI portion of the model, while spatial isolation and start date of flowering influenced the proportion of fruits that contained a seed as modeled by the beta-binomial process (Table 1).

*Style Persistence* – We observed style persistence for  $N = 5354$  individuals. Some plants' rows of styles shriveled within an average of one day, indicating pollination occurred on day that styles emerged; others' styles persisted for up to an average of 11.5 days, indicating low pollination rate. As we observed for seed set, predicted style persistence consistently declined with flowering synchrony (Figure 1D), with highly synchronous individuals (mean overlap in flowering time = 90%) having 1.56x lower style persistence than low synchrony individuals (mean overlap = 10%). Unlike the

pattern we observed for seed set, however, the relationship between style persistence and synchrony was not contingent upon the degree of spatial isolation. Individuals that were more isolated had higher predicted style persistence than those in dense clusters, but the effect of spatial isolation alone dropped out during model selection (Table 2).

Individuals in large populations typically had lower style persistence than those in small populations, but the magnitude of difference depended on individuals' spatial isolation. For example, predicted style persistence in large populations (Pop. Size = 1000) was 4.3x that of individuals in small populations (Pop. Size = 10) when considering plants in the most dense clusters ( $Dist_{k4} = 0.18$  m) (0.81 in large populations vs. 0.19 in small populations). When considering highly isolated plants ( $Dist_{k4} = 2502$  m), predicted seed set in small populations was indistinguishable from or potentially greater than in large populations (Figure 1E). Predicted style persistence declined with start date of flowering, taking an expected 2.46 days per row to shrivel for individuals that flowered at the onset of the season and 1.58 days per row for individuals flowering at the end of the season (Figure 1F).

### H3: Scale Dependence Analyses

Distance to individuals' third nearest flowering neighbor ( $k = 3$ ) best predicted its seed set, as indicated by the model performance of models considering spatial isolation to different neighbor ranks (Figure 2, seed set; Figure S7, style persistence). Similarly, style persistence was sensitive to the rank of neighbor to which we measured isolation, that is, 'the scale of isolation,' and was also best predicted at an intermediate scale,  $k = 7$ . The pattern of how well distances to neighbors of different ranks explained reproductive success (seed set or style persistence) was remarkably consistent across separate subsets of individuals that flowered across contexts (Figure 3; Figure S8). With one exception discussed below, individuals' distances to intermediate neighbors ( $k = 3-5$  for seed set and  $k = 2-7$  for style persistence) still best explained variation in reproductive success, even when the distance to individuals' first, second, etc. nearest neighbor varied on

average among subsets of the data. The rank of neighbor to which we considered spatial isolation was especially consequential for individuals in small populations, which often had fewer than 30 plants flowering in a given year. For seed set of individuals from small populations,  $k = 3$  led to the lowest AIC; distance to distant neighbors,  $k = 20-30$ , led to poor model performance and AIC scores ~80 units higher.

The exception to the pattern that distance to intermediate neighbors was most influential for reproductive success comes from large populations. Considering seed set of individuals from large populations, using distance to the  $k = 17^{\text{th}}$  nearest neighbor yielded slightly better model performance than isolation to any other neighbor rank between 1 and 30. For style persistence, performance peaked at  $k = 14$ . However, the range of AIC scores between all models fit to the large-population datasets of seed set and style persistence was small, especially for seed set (Figure 3 ‘large’). While the AIC scores for models of seed set varying  $k$  for other subsets of the data ranged by at least 20 units, for large populations, AIC scores were between 1848.1 and 1849.6. The lack of variation in model performance across values of  $k$  in large populations indicates little sensitivity to the scale of spatial isolation when considering individuals in this context.

## DISCUSSION

Individuals’ success in finding mates depended on the spatial proximity and flowering synchrony with conspecifics, the size of their population, and the time of season that they flowered (Figure 1). These factors were associated with a wide range of variation in reproductive outcomes, from total reproductive failure (seed set of zero) to 100% of the fruits we sampled from an individual containing a seed (seed set of one). We highlight that an exclusive focus on proxies for density at the population level (e.g., population size), or similarly on spatial dimensions of isolation alone, would have vastly underestimated the variation we observed. Specifically, we found that isolation in space and isolation in time both reduced seed set with effects similar in magnitude (Figure 1A, B). Furthermore, spatial and temporal isolation amplified the other’s effect; for example,

the effects of asynchrony were most severe when individuals were spatially isolated (Figure 1A). While we did not detect a main effect of spatial isolation on style persistence, spatial isolation led to greater rates of reduced rates of pollination in small populations as compared to large ones (Figure 1D, E).

Independent of flowering synchrony, spatial isolation, and population size, seed set exhibited a consistent seasonal decline (Figure 1C). A seasonal decline independent of flowering synchrony could indicate, for instance, phenological mismatch with pollinators. Interestingly, the seasonal decline in seed set contrasted with the pattern we observed for style persistence. Style persistence increases with individuals' failure to find mates, so based on the trend we observed for seed set, we might expect style persistence to increase over the course of the season. However, style persistence also declined through the season. One possible explanation for this trend is that styles late in the season might persist for less time through mechanisms unrelated to pollination. For instance, abiotic conditions that increase the physiological costs of floral longevity (e.g., hotter days or drier conditions; Teixido and Valladares 2015) relative to its benefits may become more common later in the flowering season (Primack 1985; Ashman and Schoen 1996). Moreover, while overall, style persistence and seed set were correlated ( $R = -0.30$ ; Figure S4), the discrepancy in their responses to date of season also adds to growing evidence that seasonal timing of an event (e.g., an individual's start date of flowering) should not be conflated with its degree of synchrony with others in the population.

Population size related positively to reproductive success and mediated the relationship between spatial isolation with seed set. Specifically, seed set of individuals in larger populations was buffered to a modest extent from the negative effects of spatial isolation (Figure 1B). Using a zero-inflated modeling approach allowed us to see that population size specifically influenced the probability that individuals set zero seeds. Thus, population size seems to influence the probability that a plant receives no effective pollinator visits. Several mechanisms could have led to this outcome. First, in smaller populations, individuals of this self-incompatible plant may be more likely to be

genetically incompatible. Thus, even if visitation occurs, the pollinator may not be carrying compatible pollen (Wagenius and Lyon 2010). Alternatively, pollinator foraging patterns at the landscape level might explain this result. Bees might pass over small populations, and thus plants in small populations might be more likely to receive no visits. However, we note that our measure of population size is a census of all adult plants, flowering and non-flowering, and not a measure of population-level flowering density. Population size could co-vary with other factors, such as habitat disturbance, that could also influence pollinator abundance or foraging choices. Our investigations of scale-dependence in the response of reproductive success to spatial isolation reflect better the scale at which pollinator visitation may have responded to floral density.

Distance to individuals' intermediate (~3-8<sup>th</sup>) nearest neighbors best explained reproductive success overall (Figure 2), in small and medium populations (Figure 3), and in plants flowering across the season (Figure 3). This finding is consistent with the previous investigation in this system (Wagenius 2006), which did not consider how variation in seasonal context or population size might alter the scale at which reproductive success responds to spatial isolation. Failure of distance first nearest neighbor to predict reproductive success could reflect a tendency for nearest neighbors to be incompatible, thus rendering their proximity irrelevant for mating outcomes. Alternatively, pollinators might respond to density at the scale of patches of plants, rather than the isolation of one or two individuals. While consistent with prior work, the finding that the scale of plant isolation that influenced reproductive success was constant across the season and a wide range of population sizes was surprising. Small populations included as few as four plants while medium populations included as many as 796. The consistent pattern across this wide range of population sizes suggests that pollinators foraging is responsive to density on a relatively small scale and that pollinators may visit the same number of plants in a foraging bout regardless of distance between them, which varies with population size and time of season (Figure S9). The only exception to this pattern was in large populations, where distance between individuals 1-30<sup>th</sup> nearest neighbor all predicted reproductive success similarly. This is consistent with work by

Groom (1998) showing that individual isolation has less of an effect on seed production in large patches of flowers, perhaps because pollinators are more abundant or forage more thoroughly in that context (Westphal et al. 2003).

### *Implications for Conservation*

Knowledge of the mechanisms that underlie mate-finding Allee effects can offer insights for conservation. For example, we found that individuals in small populations were more sensitive to spatial isolation. To improve reproductive outcomes for small populations, based on our findings, we can envision three options for a conservation manager. First, one could seek to minimize a plausible cause for the population size effect by increasing genetic diversity, such as through the addition of new seeds or individuals. Second, one could reduce spatial isolation, such as by creating small patches of individuals, e.g., at least three to six individuals, in close proximity, as our scale-dependence analysis suggests this range best predicts reproductive outcomes (Figure 3). We found that individuals in dense patches, e.g., those that have four neighbors within 1 m, were buffered from the effects of reproductive asynchrony (Figure 1A), so planting individuals within a small radius could be effective. If manipulating spatial proximity is not feasible, a third approach could be to seek methods to increase reproductive synchrony, such as through prescribed burns, which increase reproductive synchrony in our system (Wagenius et al. 2020). In a restoration context, where seeds sourced from different locations may have mismatched phenology (Wadgyman and Weis 2017), efforts to minimize temporal isolation would improve reproductive outcomes.

It is important to recognize that while we have demonstrated how isolation influences reproductive components of individual fitness (i.e., a “component Allee effect”) the matter of chief concern to conservation biologists is whether limitations to mate finding affect population demography (Gascoigne et al. 2009). Trade-offs with other fitness components could mean that mate-finding Allee effects are of little consequence for population growth. Our other investigations show that plants with more

mates in close proximity do have more offspring, even after accounting for high rates of juvenile mortality over eight years (see Chapter 3). However, the fitness differences associated with mate density eroded over time. Thus, the long-term demographic consequences of mate-finding Allee effects in our system are suggestive but remain unclear.

## CONCLUSIONS

Individual-level isolation in both space and time correlated with patterns of reproductive failure. We found strong evidence that spatial and temporal dimensions of isolation interactively influenced seed set. Furthermore, the relationship between reproductive success and distance to intermediate neighbors was consistent across time and between populations of different sizes, suggesting that foraging patterns are consistent across a wide range of contexts. This could offer a potential explanation for the apparent resilience of small and isolated populations in fragmented landscapes. At the same time, in large populations, individuals' reproductive success declined less with spatial isolation and reproductive asynchrony compared to small populations.

Disentangling the mechanisms that produce this pattern, e.g., mate incompatibility and/or pollinator foraging patterns, could offer insight to conservation practitioners to improve management of small populations.

## ACKNOWLEDGEMENTS

A. Waananen contributed to data collection and processing between 2015 and 2020, designed and performed the analysis, and wrote the manuscript. J. Beck, S. Wagenius, and R. Shaw helped develop the questions and provided feedback on the analysis and manuscript; J. Beck calculated style persistence and S. Wagenius collected the data from 1996-1999. Many members of Team Echinacea, especially G. Kiefer, contributed to data collection in the field. Volunteers at the Chicago Botanic Garden, led by interns D. Hanson, S. Nordstrom, and M. Stevens, processed seed heads. Long term funding to R. Shaw and S. Wagenius from the National Science Foundation made this work possible.

The Fish and Wildlife Service, the Pope-Douglas Solid Waste Board, and private landowners granted us to access their property and collect plant materials.



## ILLUSTRATIONS

Table 1. Model selection for seed set predicted as a function of distance to 4<sup>th</sup> nearest neighbor ('Dist'), flowering synchrony ('Sync'), date of flowering ('Jdate'), population census size ('N'), and interactions between these predictors. The full model was a zero-inflated beta-binomial model: Seed Set ~ Dist + Sync + Jdate + N + Jdate:Dist + N:Dist + Sync:N + Dist:Sync; the zero-inflated (ZI) model was Prob[Observation is a Structural Zero] ~ Dist + Sync + Jdate + N + Jdate:Dist + N:Dist + Sync:N + Dist:Sync. We included random effects for site and year in the main portion of the model. We compared a reference model to models dropping a single term, beginning with models that dropped ZI interaction terms, and establishing new reference models sequentially as indicated by moving down the table below. We retained italicized terms in the final model.

Dropped Term	Chi-Square	Df	P-Value
ZI Jdate:Dist	0.02	1	0.87
ZI N:Dist	0.77	1	0.38
ZI Sync:N	0.73	1	0.39
ZI Dist:Sync	0.19	1	0.66
New reference model for tests below: <i>omit all interactions from ZI portion of the model</i>			
Jdate:Dist	0.002	1	0.97
<i>N:Dist</i>	3.57	1	0.06*
Sync:N	0.02	1	0.89
<i>Dist:Sync</i>	3.34	1	0.07*
New reference model for tests below: <i>also omit Jdate:Dist and Sync:N from main model</i>			
<i>ZI Dist</i>	4.95	1	0.03*
<i>ZI Sync</i>	6.87	1	0.009*
ZI Jdate	0.11	1	0.73
<i>ZI N</i>	8.94	1	0.003*
<i>Dist</i>	17.59	1	< 0.001*
Sync	1.98	1	0.16
<i>Jdate</i>	27.5	1	< 0.001*
N	0.67	1	0.41
Final model: <i>ZI Model: ~ Dist + Sync + N</i> <i>Betabinomial Model: ~ N:Dist + Dist:Sync + Dist + Jdate</i> <i>+ (1/Site) + (1/Year)</i>			

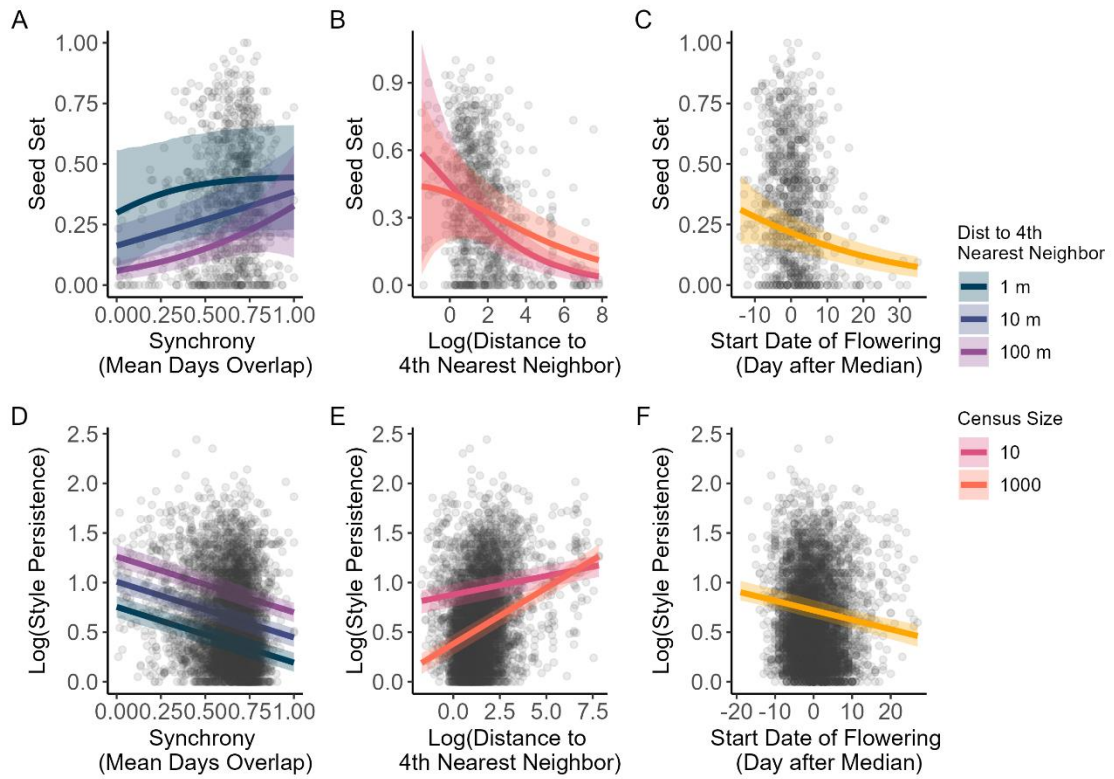


Figure 1. Relationships between seed set (top row) or style persistence (bottom row) and the predictors of primary interest. Model predictions are shown for hypothetical individuals across the range of values for the covariate on the x-axis while the values of all other covariates in the model are either held at the median value observed in the data or, for interactions, predicted at specific values of the interacting variable.

Table 2. Results of model selection for style persistence predicted as a function of distance to 4<sup>th</sup> nearest neighbor ('Dist'), flowering synchrony ('Sync'), date of flowering ('Jdate'), population census size ('N'), and interactions between these predictors. The full model was a linear mixed model: Style Persistence ~ Dist + Sync + Jdate + N + Jdate:Dist + N:Dist + Sync:N + Dist:Sync plus random effects for site and year. We compared a reference model to models dropping a single term, beginning with models that dropped interaction terms and establishing a new reference models as indicated by moving down the table below. We retained italicized terms in the final model.

Dropped Term	Chi-Square	Df	P-Value
Jdate:Dist	0.07	1	0.78
<i>N:Dist</i>	8.23	1	0.004*
<i>Sync:N</i>	1.42	1	0.23
<i>Dist:Sync</i>	2.16	1	0.14
New reference model for tests below: <i>omit Jdate:Dist, Sync:N and Dist:Sync</i>			
Dist	2.43	1	0.11
<i>Sync</i>	200.33	1	< 0.001*
<i>Jdate</i>	88.39	1	< 0.001*
<i>N</i>	15.01	1	< 0.001*
Final model: <i>Betabinomial Model: ~ N:Dist + Sync:N + Dist:Sync</i> <i>+ Sync + Jdate + N + (1/Site) + (1/Year)</i>			

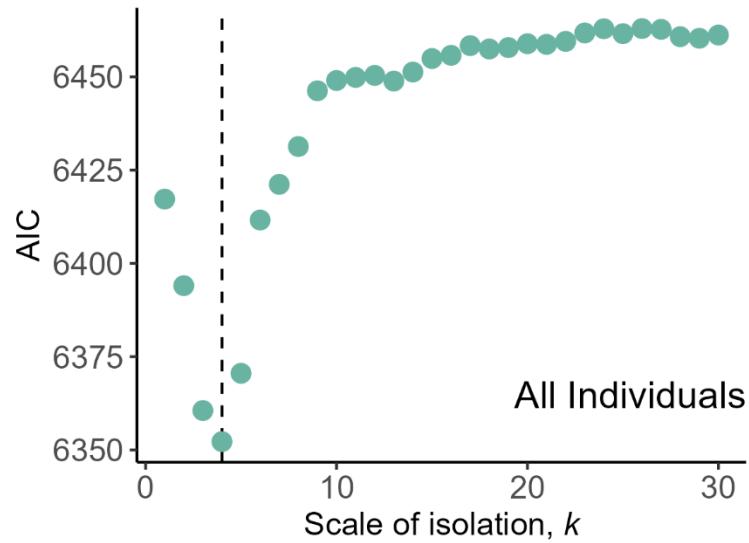


Figure 2. Scale dependence of the relationship between seed set and the scale of spatial isolation when considering all individuals. Each point represents the performance, measured as AIC, of a model that included a predictor for distance to individuals'  $k$ th nearest neighbor. Lower AIC values indicate better model performance. The dashed line highlights the value of  $k$  where the corresponding model AIC was minimized across the set of models.

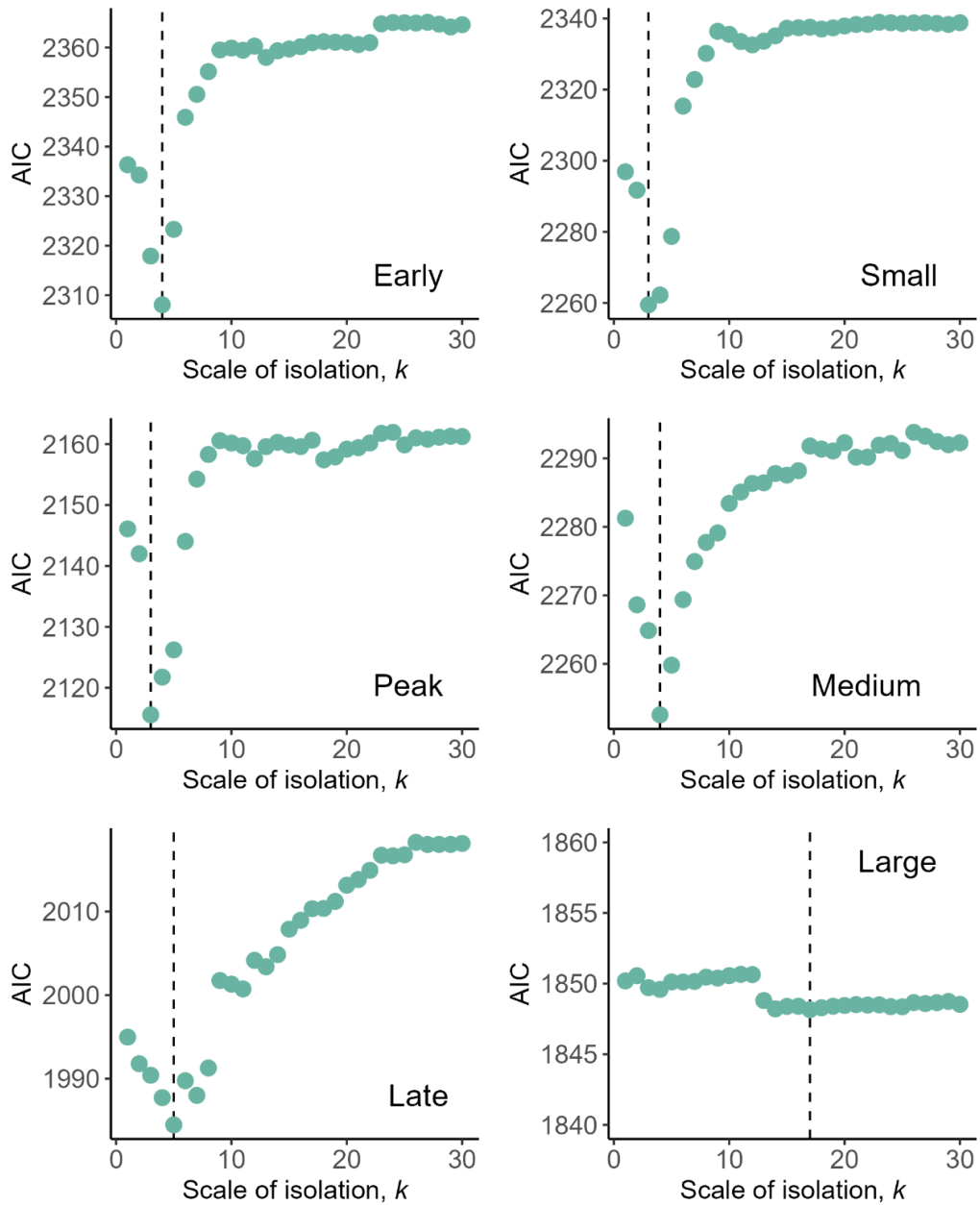


Figure 3. Assessment of variation performance of models considering different scales of spatial isolation (distance to  $k$ th nearest neighbors) as predictors of seed set in subsets of the data. Lower AIC values indicate better model performance. The ‘Early’ panel shows model performance based individuals that had flowering times within the earliest third of the data (but across all populations), and so on.

## BIBLIOGRAPHY

- Alonso-López, M. T., P. J. Garrote, and J. M. Fedriani. 2022. Spatial isolation impacts pollinator visitation and reproductive success of a threatened self-incompatible Mediterranean tree. *Acta Oecologica* 117:103866.
- Ashman, T.-L., and D. J. Schoen. 1996. Floral Longevity: Fitness Consequences and Resource Costs. Pp. 112–139 *in* *Floral Biology*.
- Augspurger, C. K. 1983. Phenology, flowering synchrony, and fruit set of six Neotropical shrubs. *Biotropica* 15:257–267.
- Bates, D., M. Maechler, B. Bolker, S. Walker. 2015. Fitting linear mixed-effects models using lme4. *Journal of Statistical Software*, 67:1-48.
- Blasco-Moreno, A., M. Pérez-Casany, P. Puig, M. Morante, and E. Castells. 2019. What does a zero mean? Understanding false, random and structural zeros in ecology. *Methods Ecol. Evol.* 10:949–959. British Ecological Society.
- Bogdziewicz, M., M. Pesendorfer, E. E. Crone, C. Pérez-Izquierdo, and R. Bonal. 2020. Flowering synchrony drives reproductive success in a wind-pollinated tree. *Ecol. Lett.* 23:1820–1826.
- Bolmgren, K., O. Eriksson, and H. P. Linder. 2003. Contrasting flowering phenology and species richness in abiotically and biotically pollinated angiosperms. *Evolution* 57:2001–2011.
- Brooks, M. E., K. Kristensen, K. J. Van Benthem, A. Magnusson, C. W. Berg, A. Nielsen, H. J. Skaug, M. Machler, and B. M. Bolker. 2017. glmmTMB balances speed and flexibility among packages for zero-inflated generalized linear mixed modeling. *R J.* 9:378–400.
- Calabrese, J. M., W. F. Fagan, and A. E. C. A. Pfister. 2004. Lost in time, lonely, and single: Reproductive asynchrony and the Allee effect. *Am. Nat.* 164:25–37.
- Elzinga, J. A., A. Atlan, A. Biere, L. Gigord, A. E. Weis, and G. Bernasconi. 2007. Time after time: flowering phenology and biotic interactions. *Trends Ecol. Evol.* 22:432–439.
- Fagan, W. F., C. Cosner, E. A. Larsen, and J. M. Calabrese. 2010. Reproductive asynchrony in spatial population models: How mating behavior can modulate allee effects arising from isolation in both space and time. *Am. Nat.* 175:362–373.
- Forrest, J., and J. D. Thomson. 2009. Pollinator experience, neophobia and the evolution of flowering time. *Proc. R. Soc. B Biol. Sci.* 276:935–943.

- Gascoigne, J., L. Berec, S. Gregory, and F. Courchamp. 2009. Dangerously few liaisons: a review of mate-finding Allee effects. *Popul. Ecol.* 51:355–372.
- Greenleaf, S. S., N. M. Williams, R. Winfree, and C. Kremen. 2007. Bee foraging ranges and their relationship to body size. *Oecologia* 153:589–596.
- Groom, M. J. 1998. Allee effects limit population viability of an annual plant. *Am. Nat.* 151:487–496.
- Harrell, F. E., and C. Dupont. 2023. Hmisc: Harrell miscellaneous. R package version 5.0-1. R Found. Stat. Comput. <https://CRAN.R-project.org/package=Hmisc>.
- Hartig, F. 2022. DHARMA: Residual Diagnostics for Hierarchical (Multi-Level / Mixed) Regression Models. R package version 0.4.6, <<https://CRAN.R-project.org/package=DHARMA>>.
- Hayes, L., and C. Grüter. 2023. When should bees be flower constant? An agent-based model highlights the importance of social information and foraging conditions. *J. Anim. Ecol.* 92:580–593.
- Ison, J. L., and S. Wagenius. 2014. Both flowering time and distance to conspecific plants affect reproduction in *Echinacea angustifolia*, a common prairie perennial. *J. Ecol.* 102:920–929.
- Ison, J. L., S. Wagenius, D. Reitz, and M. V Ashley. 2014. Mating between *Echinacea angustifolia* (Asteraceae) individuals increases with their flowering synchrony and spatial proximity. *Am. J. Bot.* 101:180–189.
- Kunin, W. E. 1997. Population size and density effects in pollination: pollinator foraging and plant reproductive success in experimental arrays of *Brassica kaber*. *J. Ecol.* 225–234.
- Levin, D., and H. Kerster. 1969. The dependence of bee-mediated pollen and gene dispersal upon plant density. *Evolution* 23:560-571.
- Lüdecke, D. 2018.ggeffects: Tidy data frames of marginal effects from regression models. *J. Open Source Softw.* 3:772.
- Muller, H., H. Grossmann, and L. Chittka. 2010. ‘Personality’ in bumblebees: individual consistency in responses to novel colours? *Anim. Behav.* 80:1065–1074.
- Munguía-Rosas, M. A., J. Ollerton, V. Parra-Tabla, and J. A. De-Nova. 2011. Meta-analysis of phenotypic selection on flowering phenology suggests that early flowering plants are favoured. *Ecol. Lett.* 14:511–521.

- Nooten, S. S., and S. M. Rehan. 2019. Agricultural land use yields reduced foraging efficiency and unviable offspring in the wild bee *Ceratina calcarata*. *Ecol. Entomol.* 44:534–542.
- Ogilvie, J. E., and J. R. K. Forrest. 2017. Interactions between bee foraging and floral resource phenology shape bee populations and communities. *Curr. Opin. insect Sci.* 21:75–82.
- Osborne, J. L., A. P. Martin, N. L. Carreck, J. L. Swain, M. E. Knight, D. Goulson, R. J. Hale, and R. A. Sanderson. 2008. Bumblebee flight distances in relation to the forage landscape. *J. Anim. Ecol.* 77:406–415.
- Page, M. L., J. L. Ison, A. L. Bewley, K. M. Holsinger, A. D. Kaul, K. E. Koch, K. M. Kolis, and S. Wagenius. 2019. Pollinator effectiveness in a composite: a specialist bee pollinates more florets but does not move pollen farther than other visitors. *Am. J. Bot.* 106:1487–1498.
- Peters, M. A. E., and A. E. Weis. 2019. Isolation by phenology synergizes isolation by distance across a continuous landscape. *New Phytol.* nph.16041.
- Primack, R. B. 1985. Longevity of individual flowers. *Annu. Rev. Ecol. Syst.* 16:15–37.
- R Core Team. 2022. R: A language and environment for statistical computing. R Foundation for Statistical Computing, Vienna, Austria. URL <https://www.R-project.org/>.
- Richardson, L. K., and S. Wagenius. 2022. Fire influences reproductive outcomes by modifying flowering phenology and mate-availability. *New Phytol.* 233:2083–2093.
- Samson, F., and F. Knopf. 1994. Prairie conservation in North America. *Bioscience* 44:418–421.
- Sánchez-Castro, D., G. Armbruster, and Y. Willi. 2022. Reduced pollinator service in small populations of *Arabidopsis lyrata* at its southern range limit. *Oecologia* 200:107–117.
- Teixido, A. L., and F. Valladares. 2015. Temperature-limited floral longevity in the large-flowered mediterranean shrub *Cistus ladanifer* (Cistaceae). *Int. J. Plant Sci.* 176:131–140.
- Waananen, A., G. Kiefer, J. L. Ison, and S. Wagenius. 2018. Mating opportunity increases with synchrony of flowering among years more than synchrony within years in a nonmasting perennial. *Am. Nat.* 192:379–388.



- Wadgyamar, S. M., and A. E. Weis. 2017. Phenological mismatch and the effectiveness of assisted gene flow. *Conserv. Biol.* 31:547–558.
- Wagenius, S. 2006. Scale dependence of reproductive failure in fragmented *Echinacea* populations. *Ecology* 87:931–941.
- Wagenius, S. 2004. Style persistence, pollen limitation, and seed set in the common prairie plant *Echinacea angustifolia* (Asteraceae). *Int. J. Plant Sci.* 165:595–603.
- Wagenius, S., J. Beck, and G. Kiefer. 2020. Fire synchronizes flowering and boosts reproduction in a widespread but declining prairie species. *Proc. Natl. Acad. Sci.* 117:3000–3005.
- Wagenius, S., and S. P. Lyon. 2010. Reproduction of *Echinacea angustifolia* in fragmented prairie is pollen-limited but not pollinator-limited. *Ecology* 91:733–742.
- Westphal, C., I. Steffan-Dewenter, and T. Tscharntke. 2003. Mass flowering crops enhance pollinator densities at a landscape scale. *Ecol. Lett.* 6:961–965.
- Yourstone, J., V. Varadarajan, and O. Olsson. 2023. Bumblebee flower constancy and pollen diversity over time. *Behav. Ecol.* In press.
- Zurbuchen, A., S. Cheesman, J. Klaiber, A. Müller, S. Hein, and S. Dorn. 2010. Long foraging distances impose high costs on offspring production in solitary bees. *J. Anim. Ecol.* 79:674–681.

## CHAPTER 2

Flowering asynchrony moderates fitness effects of outcrossing distance in fragmented populations of an herbaceous forb

### SYNOPSIS

Individuals' location and timing of reproduction constrain which pairs can mate. A limited mating pool, over generations, can lead to genetic drift, with more proximate individuals becoming more similar to one another. At the same time, location and timing often correlate with axes of environmental variation to which individuals may adapt, such as climate or resource availability. Genetic drift and adaptation to different environments can both result in genetic differentiation between population fragments separated by space or timing of reproduction. However, these two mechanisms are expected to lead to opposing consequences for mating across space or time. Mating between individuals separated by space or time (i.e., outcrossing) could alleviate inbreeding depression resulting from genetic drift, increasing fitness, but it could also disrupt local adaptation, decreasing fitness. While studies have often investigated the effects of outcrossing over space, the effects of outcrossing over time remain unknown. Here, we assess the fitness outcomes of outcrossing over both space and time in populations of a tallgrass prairie forb, *Echinacea angustifolia*. Surprisingly, we found that interparent distance and asynchrony interacted to affect offspring fitness, such that the offspring with the highest fitness had parents from highly distant source populations and a maternal plant that flowered late relative to the paternal plant. We discuss possible causal mechanisms for this result and its implications for conservation and management.

## INTRODUCTION

Mating patterns—i.e., who mates with whom—can exert a profound influence on offspring fitness. In plants, there is strong evidence for relationships between spatial distance and mating. For many species, likelihood of mating increases with the proximity of two individuals (Levin and Kerster 1969; Fenster 1991a; Ison et al. 2014) while long-distance mating events occur infrequently (Pasquet et al. 2008; Ahmed et al. 2009; Jha and Dick 2010; Castilla et al. 2017). Several independent mechanisms may then lead to a relationship between the distance separating mates (‘interparent distance’) and the fitness of their offspring. Over generations, limited dispersal can result in spatial genetic patterns such that the relatedness of individuals decreases with distance (i.e., ‘isolation-by-distance’) at a scale dependent on the organism’s dispersal ability (Wright 1943). As a result, mating between more distant plants could alleviate inbreeding and subsequent inbreeding depression (Keller and Waller 2002).

At the same time, individuals that are more distant may be more likely to be adapted to distinct local conditions (Sexton et al. 2014). Thus, mating between distant plants may simultaneously alleviate inbreeding, increasing offspring fitness (‘heterosis’), and compromise adaptation to local conditions, reducing fitness (‘outbreeding depression’). Alternatively, intermediate interparent distances could maximize offspring fitness by finding a compromise between the opposing consequences of heterosis and adaptation to local conditions. To investigate which scenario is most likely, researchers conduct experimental crosses over a range of interparent distances and measure offspring fitness (Price and Waser 1979; Fenster 1991b; Edmands 1999; Waser et al. 2000; Caruso et al. 2015). Such studies have taken place over a wide range of geographical scales (e.g., 4m – 15km, Billingham et al. 2007 and within populations (e.g., Price and Waser 1979; Fenster 1991b; McCall et al. 1991). These studies reveal that the strength and scale of genetic drift and selection vary widely across space (reviewed in Waser and Williams 2001). However, comparatively few studies have considered other possible axes of genetic differentiation (e.g., genetic distance, but see Pelabon et al. 2005; or

environmental distance) and fewer still have considered multiple potential axes simultaneously. Examining each dimension individually could obscure multidimensional patterns.

One potentially important axis of differentiation is timing of reproduction. Timing of reproduction, like individuals' spatial distribution, influences mating patterns. When reproduction is not synchronous among all individuals in a population, timing of reproduction determines an individual's potential mates. Temporally non-random mating patterns can lead to genetic differentiation among individuals that reproduce at different times during a season (i.e., temporal genetic structure) when variation in timing of reproduction has a genetic component (Hendry and Day 2005). Pollination is restricted to synchronously flowering individuals and there is often a substantial genetic component of variance in flowering phenology (Geber and Griffen 2003; Hendry and Day 2005, Reed et al. 2022). On these first principles, when variation in timing of flowering exists and is heritable, individuals with similar timing will mate and produce offspring with similar timing of flowering (Weis and Kossler 2004; Hendry and Day 2005). Following this reasoning over generations, individuals that flower at similar times of the season will be more likely to share ancestry, though the magnitude of genetic structuring will depend on both the heritability of timing of flowering and the extent to which individuals mate assortatively by time. Empirical studies have borne out these predictions (Ison et al. 2014; Ison and Weis 2017) and theory suggests that the consequences of temporal assortative mating may be analogous to those of isolation-by-distance (Hendry and Day 2005). Furthermore, a simulation study found that spatial and temporal isolation together accelerate population genetic subdivision (Peters and Weis 2019). Thus, the consequences of outcrossing across space and time may be strong in fragmented populations. Mating across a temporal gradient may also have important implications in the context of ecological restorations; several recent studies have documented that seeds sourced from different provenances maintain differences in phenology when sown together (Wadgyamar and Weis 2017; Rushing et al. 2021).

Offspring size and quality may vary depending on when during the parental plants' reproductive period mating occurred (Wyatt 1982). As a result, directional reproductive asynchrony between the paternal plant and maternal plant (i.e., which parent flowers earlier and by how much), rather than simply the magnitude of the difference, could also affect offspring fitness. Within an inflorescence (i.e., a group of multiple flowers of one plant), seed size often decreases with the timing of its corresponding flower's development (Diggle 1995). This may reflect reduced maternal resources available for later-pollinated seeds (i.e., resource competition among ovaries) (Lloyd 1980; Herrera 1991; Ashman and Baker 1992), morphological constraints (Watson and Casper 1984; Diggle 1995; Wang et al. 2022), or both.

Similarly, individual plants can vary in either pollen viability or style receptivity across their duration of flowering within a season (Marshall et al. 2010). For instance, individuals may become more receptive to self-pollination (Gibbs 2014) or less discriminating among pollen donors (Marshall et al. 2007) as their flowering period progresses, resulting in lower fitness offspring. Thus, a maternal plant mating early in its flowering period might produce higher fitness offspring than a maternal plant mating late within its flowering period (Marshall et al. 2010). Furthermore, a paternal plant that flowers earlier than a maternal plant, then, might be more able to access the early, highest fitness portions of the maternal plant's inflorescence, particularly if plants shift resources towards male reproductive function later within an individual's flowering period (Brunet and Charlesworth 1995). Altogether, these mechanisms provide rationale for considering reproductive asynchrony not simply as an absolute distance in time, but as a directional measure, and to consider at what point within the maternal plant's reproductive period mating occurred.

In this study, we use a long-term dataset of survival and reproduction of the narrow-leaved purple coneflower, *Echinacea angustifolia* (Asteraceae), an herbaceous perennial forb native to the North American tallgrass prairie, to assess the fitness consequences of mating between plants isolated by space and time. In particular, we test

alternative hypotheses that offspring fitness (H1) increases with interparent isolation (in space or time), exhibiting heterosis, (H2) decreases with interparent isolation, reflecting outbreeding depression, or (H3) peaks at intermediate interparent distance, which would suggest a balance between inbreeding and outbreeding depression over a span of temporal difference. We also evaluate the extent to which (H4) offspring fitness is associated with the direction of interparent asynchrony, which could reflect the effect of timing of mating within a parental plant's flowering bout on offspring quality.

## MATERIALS AND METHODS

Our overall approach was to collect seeds from thirteen isolated remnant populations of *E. angustifolia* and plant them together in a common environment, where we monitored their timing of flowering and allowed open pollination. Then, we collected seeds from a sample of these plants and analyzed their paternity, linking the identity of the parental plants to their source populations and timing of flowering. We planted the offspring in a separate experiment plot, where we monitored their survival and reproduction for 11 years. To estimate offspring fitness and its relationship with interparent distance and asynchrony, we compare models of offspring fitness, measured by offspring survival and reproduction through age 17, as predicted by the distance between their parents' source populations and flowering asynchrony. Then, we use model selection to test our hypotheses about the relationships between interparent distance and interparent asynchrony and offspring fitness.

### Study Area and Organism

*Echinacea angustifolia* is a long-lived, self-incompatible perennial forb that is widespread throughout the North American tallgrass prairie, which has experienced extensive habitat loss over the past 150 years. Prior work in *E. angustifolia* suggests that the formation of spatial and temporal genetic structure that could lead to fitness effects of outcrossing may be plausible. In *E. angustifolia*, mating is more likely between plants that are closer together or flower more synchronously (Ison et al. 2014). One likely cause

for spatial patterning is that *E. angustifolia*'s main pollinators are small-bodied bees (Page et al. 2019) with typical foraging ranges that are likely limited to <200 m (Greenleaf et al. 2007). The fruits (achenes) of *E. angustifolia* are also heavy and gravity-dispersed, meaning that offspring remain in close proximity to their maternal source. Studies of genetic structure in our study area indicate fine-scale genetic structure within a large remnant (Wagenius 2000) and among smaller remnants (Ison 2010) at scales of ~50m. In addition, individuals' start date of flowering shows substantial heritability (~20%, Reed et al. 2022). Although *E. angustifolia* is iteroparous and date of flowering varies with annual conditions, individuals' flowering rank within the population is consistent (English et al., in prep). Furthermore, previous studies of the populations in our study area have found severe inbreeding depression (Wagenius et al. 2010), suggesting that there may be positive consequences of increasing outcrossing distance over space or time.

Other aspects of *E. angustifolia* life history and flowering biology also inform our approach. *E. angustifolia* has a long pre-reproductive period; when germinated in the greenhouse and planted as plugs, individuals rarely flower before four growing seasons have passed. After flowering for the first time, individuals do not typically flower each year, emerging instead as basal rosettes between flowering years. Some individuals flower nearly every year, while others flower less than once in ten years (Waananen et al. 2018). When they flower, individuals most often produce a single composite flowering head, though we have observed individuals with up to 21 heads. Average head count increases after spring fire (Wagenius et al. 2020). Individual flowering heads are cone-shaped and comprise numerous hermaphroditic florets (typically 60-180) that each produce one monocarpic fruit (an achene). Flowers open sequentially in rows from the bottom of the head (more proximal to the peduncle) to the top, with anthers emerging from one row each day (Wagenius 2004). Anthers persist for one day, after which styles emerge through the anther tube. Upon receipt of compatible pollen, styles typically shrivel within 24 hours. If a style does not receive compatible pollen, it will eventually shrivel due to age, usually within seven days. The rate of shriveling due to age seems to

be variable depending on weather conditions (e.g., shriveling seems to occur sooner when it is hot and dry as compared to when it is cool and humid).

#### Establishment of the Parental Cohort

Our analysis focuses on the effects of outcrossing between 13 *E. angustifolia* populations in Grant and Douglas County, Minnesota (Figure 1). These populations primarily persist along roadside rights-of-way, though one large population is located within a preserve managed by The Nature Conservancy, one is partially located on a U.S. Fish and Wildlife Waterfowl Protection Area, and two are on private land. Between 1995 and 1999, we established a common garden experiment consisting of seeds collected from randomly selected individuals in our 13 focal populations. Methods for this planting are detailed in Shaw et al. 2008; briefly, we germinated the seedlings under laboratory conditions and planted seedlings in randomized locations within blocks in a restored old-field prairie. We planted cohorts adjacent to one another, except for one group of seedlings from the 1999 cohort, which we planted 200 m away. In subsequent years, we planted other experimental plantings adjacent to the main common garden area. Collectively, we refer to these common garden plantings as Experimental Plot 1, hereafter ExPt1. We retained information on the source population for most individuals in ExPt1, but the source population for a small number of plants in ExPt1 is unknown.

In 2005, 223 plants in ExPt1 flowered; our study focuses on these plants and the fitness of their offspring. We recorded start and end date of flowering for all 223 flowering individuals in 2005 (Ison et al. 2014). To do this, we identified bolting individuals early in the season and revisited each individual daily to record its flowering status. We collected and dried a sample of leaf tissue from all flowering individuals within ExPt1, except for two plants, which were diseased and likely did not sire offspring. At the end of the season, we randomly sampled 37 flowering individuals representing unique maternal lines from which to harvest one seedhead.

#### Establishment of the Offspring Cohort and Annual Fitness Measurements



We selected 30 achenes from each maternal line to undergo germination treatment, randomly choosing 10 achenes from each of the top 30 achenes, the bottom 30 achenes, and the remaining ‘middle’ achenes (Ison et al. 2014). For the ‘top’ achenes, we noted whether the achene was sourced from the top 10 achenes from a head or the top 11-30 achenes. When a head had fewer than 30 achenes, we attempted to germinate all of them. We followed the protocol of Feghahati and Reese (1994), as modified by Wagenius (2004), and transferred germinants to plug trays. We grew the seedlings until the first true leaf was large enough to sample, about one week. In total, we collected leaf tissue samples from 927 offspring. We continued to grow the seedlings under greenhouse conditions until they were 4-6 weeks old. Then, we planted all surviving offspring (3861 plants) on a 1 m by 1 m grid within a new experimental plot, Experimental Plot 2, hereafter referred to as ‘ExPt2’. To assess the paternity of the individuals in ExPt2, we extracted DNA from samples of leaf tissue that we collected from the plants that flowered in 2005 in ExPt1 and from a sample of the progeny that we planted in ExPt2. We amplified the DNA at 11 microsatellite markers (Ison et al. 2013) and used the paternity inference program Cervus (Kalinowski et al. 2007) to assign the most likely paternal plant to each seedling based on these markers; we describe our paternity assignment methods in detail in Ison et al. 2014. In subsequent years, we genotyped an additional 157 individuals in ExPt2 that flowered in the years 2014-2016, following the same methodology, as described in Reed et al. (2022).

We assessed the survival and flowering of each individual in ExPt2 annually in July or August between 2006 and 2022. We also counted how many flowering heads each plant produced. In some cases, individuals initiated flowering but failed to produce pollen or seeds (e.g., due to frost damage, herbivory, or disease). In these cases, we recorded individuals as flowering but producing zero flowering heads. When we failed to find an individual at its planting location, we recorded this and continued to search for it for three subsequent years. If we found it alive in those years, we updated the status of all previous records from missing to alive and non-flowering. If we failed to find the

individual after three years, we updated its status to dead in the first year that we did not find it.

### Aster Analysis

We used unconditional fixed effect aster models to make inferences about an integrated measure of fitness that accounts for variation in survival, flowering status, and fecundity. We estimated fecundity as the count of flowering heads that individuals produced in each year over the first 17 years since planting (2006-2022). Fitness in many natural populations violates the statistical assumption of linear regression approaches that residuals are normally distributed, for example, due to the tendency for a large portion of individuals to fail to survive to reproduction (Mitchell-Olds and Shaw 1987). Aster models address these issues by modeling fitness with different distributions for each transition between life-history stages, e.g., survival from one year to the next, or initiation of flowering given survival (Geyer et al. 2007). Through their graphical structure, Aster models validly model fitness by accounting for the dependence of life-history transitions on previous life stages in a joint analysis of survival and reproduction even in organisms with complex life histories, such as iteroparous plants (Shaw et al. 2008).

Using Aster models, we assessed the relationships between fitness, interparent distance, and interparent asynchrony. The offspring that we sampled for genotyping after they began flowering are not a random sample of the population that survived through at least 2014. To avoid confounding effects of this bias and still make use of our data, we performed two analyses using different subsets of individuals and their life histories. First, we analyzed all of the offspring that we genotyped initially, considering their survival and reproduction for the full study period, 2006-2022. Then, we performed an analysis of all genotyped offspring that survived at least until 2014, including those that we sampled after they flowered, and restricted our life history analysis to individuals' survival and reproduction between 2014 and 2022. This analysis yielded qualitatively similar results, so, for simplicity, we detail it in full in Appendix D. Hereafter, we focus

on the set of individuals genotyped initially with fitness assessed over the full study period.

We modeled transitions representing survival from one year to the next as Bernoulli distributed (where 1 = survived, 0 = died). Likewise, we modeled transitions from survival status to flowering status with a Bernoulli distribution (where 1 = produced at least one flowering head that produced pollen, 0 = did not produce a flowering head that produced pollen). In contrast, we modeled the transition from flowering status to flowering head count with a zero-truncated Poisson distribution (flowering head count = 1, 2, 3...). In 2018, we cut flowering heads from some individuals in the common garden for a different experiment; some plants re-sprouted heads before the end of the season, complicating our measure of head count in that year. Thus, we omitted fitness data from 2018 in our model. The graphical model included nodes for annual survival from 2006-2017 and 2019-2022 and flowering head count for 2009-2017 and 2019-2022, excluding 2018 from the analysis. Because of this, one node (“Survival 2019” in Figure S1) represents survival over both 2018 and 2019. None of the genotyped individuals produced flowering heads prior to 2009. Cumulative head count over all years represents fitness in our model. We performed all statistical analyses in R version 4.0.3 using the R package ‘aster’ version 1.0-3 (Geyer, 2021).

The goal of our analysis was to assess the relationship between fitness and interparent distance and asynchrony. We used the flowering phenology data collected in ExPt1 in 2005 to calculate interparent asynchrony. Specifically, we measured interparent asynchrony (hereafter ‘asynchrony’) as difference in start date of flowering of the parental plants (i.e., maternal start date of flowering minus the paternal start date of flowering). Note that this measure accounts for the direction of asynchrony between maternal and parental plants because positive values indicate a maternal plant began flowering after the paternal plant and vice versa for negative values. To calculate interparent distance, hereafter, ‘distance’, we found the Euclidian distance between the center of the maternal and paternal source populations, i.e., sites where we collected the

seeds that became the maternal and paternal plants. We estimated population centers with the median easting and median northing coordinate, the mediod, of all *E. angustifolia* individuals we have observed during annual censuses in each population between 2012 and 2022. Outlier points, which may reflect ambiguity in population boundaries, influence a mediod less than a centroid, the mean coordinates of a group of points.

## Model Selection

We hypothesized the relationships between interparent distance and asynchrony differs in direction (H1 vs H2) or form (H3), depending on the mechanism underlying fitness differences with outcrossing. To determine the best overall model, we first assessed our hypotheses for distance and asynchrony separately using Akaike's information criterion (AIC) to compare candidate models. Then, we used likelihood ratio tests to test effects of distance and asynchrony jointly on offspring fitness.

*Interparent Distance* – To create models corresponding to our alternate hypotheses about interparent distance, we began with the 'Null' model that included only row, position, and the graph nodes, as described previously. We compared a model that included distance between parental source populations as a linear predictor, which would capture monotonic increases (H1) or decreases (H2) in offspring fitness with changes in distance. We also created a model that included the quadratic form of distance, which would best capture the scenario in which offspring fitness peaks at intermediate distances (H3). To improve model convergence, we linearly transformed interparent distance, centering it at zero and scaling it to a standard deviation of one.

To compare the models representing our *a priori* hypotheses H1-H3 (Table 1), we used Akaike's information criterion (AIC)(Akaike 1974). Models that are more accurate and use fewer parameters have lower AIC values. We calculated Akaike weights, which indicate the probability that a model minimizes the estimated information loss (i.e., minimizes the AIC index) compared to the other candidate models. Specifically, we calculated the difference between the minimum AIC and that of each other model ( $\Delta AIC$ )

and calculated an index of each model's plausibility as its Akaike weight, or  $\exp(\Delta AIC/2)$  (Wagenmakers and Farrell 2004). To represent the models' relative plausibilities, we calculated the proportion of each candidate model's Akaike weight in the sum of all candidate models' Akaike weights.

*Interparent Asynchrony* – To assess the relationship between interparent asynchrony and offspring fitness, we created a set of models beginning with a 'Null' model. This included, in addition to the graph nodes, the offspring row and position within ExPt2 as covariates to account for dependence of fitness on spatial environmental variation within the common garden. We then created models by adding to the 'Null' model different forms of effect of interparent asynchrony, representing our alternative hypotheses. Because we use a directional measure of asynchrony, to assess increases (H1) or decreases (H2) with interparent dissimilarity in timing of flowering, regardless of direction (or sign) of difference between the maternal and paternal plants' timing of flowering, we created a model including the term '|Asynchrony|'. Similarly, to test whether offspring fitness is maximized at intermediate values of parental dissimilarity (H3), we created a model with the term '|Asynchrony| + Asynchrony<sup>2</sup>.' This specification was necessary because if intermediate values of interparent dissimilarity maximize fitness, fitness would display a bimodal distribution with asynchrony (i.e., peaking at intermediate negative values and at intermediate positive values). By using the absolute value of asynchrony, we fit a relationship between fitness and dissimilarity, rather than difference; by adding the quadratic term, we allow for curvature, and therefore fitness peaks at intermediate values, in that relationship. We also tested for directional effects of interparent asynchrony on offspring fitness (H4), creating a model with the term 'Asynchrony.' We compared model performance using AIC, as described above.

*Overall Model* – We used likelihood ratio tests to compare a hierarchical set of models, beginning with the most complex model that included the best terms for asynchrony and distance, as indicated by the AIC comparisons on each term individually, and an interaction between the two, the 'Interaction' model. We compared the

‘Interaction’ model to a model that dropped the interaction, the ‘Additive’ model, and the additive model to a model that dropped the term for asynchrony, ‘Minus Asynchrony’ model, and a model that dropped the term for distance, ‘Minus Distance’ model. When likelihood ratio tests indicated a significant gain in model performance with the inclusion of either the interaction or an additional term, we interpreted this as evidence to retain the term in selecting the best model. To gain intuition for the effects predicted by the best model, we created and visualized model predictions for hypothetical individuals across the range of observed interparent distance and asynchrony.

To investigate potential causal mechanisms related to our findings, we performed several post-hoc tests. First, we investigated the relationship between offspring fitness and its position within the maternal plant inflorescence, or the ‘achene position.’ Because *E. angustifolia* flower heads develop sequentially and upwards from the bottom of the flower head to the top, we might expect a relationship between achene position and the direction of interparent asynchrony. For instance, offspring with high values of interparent asynchrony (maternal plants flowered later than paternal plants) might tend to come from a low achene position (i.e., near the beginning of the maternal plant’s flowering). We created ordinal categories for achene position. We scored achenes selected from the top 10 within a head as 4, those from the top 11-30 as 3.5, those from the middle of the head as 2, and those from the bottom 30 as 1. We quantified the correlation between achene rank and asynchrony using Kendall’s Tau rank correlation. We also used likelihood ratio tests to compare aster models that included ordinal achene position in addition to or in replacement of asynchrony.

To examine the extent to which parental start date of flowering, rather than interparent asynchrony *per se*, predicts fitness differences among offspring, we also visualized the correspondence between maternal and paternal start dates of flowering (the day of year that individuals began shedding pollen) and the interparent asynchrony of the offspring. We tested how much including maternal start date of flowering as an additional covariate, or in place of interparent asynchrony, would improve model performance. We

also investigated the correlation of interparent asynchrony with maternal or paternal source populations. We visualized variation in start date of flowering and subsequent interparent asynchrony among parental plants that originated from different source populations. However, because we chose the offspring in our study as seeds from a limited number of maternal plants, maternal and paternal source populations had low replication in our dataset and were confounded with maternal plant identity. Thus, we could not formally analyze relationships between interparent asynchrony and parental source population identities.

## RESULTS

Offspring fitness varied widely, as did interparent distance and asynchrony. We assigned paternity with >80% confidence to 758 plants in ExPt2 for which we could obtain records of interparent distance and interparent asynchrony. Of these, 436 were genotyped prior to planting, and thus were included in our analysis. Offspring produced between 0 and 32 flowering heads, which reflected if and in how many years individuals flowered. More than half of all plants died before producing any flowering heads (236 of 436, 54%); at the other extreme, two flowered ten times and produced >25 flowering heads (Appendix C Figure S2B). The distance between the source populations of parents of these offspring (i.e., interparent distance) ranged from 0 m (parents were from the same source population) to 9014 m (see distribution in Appendix C Figure S2C). The difference in start dates between the parents of these offspring (i.e., interparent asynchrony) ranged from -13 days (i.e., the maternal plant started flowering 13 days prior to the paternal plant) to 12 days (Appendix C Figure S2D). Interparent distance and interparent asynchrony were not correlated (Pearson's product-moment correlation;  $r = -0.007$ , 95 CI = -0.10 – 0.09,  $t = -0.15$ ,  $df = 434$ ,  $p = 0.88$ ; Appendix C Figure S2E). Timing of flowering appeared to vary among parents from different source populations, but samples sizes were insufficient to analyze variance within and among source population groups (Appendix C Figure S3).

The best performing model included the interactive effect of interparent distance and asynchrony ('+ Interparent Distance \* Interparent Asynchrony', Table 2). We used AIC analysis to test models representing the effects of interparent distance and interparent asynchrony corresponding to our *a priori* hypotheses (Table 1). For both variables, the best candidate models included a term indicating a linear, monotonic increase (i.e., +Asynchrony and +Distance, Table 1). We then used likelihood ratio tests to determine the best model considering both predictors (Table 2). Offspring fitness increased slightly with interparent distance (i.e., Distance:  $p = 0.001$ ; Table 3, Figure 2), according to the best overall model (Table 2); however, the effect of interparent distance depended strongly on the value of interparent asynchrony (Distance x Asynchrony:  $p = 0.02$ ; Table 3). In fact, our model predicted that offspring of maternal plants that flowered before the paternal plant (negative interparent asynchrony; Figure 2) would have decreasing fitness as interparent distance increased. In contrast, we failed to detect a significant relationship with interparent asynchrony independent of interparent distance (Asynchrony:  $p = 0.21$ ; Table 3). Visualizing predicted offspring fitness across the range of interparent distances and asynchrony revealed a saddle-shaped relationship (Figure 3). The model predicted that more extreme combinations of parental differences, especially highly positive asynchrony (maternal plants flowering later than paternal) and large distances between source populations, yielded the highest fitness offspring, while combinations of small distance with positive asynchrony or large distance with negative asynchrony minimized offspring fitness.

The best performing model included strong effects of an individual's location (i.e., their row and position) within the plot on survival (Row x Survival:  $p = 0.001$ ; Position x Survival:  $p < 0.001$ ; Table 3). Row within the plot also influenced the probability that an individual flowered (Row x Flowering:  $p < 0.001$ ; Table 3), but location within the plot was not significantly related to the number of flowering heads an individual produced (Row x Head Count:  $p = 0.14$ ; Position x Head Count:  $p = 0.82$ ; Table 3). Because we assigned locations to individuals randomly, this spatial variation does not affect our inferences regarding interparent distance or asynchrony.



Ordinal achene position correlated negatively with interparent asynchrony (Kendall's  $\tau = -0.22$ ,  $p < 0.001$ ) (Appendix C Figure S4). However, there was no evidence that achene position within a head improved model fit (Interparent Distance x Interparent Asynchrony vs. Interparent Distance x Interparent Asynchrony + Achene Position, Deviance = 1.06,  $df = 1$ ,  $p = 0.30$ ). Similarly, we found no evidence that start date of flowering (Julian date) of either the maternal or paternal plant improved model performance. This was true both when included in addition to interparent asynchrony (Interparent Distance x Interparent Asynchrony vs. Interparent Distance x Interparent Asynchrony + Start Date (either Maternal or Paternal), Deviance = 0.29,  $df = 1$ ,  $p = 0.59$ ) and in replacement of interparent asynchrony (Interparent Distance x Interparent Asynchrony vs. Interparent Distance x Start Date (Maternal),  $\Delta AIC = 6.8$ , Prop. AIC Weight = 0.97 vs. 0.03). Model comparisons with paternal start date indicate the same pattern ( $\Delta AIC = 7.2$ , Prop. AIC Weight = 0.97 vs. 0.03).

## DISCUSSION

The interaction between interparent distance and asynchrony exemplifies the importance of considering multiple potential dimensions of reproductive isolation simultaneously. The role of interparent asynchrony modulating the effect of interparent distance transforms interpretation of the relationship between interparent distance and offspring fitness from weak support for heterosis (Table 1), to a more nuanced understanding of how isolation in space and time may interact (Figure 2, Figure 3). Interestingly, we found that interparent distance interacted with *directional* interparent asynchrony (Table 1, Table 2). When paternal plants flowered before maternal plants, offspring fitness increased strikingly with interparent distance. In contrast, when maternal plants flowered first, offspring fitness declined with interparent distance, albeit to a lesser degree. We discuss several possible explanations for this finding below, including that it, to some extent, may reflect the relationship between directional asynchrony and parental start dates of flowering (Figure 4).

The differences between these scenarios were most apparent at large interparent distances; at small interparent distances (i.e., when mating occurred between parents from the same source populations), predicted offspring fitness varied little with respect to interparent asynchrony (i.e., the far left side of Figure 3). This may be because there is little genetic differentiation within these populations by timing of flowering; populations flower synchronously enough that most individuals have opportunities to mate, especially considering that opportunities may arise over multiple reproductive bouts. Thus, gene flow across the season could impede the formation of temporal genetic structure. Our results—that fitness effects of interparent asynchrony within populations were both small and related to directional aspects of asynchrony, rather than absolute measures that would measure isolation in time—suggests that variation in timing of flowering within populations does not reflect adaptation to isolation-by-time (H1), temporal environments across the season (H2), nor a combination of the two (H3).

In contrast, when parents' source populations were distant from one another (i.e., the far right side of Figure 3), fitness varied among offspring in relation to the asynchrony of their parents. Again, offspring fitness varied according to the extent to which the maternal plant flowered prior to the paternal plant—the directional, not absolute, difference in timing of flowering between parents. When maternal and paternal plants originated from distant source populations, offspring of maternal plants that flowered later than paternal plants had substantially higher fitness. What mechanisms could cause this surprising pattern? Below, we discuss several hypotheses that warrant further investigation.

First, (1) isolation-by-time might occur when reinforced by spatial or environmental gradients and its fitness effects evident only when aligned with directional flowering asynchrony. In distant populations, as compared to within a population, there are more opportunities for genetic divergence to occur over timing of flowering. This might occur if environmental differences associated with geographic distance could reinforce dissimilarities in timing of flowering (i.e., if divergence in timing is aligned

with environmental gradients) (Franke et al. 2006). This would be consistent with previous work showing the interaction between isolation in space and time can accelerate the formation of population genetic structure (Weis and Peters 2019). Despite this, we only found evidence that interparent asynchrony related to offspring fitness when we considered directional interparent asynchrony. Mechanisms related to directional asynchrony—such as fitness effects related to temporal resource allocation or floral architecture (Diggle 1995)—are not mutually exclusive from those related to the formation of temporal genetic structure, either through isolation-by-time or local adaptation to temporal environments. If both processes occurred, and isolation-by-time is weak, we might only detect directional effects. Specifically, we might expect to see a pattern of increasing offspring fitness with interparent asynchrony if offspring fitness increased with interparent dissimilarity in timing (i.e., heterosis, H1), but this effect was dominated by directional effects such that lower (more negative) asynchrony mating yields lower fitness offspring.

A second possible explanation for the interaction we observed is that there was a (2) relationship between floral architecture and timing of flowering that was modified by interparent distance. Offspring with high interparent asynchrony had maternal plants that flowered late and paternal plants that flowered early relative to both each other and the population (Figure 3). Because *E. angustifolia* develops sequentially from the bottom of the head to the top, these offspring tended to originate at the bottom of the maternal plant's flowering head (Appendix C Figure S4). Within *E. angustifolia*'s cone-shaped seedheads, achenes at the bottom of a head tend to be larger than achenes at the top of a head (unpublished data). As a result, high asynchrony offspring might come from larger seeds that yield higher fitness offspring due to floral architecture constraints, rather than resource allocation (Diggle 1995). However, individuals vary in their floral architecture and some populations may have less extreme gradients in seed size within a seed head. Interparent distance could modify the relationship between interparent asynchrony and offspring fitness if floral morphology differs among populations, such that the pairs of closer populations tended to have maternal plants with lower intra-head variation in seed

size. Detailed data on within-individual variation in seed size and its relationship with interparent distance would clarify whether there is support for this hypothesis. Our analysis, however, indicated that the region of the maternal seed head from which an offspring achene originated did not explain a significant portion of variance in offspring fitness.

Third, (3) flowering later might lead to higher fitness offspring due to variation in maternal resource allocation, but this relationship is modified by interparent distance. An interaction such as the one we observed might arise if the positive relationship between maternal plants' timing of flowering and offspring fitness depends upon parents' distance. For instance, maternal plants might invest more in later offspring when a pollen donor is from a distant population. Temporally variable resource allocation is common (Brunet and Charlesworth 1995). Maternal plants flowering later in the season or mating later in their flowering period may allocate resources among fewer offspring, resulting in better provisioned seeds (e.g., a seed number and resource allocation trade-off; Smith and Fretwell 1974; Venable 1992). At the same time, there is evidence that mate choice can occur through pollen-pistil interactions (Broz and Bedinger 2021; Tonnabel et al. 2021)—this includes self-recognition mechanisms that prevent self-fertilization (Bedinger et al. 2017), but may also involve more nuanced aspects of mate choice, e.g., related to pollen traits (Madjidian et al. 2020). Perhaps maternal plants allocate more resources later in the season, but only if the pollen is sufficiently distinguishable, as it may be if it originates from an individual from a more distant source population. An experimental crossing design to assess pollen-pistil interactions and how these vary depending on the distance from the pollen source and time of season could clarify the possibility of this mechanism. However, we note that we did not find any evidence that including maternal plant's start date of flowering in addition to or replacement of interparent asynchrony improved our model of offspring fitness, suggesting that the effect of directional interparent asynchrony is not reducible to the maternal plant's timing of flowering.

Finally, timing could be non-causal and associated with offspring fitness simply through correlation with (4) fitness effects associated with maternal plant or population identity. It might not be asynchrony *per se* but rather the identity of populations or specific maternal plants that led to fitness effects when considered in interaction with interparent distance (Appendix C Figure S3). For instance if mating between certain distant populations that differed in timing of flowering produced particularly high fitness offspring, we might expect results similar to what we found. Did offspring fitness vary among source population pairs of the maternal or paternal plants, such that we might have observed an association between offspring fitness and asynchrony when the distance between parental source populations was large? Because the offspring in our study resulted from open pollination, not a balanced crossing design, and the 37 maternal lines in ExPt2 were not selected based on source population, we lacked the replication of source population pairings necessary to answer to this question rigorously. Only a single maternal or paternal individual represented some populations, preventing us from disentangling population and parental effects. Furthermore, the populations with the highest flowering asynchrony were not more isolated from other populations; overall, interparent asynchrony and interparent distance were not correlated (Appendix C Figure S2E).

### *Conservation Implications*

Our finding that, overall, offspring fitness increased with interparent distance indicates that more distant cross-population mating has a positive effect on *E. angustifolia* fitness within our study area; however, the average positive effect of distance was of a smaller magnitude than the interaction with asynchrony. These results suggest that efforts to enhance habitat connectivity or gene flow in the area would be beneficial, particularly if it were possible to facilitate outcrossing between late flowering maternal plants and early flowering pollen donors. Common methods to enhance habitat connectivity for plants include designing landscapes to facilitate pollinator movement, such as through the installation of hedgerows or habitat corridors in agricultural

landscapes (e.g., Kormann et al. 2016; Minnesota Prairie Plan Working Group 2011), while gene flow can be more directly promoted through seeding. In particular, using a “regional admixture” approach to seed sourcing—i.e., sowing seeds from nearby populations—could have a similar effect to improving habitat connectivity (Rushing et al. 2021). All the populations considered in this study are relatively near to each other (<10 km) and are subject to no obvious environmental gradients. The standards of most seed sourcing guidelines would treat even the populations separated by the greatest distance in our study to be “local” or a single source. Outbreeding depression is more likely at larger spatial scales. For instance, annual average precipitation ranges from the 40 cm that the western edge of *E. angustifolia*’s range receives to 62 cm in our study area, near the eastern edge of the range (Dykstra 2013). Study across the geographic scale of seed sourcing boundaries would be necessary to provide insight to the question where to source seeds for ecological restorations.

We can envision several strategies one might take to either promote mating between late flowering maternal and early flowering paternal individuals or to source seeds from high asynchrony mating events. High interparent asynchrony correlated with maternal plants flowering late relative to the entire population (Figure 4); one could visit a population late in its flowering period to flag still-flowering individuals to target for seed collection. Additionally, one could screen seed lots for diversity of flowering phenology; whereas this would not prevent mating between individuals with low or intermediate asynchrony, it could improve the chances of mating with high positive asynchrony. Similarly, one could attempt to increase the chances of mating between plants that would typically flower too early or too late to mate with one another by increasing reproductive synchrony of the population as a whole. For example, in our populations, spring fires increase reproductive synchrony at the population level (Wagenius et al. 2020). Individuals that do not overlap in flowering time in a non-burn year might be more likely to do so following a burn. Collecting seeds after a spring burn, especially from maternal plants that were relatively late flowering, could help improve

chances that offspring represent a temporally diverse and potentially high fitness pedigree.

### *Caveats*

We note three caveats to our findings. First, our metric of asynchrony may not precisely represent temporal genetic differentiation for several reasons. The degree of isolation in time between two plants is a somewhat ambiguous quantity. Despite a substantial genetic basis for variance in start date of flowering ( $h^2 = \sim 0.15-0.2$ ; Reed et al. 2022), environmental effects, as well as genotype-by-environment effects, contribute to variation in flowering time within and among years. Thus, the difference in start date between two individuals in one year may only weakly correspond to their difference in another, or their genetic distinctiveness. Second, fitness estimates based on the beginning of individuals' lives does not perfectly capture variation in lifetime fitness. Even so, this study does measure variation in reproductive effort over sixteen years. Moreover, *E. angustifolia* in our study area may reproduce less frequently with increasing age (unpublished data), suggesting that our study includes individuals' most productive reproductive years. Third, this study uses the number of flowering heads that individuals produce—a measure of reproductive effort, rather than reproductive success—as a proxy for reproductive success and does not account for offspring fitness through pollen export (i.e., male fitness). However, we defend this choice, as artificially high density of flowering within the experimental plot could mean that measures of offspring production (i.e., seed set) could be less informative than individuals' capacity for reproductive effort.

### CONCLUSIONS

This study builds on our prior efforts to describe *E. angustifolia* mating patterns in space and time. Previously, we found that mate availability varies dramatically in time (Waananen et al. 2018) and pollinator visitation rates to *E. angustifolia* are sensitive to both flowering phenology and density (Ison et al. 2018). Mating occurs most often between plants that are close together and flower synchronously (Ison et al. 2014). Here,

we show that the offspring of parents that are close together and flower synchronously tend to have relatively low fitness offspring. Because previous work has shown that early flowering maternal plants have the greatest number of offspring (Ison and Wagenius 2014), our finding here that later flowering maternal plants tended to produce higher fitness offspring (at least when mating with distant partners) implies a trade-off between offspring quantity and quality. This finding adds to mounting evidence that accounting for fitness effects of outcrossing and gene flow is critical for accurately predicting its frequency and effects (Edelaar and Bolnick 2012). Thus, characterizing both mating patterns in terms of parents' spatial and temporal isolation and their consequences for offspring fitness helps to advance an integrative perspective of outcrossing in plants (Fenster 1991a,b). Further experimental study would advance understanding of the causal pathway(s) between the interaction of interparent distance and asynchrony leading to offspring fitness effects.

#### ACKNOWLEDGEMENTS

A. Waananen contributed to data collection of offspring fitness, designed the analysis, analyzed the data, and wrote the manuscript. S. Wagenius and J. Ison established of ExPt1 and ExPt2 and collected parental phenology data and J. Ison performed the molecular lab work for paternity analysis of the offspring in ExPt2. R. Shaw contributed to the design of the analysis and S. Wagenius, J. Ison, and R. Shaw all contributed to manuscript revisions. This work was possible because landowners, including the Pope Douglas Public Waste Board, The Nature Conservancy, and the Fish and Wildlife Service, along with several private individuals, including J. and D. Wagenius, allowed access to their property. Numerous members of Team Echinacea from 2007-2022 contributed to the fitness measurements of offspring and several contributed to data management, especially G. Kiefer, M. Stevens, and L. Paulsen.



## ILLUSTRATIONS

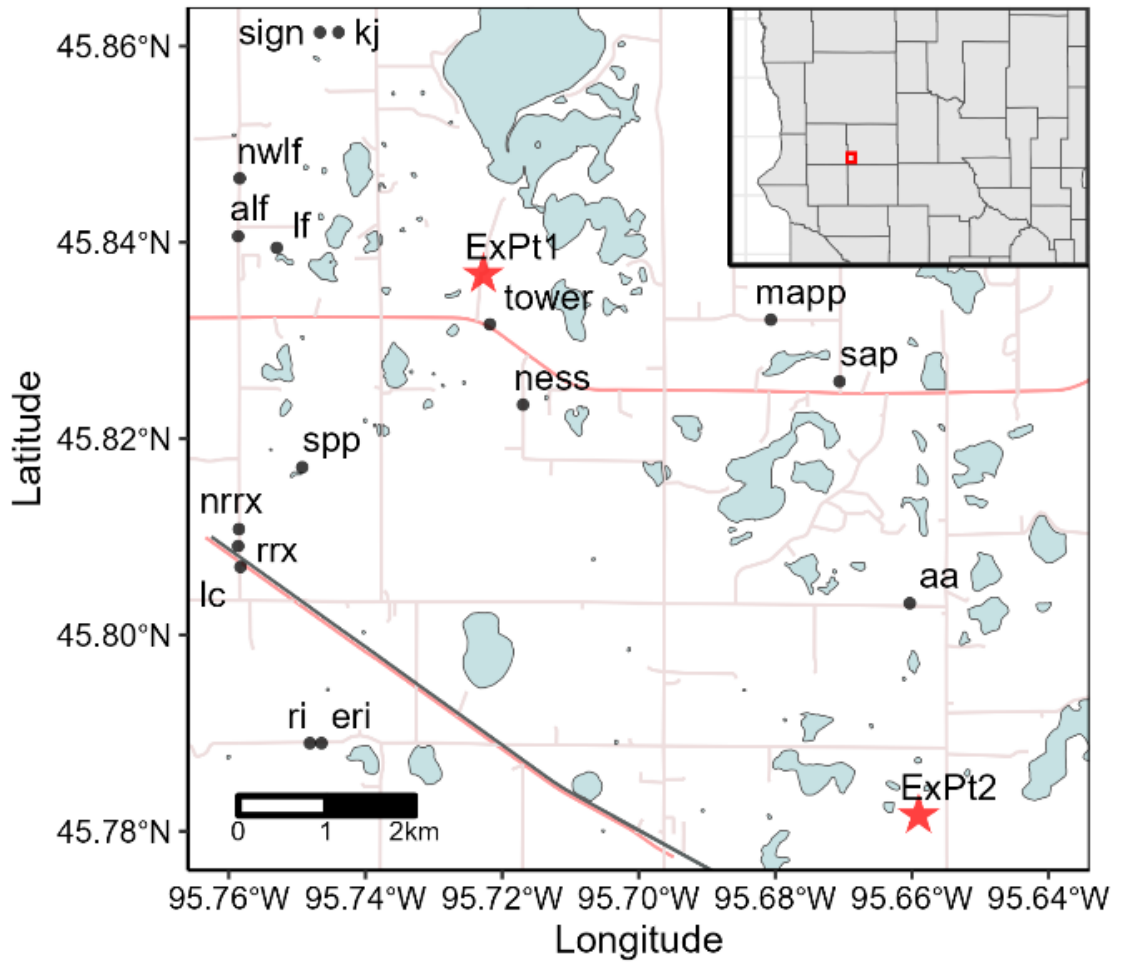


Figure 1. Map of the study area and sites in west central Minnesota, USA. The location of the experimental plots are indicated with stars, while source populations are labeled with points. Water (polygons), highways (thick lines), and streets (light lines) are from OpenStreetMaps.

Table 1. Model selection results for models of interparent asynchrony and interparent distance separately. Each row represents a candidate model: its predictors (in addition to the null model, as described below), AIC, difference between AIC and the lowest AIC of all candidate models ( $\Delta$ AIC), the Akaike weight ('Weight'), which is proportional to the probability that the model is the best of the set of candidate models, and proportional Akaike model weights (Prop. Weight). All models included predictors for location within the plot (row and position) on the different types of fitness components (or 'layers': ld, fl, hdCt) and had the structure:  $\text{resp} \sim \text{varb} + \text{layer} : (\text{row} + \text{position}) + \text{fit} : (\dots)$ , where ' $\dots$ ' is indicated by the covariates in the 'Predictors' column. The bolded row indicates the best-performing model.

Hypothesis	Predictors	No. Par	AIC	$\Delta$ AIC	Weight	Prop. Weight
<i>Asynchrony</i>						
Null	None	43	5007.13	2.64	0.27	0.19
<b>Directional Effects (H4)</b>	<b>+ Asynchrony</b>	<b>44</b>	<b>5004.49</b>	<b>0</b>	<b>1</b>	<b>0.70</b>
Heterosis (+) (H1) or Outbreeding Depression (-) (H2)	+  Asynchrony	44	5009.13	4.64	0.10	0.07
Intermediate Optimum (H3)	+  Asynchrony  + Asynchrony <sup>2</sup>	45	5010.36	5.87	0.05	0.04
<i>Distance</i>						
Null	None	43	5007.13	10.87	0.004	0.004
<b>Heterosis (+) (H1) or Outbreeding Depression (-) (H2)</b>	<b>+ Distance</b>	<b>44</b>	<b>4996.26</b>	<b>0</b>	<b>1</b>	<b>0.99</b>
Intermediate Optimum (H3)	+ Distance <sup>2</sup>	44	5009.01	12.74	0.001	0.002

Table 2. Results from likelihood ratio tests comparing nested models that included the final terms selected for interparent asynchrony and interparent distance, as indicated by AIC analysis (Table 1), and their interaction. Comparisons test the null hypothesis that a reduced model performs as well as a more complex one by comparing the difference in deviance (a goodness-of-fit measure) between nested models ( $\Delta$  Deviance) to a  $\chi^2$  distribution with degrees of freedom equal to the difference in degrees of freedom between the two models ('Df'). ' $P(\chi_{Df}^2 > \Delta \text{ Deviance})$ ' indicates the probability of a value from  $\chi_{Df}^2$  greater than  $\Delta$  Deviance.

Pairwise Model Comparison	Df	$\Delta$ Deviance	$P(\chi_{Df}^2 > \Delta \text{ Deviance})$	Interpretation
Interactive vs. Additive	1	5.55	0.02	Interactive > Additive
Additive vs. Asynchrony Only	1	13.1	< 0.001	Additive > Async. Only
Additive vs. Distance Only	1	4.87	0.03	Additive > Dist. Only

Table 3. Summary of the final model of offspring fitness, which included an interaction between interparent distance and asynchrony ('Interactive'; Table 2). The graphical model also includes terms for each life-history node (Supplemental Figure 1); for simplicity, we omit those terms here. The model terms of primary interest are bolded.

	Estimate	Std. Error	z value	Pr(> z )	Signif.
Row x Survival	0.001	0.0005	2.585	0.01	**
Position x Survival	-0.003	0.0007	-4.439	<0.001	***
Row x Flowering	-0.019	0.0035	-5.354	<0.001	***
Position x Flowering	-0.0006	0.0051	-0.114	0.91	
Row x Head Count	-0.0024	0.0016	-1.486	0.14	
Position x Head Count	0.0005	0.0023	0.223	0.82	
<b>Distance</b>	0.0645	0.0199	3.239	0.001	**
<b>Asynchrony</b>	0.0054	0.0043	1.262	0.21	
<b>Distance x Asynchrony</b>	0.0102	0.0044	2.348	0.02	*

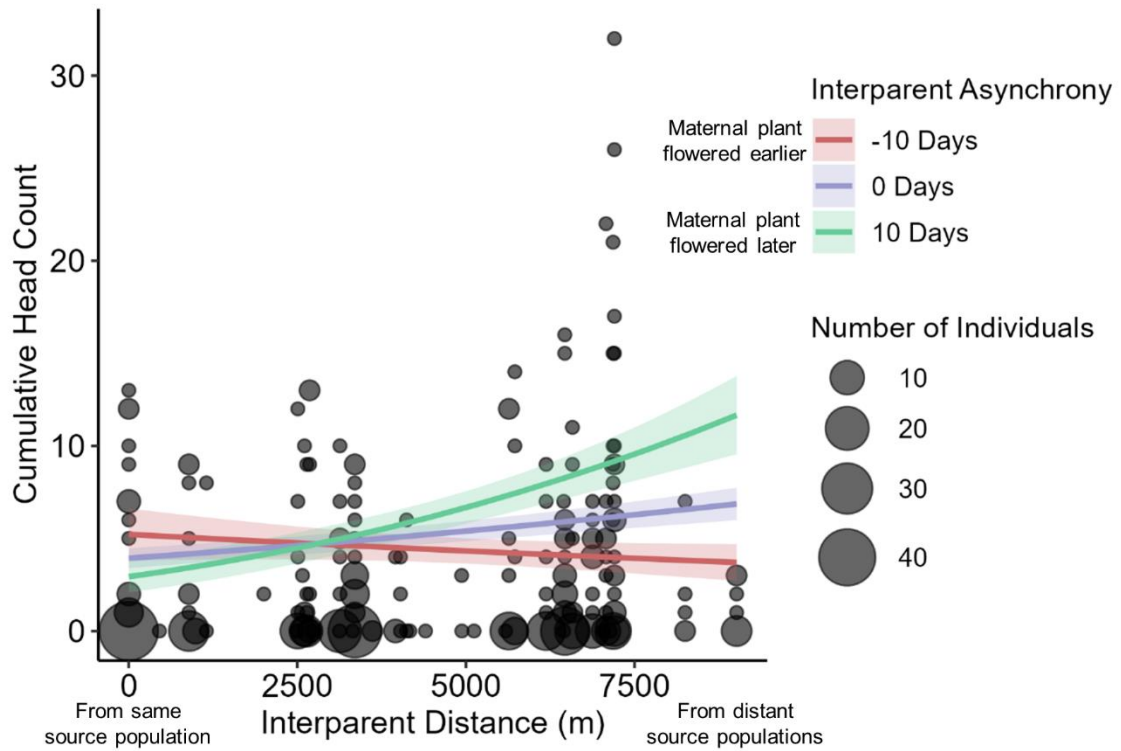


Figure 2. Effect plot of the predicted relationship between interparent distance and offspring fitness (cumulative head count) generated from the best-performing model (+ Interparent Asynchrony \* Interparent Distance; Table 1). Predictions are for hypothetical individuals located at Row 5 and Position 5 (located 5 m away from the edge of the plot). Lines show predicted fitness over the range of interparent distance, with lines representing predictions for individuals at three levels of interparent asynchrony (maternal start date minus paternal start date): -10 days, 0 days, and 10 days. Points indicate the cumulative head counts of offspring with corresponding interparent distances observed in our study; point size scales with the number of offspring with each pair of values.

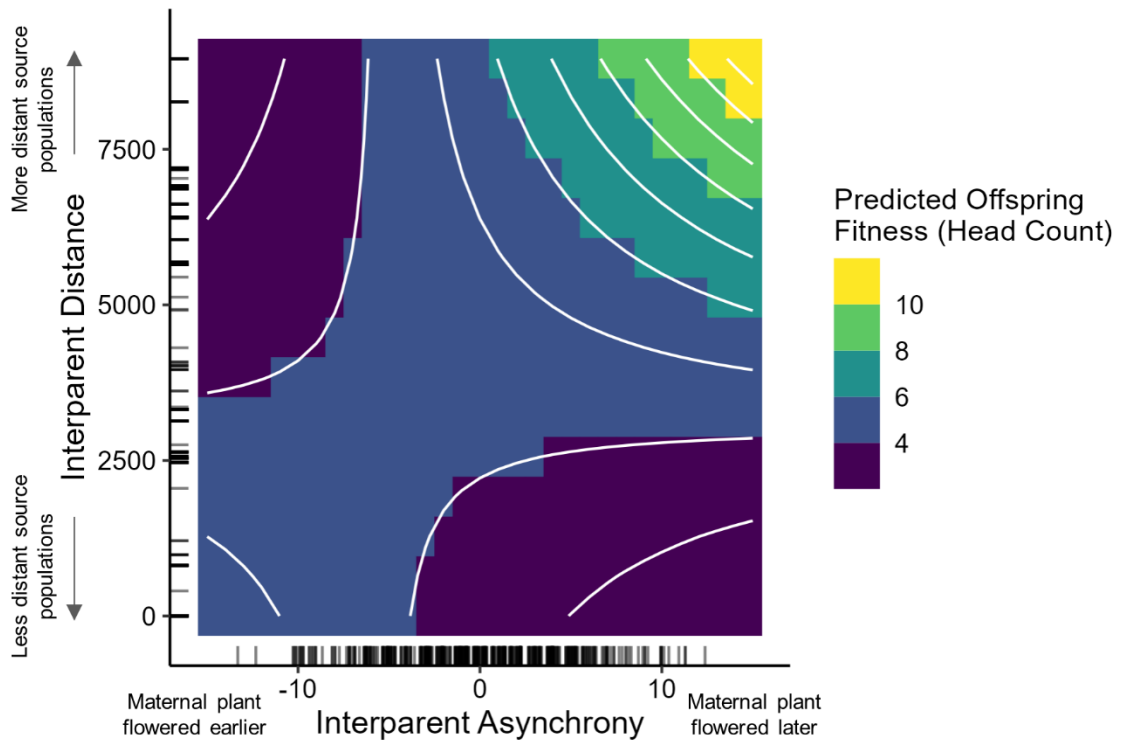


Figure 3. Predicted fitness contours across the range of observed interparent distances and asynchronies. Specifically, offspring fitness is an individual's predicted cumulative head count. Contours are spaced at increments of one offspring flowering head. Hatches along the x and y-axes indicate observed values and are slightly transparent to improve visualization with overplotting (in addition, see histograms of observed data in Supplemental Figure 2).

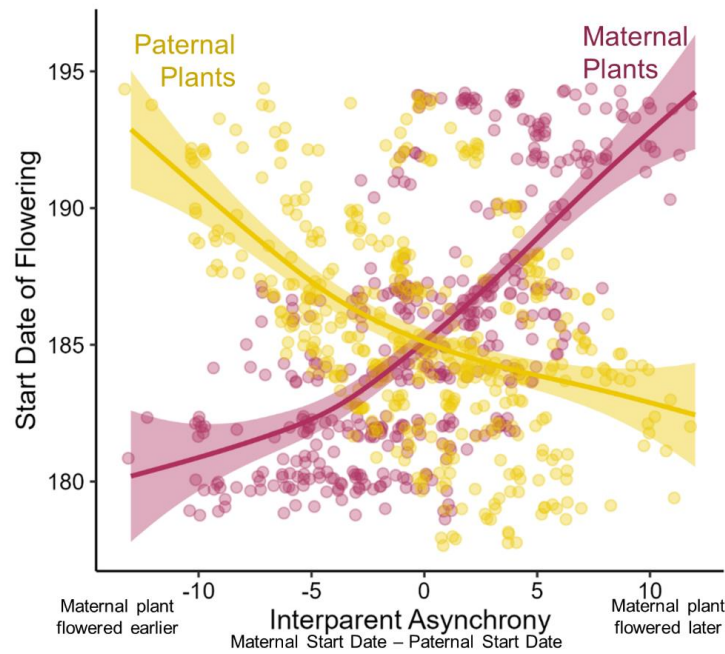


Figure 4. Interparental asynchrony correlated with the start date of flowering (Julian date of year) of the maternal and paternal plants. Points represent the parents of each offspring included in the analysis (maternal plants shown in maroon and paternal plants in gold) and are jittered to avoid overplotting. Trendlines show generalized additive models for the maternal and paternal plants' timing of flowering. This shows that at negative values of interparental asynchrony (i.e., when the maternal plant began flowering before the paternal plant), maternal plants were early-flowering relative to the population and paternal plants were late-flowering relative to the population, and vice versa for large values of interparental asynchrony.

## BIBLIOGRAPHY

- Ahmed, S., S. G. Compton, R. K. Butlin, P. M. Gilmartin, and E. A. Herre. 2009. Wind-borne insects mediate directional pollen transfer between desert fig trees 160 kilometers apart. *Proc. Natl. Acad. Sci.* 106:20342–20347.
- Akaike, H. 1974. A new look at the statistical model identification. *IEEE Trans. Automat. Contr.* 19:716–723. Ieee.
- Ashman, T.-L., and I. Baker. 1992. Variation in floral sex allocation with time of season and currency. *Ecology* 73:1237–1243.
- Bedinger, P. A., A. K. Broz, A. Tovar-Mendez, and B. McClure. 2017. Pollen-pistil interactions and their role in mate selection. *Plant Physiol.* 173:79–90. American Society of Plant Biologists.
- Billingham, M. R., T. Simoes, T. B. H. Reusch, and E. A. Serrao. 2007. Genetic sub-structure and intermediate optimal outcrossing distance in the marine angiosperm *Zostera marina*. *Mar. Biol.* 152:793–801.
- Broz, A. K., and P. A. Bedinger. 2021. Pollen-pistil interactions as reproductive barriers. *Annu. Rev. Plant Biol.* 72:615–639. Annual Reviews.
- Brunet, J., and D. Charlesworth. 1995. Floral sex allocation in sequentially blooming plants. *Evolution (N. Y.)*. 49:70–79.
- Caruso, C. M., A. M. Benschoter, N. V. Gale, E. K. Seifert, E. R. Mills, and A. L. Case. 2015. Effects of crossing distance on performance of the native wildflower *Lobelia siphilitica*: Implications for ecological restoration. *J. Torrey Bot. Soc.* 142:140–151.
- Castilla, A. R., N. S. Pope, M. O’Connell, M. F. Rodriguez, L. Treviño, A. Santos, and S. Jha. 2017. Adding landscape genetics and individual traits to the ecosystem function paradigm reveals the importance of species functional breadth. *Proc. Natl. Acad. Sci.* 201619271.
- Diggle, P. K. 1995. Architectural effects and the interpretation of patterns of fruit and seed development. *Annu. Rev. Ecol. Syst.* 26:531–552.
- Dykstra, A. B. 2013. Seedling Recruitment in Fragmented Populations of *Echinacea angustifolia*. University of Minnesota.
- Edelaar, P., and D. I. Bolnick. 2012. Non-random gene flow: an underappreciated force in evolution and ecology. *Trends Ecol. Evol.* 27:659–665.

- Edmands, S. 1999. Heterosis and outbreeding depression in interpopulation crosses spanning a wide range of divergence. *Evolution*. 53:1757–1768.
- Feghahati, S. M. J., and R. N. Reese. 1994. Ethylene-, light-, and prechill-enhanced germination of *Echinacea angustifolia* seeds. *J. Am. Soc. Hortic. Sci.* 119:853–858.
- Fenster, C. B. 1991a. Gene flow in *Chamaecrista fasciculata* (Leguminosae) I. Gene dispersal. *Evolution*. 45:398–409.
- Fenster, C. B. 1991b. Gene flow in *Chamaecrista fasciculata* (Leguminosae) II. Gene establishment. *Evolution*. 45:410–422.
- Franke, D. M., A. G. Ellis, M. Dharjwa, M. Freshwater, M. Fujikawa, A. Padron, and A. E. Weis. 2006. A steep cline in flowering time for *Brassica rapa* in Southern California: population-level variation in the field and the greenhouse. *Int. J. Plant Sci.* 167:83–92.
- Geber, M. A., and L. R. Griffen. 2003. Inheritance and natural selection on functional traits. *Int. J. Plant Sci.* 164:S21--S42.
- Geyer, C. J., S. Wagenius, and R. G. Shaw. 2007. Aster models for life history analysis. *Biometrika* 94:415–426.
- Gibbs, P. E. 2014. Late-acting self-incompatibility—the pariah breeding system in flowering plants. *New Phytol.* 203:717–734.
- Greenleaf, S. S., N. M. Williams, R. Winfree, and C. Kremen. 2007. Bee foraging ranges and their relationship to body size. *Oecologia* 153:589–596.
- Hendry, A. P., and T. Day. 2005. Population structure attributable to reproductive time: isolation by time and adaptation by time. *Mol. Ecol.* 14:901–916.
- Herrera, J. 1991. Allocation of reproductive resources within and among inflorescences of *Lavandula stoechas* (Lamiaceae). *Am. J. Bot.* 78:789–794. Wiley Online Library.
- Ison, J. L. 2010. Pollination of *Echinacea angustifolia*: effects of flowering phenology and spatial isolation. University of Illinois at Chicago.
- Ison, J. L., L. J. Prescott, S. W. Nordstrom, A. Waananen, and S. Wagenius. 2018. Pollinator-mediated mechanisms for increased reproductive success in early flowering plants. *Oikos* 127:1657–1669.



- Ison, J. L., and S. Wagenius. 2014. Both flowering time and distance to conspecific plants affect reproduction in *Echinacea angustifolia*, a common prairie perennial. *J. Ecol.* 102:920–929.
- Ison, J. L., S. Wagenius, D. Reitz, and M. V. Ashley. 2013. Development and evaluation of microsatellite markers for a native prairie perennial, *Echinacea angustifolia* (Asteraceae). *Appl. Plant Sci.* 1:1300049.
- Ison, J. L., S. Wagenius, D. Reitz, and M. V. Ashley. 2014. Mating between *Echinacea angustifolia* (Asteraceae) individuals increases with their flowering synchrony and spatial proximity. *Am. J. Bot.* 101:180–189.
- Ison, J. L., and A. E. Weis. 2017. Temporal population genetic structure in the pollen pool for flowering time: A field experiment with *Brassica rapa* (Brassicaceae). *Am. J. Bot.* 104:1569–1580.
- Jha, S., and C. W. Dick. 2010. Native bees mediate long-distance pollen dispersal in a shade coffee landscape mosaic. *Proc. Natl. Acad. Sci.* 107:13760–13764.
- Keller, L. F., and D. M. Waller. 2002. Inbreeding effects in wild populations. *Trends Ecol. Evol.* 17:230–241.
- Kormann, U., C. Scherber, T. Tschardtke, N. Klein, M. Larbig, J. J. Valente, A. S. Hadley, and M. G. Betts. 2016. Corridors restore animal-mediated pollination in fragmented tropical forest landscapes. *Proc. R. Soc. B Biol. Sci.* 283.
- Levin, D. A., and H. Kerster. 1969. Density-Dependent Gene Dispersal in *Liatris*. *Am. Nat.* 103:61–74.
- Lloyd, D. G. 1980. Sexual strategies in plants. *New Phytol.* 86:69–79.
- Madjidian, J. A., H. G. Smith, S. Andersson, and Å. Lankinen. 2020. Direct and indirect selection on mate choice during pollen competition: Effects of male and female sexual traits on offspring performance following two-donor crosses. *J. Evol. Biol.* 33:1452–1467.
- Malagon, D. A., M. D. Roche, R. M. McElderry, and S. Kalisz. 2019. Pollen performance decreases with plant age for outcrosser but not selfer: evidence for cost of male performance. *Am. J. Bot.* 106:1271–1278.
- Marshall, D. L., J. J. Avritt, S. Maliakal-Witt, J. S. Medeiros, and M. G. M. Shaner. 2010. The impact of plant and flower age on mating patterns. *Ann. Bot.* 105:7–22.

Marshall, D. L., J. Reynolds, N. J. Abrahamson, H. L. Simpson, M. G. Barnes, J. S. Medeiros, S. Walsh, D. M. Oliveras, and J. J. Avritt. 2007. Do differences in plant and flower age change mating patterns and alter offspring fitness in *Raphanus sativus* (Brassicaceae)? *Am. J. Bot.* 94:409–418.

McCall, C., T. Mitchell-Olds, and D. M. Waller. 1991. Distance between mates affects seedling characters in a population of *Impatiens capensis* (Balsaminaceae). *Am. J. Bot.* 78:964–970.

Mitchell-Olds, T., and R. G. Shaw. 1987. Regression analysis of natural selection: statistical inference and biological interpretation. *Evolution.* 41:1149–1161.

Page, M. L., J. L. Ison, A. L. Bewley, K. M. Holsinger, A. D. Kaul, K. E. Koch, K. M. Kolis, and S. Wagenius. 2019. Pollinator effectiveness in a composite: a specialist bee pollinates more florets but does not move pollen farther than other visitors. *Am. J. Bot.* 106:1487–1498.

Pasquet, R. S., A. Peltier, M. B. Hufford, E. Oudin, J. Saulnier, L. Paul, J. T. Knudsen, H. R. Herren, and P. Gepts. 2008. Long-distance pollen flow assessment through evaluation of pollinator foraging range suggests transgene escape distances. *Proc. Natl. Acad. Sci.* 105:13456–13461.

Pelabon, C., M. L. Carlson, T. F. Hansen, and W. S. Armbruster. 2005. Effects of crossing distance on offspring fitness and developmental stability in *Dalechampia scandens* (Euphorbiaceae). *Am. J. Bot.* 92:842–851.

Peters, M. A. E., and A. E. Weis. 2019. Isolation by phenology synergizes isolation by distance across a continuous landscape. *New Phytol.* 224:1215–1228.

Price, M. V., and N. M. Waser. 1979. Pollen dispersal and optimal outcrossing in *Delphinium nelsoni*. 227:294–297.

Reed, W. J., J. L. Ison, A. Waananen, F. H. Shaw, S. Wagenius, and R. G. Shaw. 2022. Genetic variation in reproductive timing in a long-lived herbaceous perennial. *Am. J. Bot.* 109:1861–1874.

Rushing, N. S., S. A. Flint, and R. G. Shaw. 2021. Latitude of seed source impacts flowering phenology and fitness in translocated plant populations. *Restor. Ecol.* 29:e13464.

Sexton, J. P., S. B. Hangartner, and A. A. Hoffmann. 2014. Genetic isolation by environment or distance: Which pattern of gene flow is most common? *Evolution.* 68:1–15.

Shaw, R. G., C. J. Geyer, S. Wagenius, H. H. Hangelbroek, and J. R. Etterson. 2008. Unifying life-history analyses for inference of fitness and population growth. *Am. Nat.* 172:E35-47.

Smith, C. C., and S. D. Fretwell. 1974. The optimal balance between size and number of offspring. *Am. Nat.* 108:499–506.

Tonnabel, J., P. David, T. Janicke, A. Lehner, J.-C. Mollet, J. R. Pannell, and M. Dufay. 2021. The scope for postmating sexual selection in plants. *Trends Ecol. Evol.* 36:556–567.

Tsitrone, A., J. Philippe, and P. David. 2003. Delayed selfing and resource reallocations in relation to mate availability in the freshwater snail *Physa acuta*. *Am. Nat.* 162: 474-488.

Venable, D. L. 1992. Size-number trade-offs and the variation of seed size with plant resource status. *Am. Nat.* 140:287–304.

Waananen, A., G. Kiefer, J. L. Ison, and S. Wagenius. 2018. Mating opportunity increases with synchrony of flowering among years more than synchrony within years in a nonmasting perennial. *Am. Nat.* 192:379–388.

Wadgymar, S. M., and A. E. Weis. 2017. Phenological mismatch and the effectiveness of assisted gene flow. *Conserv. Biol.* 31:547–558.

Wagenius, S. 2000. Performance of a prairie mating system in fragmented habitat: self-incompatibility and limited pollen dispersal in *Echinacea angustifolia*. University of Minnesota.

Wagenius, S., J. Beck, and G. Kiefer. 2020. Fire synchronizes flowering and boosts reproduction in a widespread but declining prairie species. *Proc. Natl. Acad. Sci.* 117:3000–3005.

Wagenius, S., H. H. Hangelbroek, C. E. Ridley, and R. G. Shaw. 2010. Biparental inbreeding and interremnant mating in a perennial prairie plant: fitness consequences for progeny in their first eight years. *Evolution.* 64:761–771.

Wagenmakers, E.-J., and S. Farrell. 2004. AIC model selection using Akaike weights. *Psychon. Bull. Rev.* 11:192–196.

Wang, H., Z. Zhang, B. Zhang, L. Wang, W. Guo, Y. Fang, and Q. Li. 2022. Architectural effects regulate resource allocation within the inflorescences with nonlinear blooming patterns. *Am. J. Bot.* 109:1191–1202.

Waser, N. M., M. V Price, and R. G. Shaw. 2000. Outbreeding depression varies among cohorts of *Ipomopsis aggregata* planted in nature. *Evolution*. 54:485–491.

Waser, N. M., and C. F. Williams. 2001. Inbreeding and outbreeding. *Evol. Ecol. Concepts Case Stud.* 84–96.

Watson, M. A., and B. B. Casper. 1984. Morphogenetic constraints on patterns of carbon distribution in plants. *Annu. Rev. Ecol. Syst.* 15:233–258.

Weis, A. E., and T. M. Kossler. 2004. Genetic variation in flowering time induces phenological assortative mating: Quantitative genetic methods applied to *Brassica rapa*. *Am. J. Bot.* 91:825–836.

Wright, S. 1943. Isolation by Distance. *Genetics* 28:114–138.

Wyatt, R. 1982. Inflorescence architecture: how flower number, arrangement, and phenology affect pollination and fruit-set. *Am. J. Bot.* 69:585–594.

## CHAPTER 3

High juvenile mortality overwhelms benefits of mate density for reproductive fitness

### SYNOPSIS

An individual's access to mates (i.e., its 'mating potential') can constrain its reproduction, but may also influence its fitness through effects on offspring survival. For instance, mate proximity may be associated with relatedness and consequent inbreeding depression in offspring. While offspring production and survival might respond differently to mating potential, heretofore, studies have not considered the simultaneous effects of mating potential on these fitness components. We investigated the relationship of mating potential with both the production and survival of offspring in populations of a long-lived herbaceous perennial, *Echinacea angustifolia*. Across seven years and 14 sites, we quantified the mating potential of maternal plants in 1278 mating bouts and followed the offspring from these bouts over eight subsequent years. We used aster models to evaluate the relationship of mating potential with the number of offspring that emerged and that were alive after eight years. Seedling emergence increased with mating potential. Despite this, the number of offspring surviving after eight years showed no relationship to mating potential. Low seedling emergence, high juvenile mortality, and the small magnitude of fitness differences at the end of the study were consistent with demographic stochasticity at the maternal plant level eroding the effect of mating potential over time.

## INTRODUCTION

Mating potential, defined as the abundance and proximity of potential mates, constrains the reproductive success of sexually reproducing plants, especially those that are self-incompatible and live in small populations (e.g., Wagenius et al. 2020; reviewed in Gascoigne et al. 2009). However, mating potential may also affect offspring viability. For example, if a population is structured such that relatedness increases with the proximity of reproductive individuals, resulting in increased inbreeding of offspring (Wright 1943), then a plant with many closely related mates nearby might have high mating potential in a low-quality mating pool. Alternatively, an abundance of potential mates could correspond with a diverse mating pool that could contribute to the production of more robust offspring. While many studies have assessed the effects of mating potential on seed production (e.g., Wagenius 2007), few track the fate of seeds to emergence, and fewer still beyond that, particularly in natural environments (Aguilar et al. 2019).

Studies that investigate the fitness consequences of mating potential commonly focus on its relationship with initial measures of reproductive success, such as pollination rates or fecundity, as fitness proxies. Fitness comprises multiple components that link an individual's mating success and fecundity to the production of viable offspring, but complete fitness accounts are notoriously difficult to obtain, particularly for long-lived plants. Later measurements of lifetime reproductive success, such as the number of offspring that survive to adulthood, undoubtedly yield more precise fitness estimates than early measures. What remains unclear, however, is whether early fitness proxies provide a coarse but reliable representation of fitness and its association with mating potential, or a misleading one. Early measures of reproductive success may not reliably indicate the fitness consequences of factors linked to mating success, for instance, if high juvenile mortality equalizes differences between maternal plants with variable reproductive output (Price et al. 2008; Campbell et al. 2017) or if trade-offs between the number of offspring and parental investment in each favor intermediate fecundity (Smith and Fretwell 1974).

Thus, early proxies for reproductive success, such as seed production and seedling emergence, may inaccurately reflect the fitness effects of mating potential.

Mating potential could affect separate fitness components differently in both direction and magnitude. For example, mating potential may have opposing consequences for offspring production and survival if high mating potential, i.e., access to mates, increases offspring production, but the resulting high competition among offspring reduces survival (Waser et al. 2010). In contrast, distinct effects of mating potential on separate fitness components in the same direction could compound. For example, inbred plants might initially grow to a smaller size or more slowly than non-inbred neighbors and then suffer further disadvantages from reduced access to light (Schmitt and Ehrhardt 1990). Finally, mating potential may influence one fitness component but have no effect on another. For instance, mating potential might increase the number of seedlings that emerge following a mating bout, but have no relationship with the survival of these offspring as juveniles. In this case, the initial fitness advantage (i.e., in offspring abundance) that a maternal plant with high mating potential has over one with low mating potential after a mating bout could persist or erode over time, depending on rates of juvenile mortality and demographic stochasticity at the level of maternal plants' 'clutches.' This outcome would be consistent with evidence that luck, especially related to early life-history stages, can decide fitness differences more than differences in fitness-related traits among individuals (Snyder and Ellner 2018; Snyder et al. 2020).

The goal of this study was to investigate the separate and joint effects of mating potential on an early and later measure of fitness: offspring emergence and offspring persistence following eight years, respectively. Our primary questions were: Does mating potential influence fitness components downstream from seed production? If so, does mating potential's relationship with early and late fitness components differ, leading to amplification, dampening, or negation of its overall effect? If mating potential affects

early fitness components but not later ones, how quickly do the effects of mating potential on fitness erode?

To investigate these questions in a long-lived species, we focus on components of maternal fitness, i.e., the number of offspring produced via seed, rather than via pollen export. In each summer 2006-2012, we mapped locations of all individual flowering plants in natural populations of *Echinacea angustifolia* at 14 sites in western Minnesota. Previous studies in this system found that pollination success and seed production vary with mating potential (Wagenius 2006; Ison and Wagenius 2014; Richardson et al. 2021), but did not assess offspring emergence and survival. In each spring 2007-2013, we searched for seedlings around plants in each site that had flowered the previous season, totaling 1278 observations of maternal plant mating bouts. We then tracked the survival of each year's offspring cohort for the next eight years. We used aster models (Shaw et al. 2008) to partition the effects of mating potential on maternal fitness into independent effects on progeny emergence and survival. To gain intuition for our results, we developed a model to delineate conditions under which demographic stochasticity at the maternal plant level will overwhelm initial fitness differences, such as those due to mating potential.

## MATERIALS AND METHODS

### Study Area and Organism

*Echinacea angustifolia* is a perennial forb native to the North American tallgrass prairie. We studied natural *E. angustifolia* populations in Grant and Douglas Counties, Minnesota, USA, where remnants of tallgrass prairie habitat persist in areas such as nature preserves and along road and rail rights-of-way. Of the sites in this study, six are located within roadside rights-of-way, three are on land managed by the U.S. Fish and Wildlife Service, four are on private property, and one is within a preserve managed by The Nature Conservancy. *Echinacea angustifolia* is long-lived and slow growing with an estimated generation time of 21 years in our study area (Dykstra 2013). Under natural



conditions, plants rarely flower before their seventh year (Wagenius et al. 2012), after which they may not flower every year. Individuals typically produce one composite flowering head (capitulum), but we have observed individuals with up to 20 heads (Wagenius et al. 2020). Flowering rates vary among populations and years, resulting in variation in plants' access to mates (Waananen et al. 2018; Wagenius et al. 2020; Nordstrom et al. 2021). Because *E. angustifolia* is tap-rooted and does not spread clonally, its reproduction depends upon seed production (Wagenius 2004; Wagenius et al. 2007). Previous work in our study area has found that seed set is limited by the abundance and proximity of suitable mates, rather than by visits from pollinators, which are primarily generalist bees (Wagenius 2006; Wagenius and Lyon 2010; Ison and Wagenius 2014; Richardson et al. 2021). Flowering stems of *E. angustifolia* are typically 30-60 cm in height; its fruits (achenes) are gravity-dispersed and do not form a persistent seed bank (Wagenius et al. 2012).

### Measuring Mating Potential

Each summer from 2006 to 2012, we surveyed sites for flowering *E. angustifolia*. We obtained coordinates for each flowering plant using a survey station in 2006-2011 and a TopCon GRS-1 Device in 2012, both of which offer <1 cm precision. We counted the number of flowering heads (defined as heads that successfully produced pollen) that each individual produced. We quantified mating potential as the weighted sum of the distances between a focal plant and its seven nearest potential mates.

Specifically, we calculated a weighted sum of the distances between a focal maternal plant and its  $k = 1-7^{\text{th}}$  nearest flowering conspecific neighbors (i.e., its likely pollen sources). The relationship between 1- $k$ th nearest neighbors and reproductive success (seed set) varies little between  $k = 2$  and  $k = 18$  (Wagenius 2006), suggesting that the results of this analysis should not be sensitive to the value of  $k$ . We weighted each distance by an exponential decay parameter  $\gamma = 1/13.3$  that determines the strength of the relationship between distance and a neighbor's contribution to mating potential; previous

research at these sites found that  $\gamma = 1/13.3$  best described patterns of reproduction in *E. angustifolia* (Wagenius et al. 2007). When fewer than seven individuals flowered within a site, we quantified mating potential with as many individuals as flowered in the site. A one-unit difference in mating potential could represent various differences in distances between maternal plants and their seven nearest neighbors. For example, in our data, a maternal plant with relatively low mating potential of two was isolated from its 1 - 7<sup>th</sup> nearest neighbors by 4 - 60 m while a maternal plant with mating potential of three was within 7 - 14 m of its 1 - 7<sup>th</sup> nearest neighbors. A maternal plant with a relatively high mating potential of five was 1- 8 m away from its 1 - 7<sup>th</sup> nearest neighbors; for more details about mating potential calculations, see Appendix F.

### Seedling Surveys

Between 2007 and 2013, we surveyed *E. angustifolia* seedlings at each of the 14 sites. We describe our seedling survey methods in detail elsewhere (Dykstra 2013; Nordstrom et al. 2021) and briefly here. To select our sampling locations at each site, we randomly selected 18 plants that had flowered in the previous year. We then searched for seedlings within a specified radius of each selected plant; we refer to this area as a ‘focal circle’ and to the plant at its center as the ‘maternal plant.’ Typically, we searched for seedlings within a 41 cm radius of the maternal plant. When fewer than 18 plants had flowered at the site in the previous year, we searched for seedlings at all possible maternal plants and increased the search radius of each focal circle, usually to 50 cm (30 site-years, 160 focal circles). In one instance, only one plant had flowered at a site in the previous year and we searched for seedlings within an 80 cm radius. In 2007, at two sites where flowering density was high in the previous year, we searched for seedlings within 32 cm of the focal circle.

A modest percentage of our focal maternal plants were within 41 cm of another plant that had also flowered in the previous year (16%, 204 of 1278 focal circles). To assess capacity for dispersal of seeds beyond our search radii, we also conducted searches

for seedlings in 163 additional circles (~2 per site in each year) centered at random points within 4 meters but beyond 1.5 meters of any plant that had flowered in the previous year. Altogether, these searches yielded two seedlings, indicating that dispersal beyond the range of the focal circles is rare. This suggests that (1) seedling counts per focal circle are an accurate measure of emergence per maternal plant and (2) seedlings within a circle are likely to have been produced by the focal plant, not a neighbor. We searched for seedlings in May or early June, when seedling cotyledons remained evident. To facilitate finding the individual progeny in later years, we mapped the location of each seedling relative to other seedlings, the focal plant, and other established *E. angustifolia* within or near the search radius. In total, we searched for seedlings in 1278 focal circles, not including the 163 circles centered at randomly selected locations, and tracked cohorts that emerged across seven years and at 14 sites.

For each annual seedling cohort, 2007-2013, we tracked offspring survival for eight subsequent years. We searched each circle in the late summer following emergence to assess survival over the first growing season. Thereafter, we visited focal circles annually to assess the survival of the progeny identified in the seedling search. When we did not find one of the progeny in a given year, we noted this and searched for it again for at least two more years. If we found the individual in one of these years, we revised its demographic status in previous years to “alive.” If we did not find the juvenile in either of the subsequent two years, we no longer searched for it in following years and revised our records to “dead” in all years that we did not find it.

### Statistical Analysis

We used aster analyses (Geyer et al. 2007; Shaw et al. 2008) to evaluate the relationship between mating potential and maternal fitness. Aster analyses model the joint distribution of life-history components based on graphical models that represent the dependence of later observed components on those expressed earlier and statistical distributions suitable for each component. Each component corresponds to a distinct

‘node’ in the graph (Figure 1). In this case, the number surviving at the end of eight years depended on the initial number of progeny emerging and their survival in each successive year. We implemented these models using the aster package (Geyer 2021) in R software version 4.0.3 (R Core Team 2022). Such a modeling approach is necessary because fitness, as a multi-component measure, generally does not conform to any standard statistical distribution. Appropriate specification of distributions for each fitness component is required to obtain valid estimates of sample variance, and thus valid inference. We included fitness components for the number of seedlings emerging after a mating bout (Poisson distributed), the number of seedlings surviving at the end of the first growing season after emergence (binomially distributed), and the number of progeny surviving in each of eight subsequent years (each year binomially distributed).

To assess how mating potential affected maternal plant fitness via progeny emergence and survival, we constructed four models that accounted for the effects of mating potential at different life history stages: “Null,” “Null + Emergence,” “Null + Survival,” and “Null + Emergence + Survival.” Each aster model consisted of a joint analysis of all fitness components. The “Null” model included cohort year, site, and the maternal plant’s number of flowering heads (‘head count’) as covariates affecting both the emergence and survival nodes and the radius of the focal circle (‘search radius’) as a covariate affecting the initial emergence node. The “Null + Emergence” model included all of the covariates in the “Null,” as well as a parameter to estimate the effects of mating potential specifically on seedling emergence. Similarly, the “Null + Survival” model included all of the covariates in the “Null” model and a parameter for the effects of mating potential specifically on progeny count in year eight. Finally, the “Null + Emergence + Survival” model included the “Null” model covariates and parameters for the effects of mating potential on both seedling emergence and final progeny count in year eight.

We compared the fit of nested models using likelihood ratio tests; we compared the “Null + Emergence” and “Null + Survival” models to both the “Null” model and to

the “Null + Emergence + Survival” model. To visualize the effect of mating potential on maternal fitness via seedling emergence and survival through year eight, we obtained model predictions of seedling emergence and progeny count at year eight for hypothetical plants from a site and cohort that had intermediate emergence and survival using the “Null + Survival + Emergence” model. We used Kendall’s Tau-b correlation coefficient to describe the strength of the association between maternal plants’ number of offspring at emergence and after eight years. Kendall’s Tau-b is a rank-based measure of association that does not rely upon the data conforming to a bivariate normal distribution; its values range between -1 and 1. The strength and direction of the association provides a metric to assess whether the separate relationships between mating potential and early and late fitness components leads to amplification (strong positive association between early and late components), negation (negative association), or attenuation (weak positive association) in their cumulative effects.

Finally, to assess how other model covariates related to early and late fitness components, we visualized the effects of site and cohort on seedling emergence and progeny count at year eight by obtaining model predictions for hypothetical plants with average mating potential at each site and in each year of emergence, using the best-performing model. In particular, we sought to assess the association between initial and later maternal fitness components (i.e., number of offspring at emergence and at year eight) by site and cohort by comparing their predicted ranks at both life stages.

To investigate the relative effects of mating potential, cohort year, site, and head count on maternal plants’ number of progeny eight years following a mating bout, we visualized the effect sizes of the model coefficients in the best performing model. We note, however, that, as with other generalized linear models, interpretation of the parameter estimates is not entirely straightforward, due to the non-linear relationship between the underlying ‘canonical’ scale of the analysis and the scale of biological measurement. In addition, to assess the relevance of model covariates beyond mating potential, we constructed a set of models that included all combinations of cohort year,

site, and head count in the best performing model. To compare the adequacy of these non-nested models, we found the Akaike Information Criterion (AIC), which assesses the extent to which the models captured information about the underlying processes influencing fitness (Akaike 1974), for each model. We calculated the difference in AIC values between models ( $\Delta$ AIC) and normalized these values to calculate Akaike weights, which reflect the probability that the model is the best of the set (Wagenmakers and Farrell 2004).

## RESULTS

On average, each maternal plant had few offspring emerge (on average, 0.71 seedlings per maternal plant) and survive. In total, we found 914 seedlings. Of these, only 98 remained after eight years. The distribution of seedling emergence was highly skewed; we found no seedlings in 76% of our initial searches (973 of 1278). Half of the remaining searches (155 of 305) produced just one seedling. In one focal circle, we found 45 seedlings, which exceeded the circle with the second-most by 19 seedlings. After eight years, however, no maternal plant had more than seven surviving progeny; the maternal plant that produced 45 seedlings had three. Maternal plants' mating potential, dependent upon the proximity of conspecific neighbors (Appendix E Figure S1), also varied widely. For example, the maternal plant with the highest mating potential had seven neighbors within 40 centimeters, while the maternal plant with the lowest mating potential had only one conspecific neighbor flowering within the same site, and that plant was 130 m away. In contrast, maternal plant head count varied little: 996 of 1278 (78%) of maternal plants had one flowering head in the year before our search for its seedlings.

The number of seedlings that emerged increased with a maternal plant's mating potential. Likelihood ratio tests indicated that the "Null + Emergence" model, which included the effect of mating potential on the number of seedlings emerging, but no direct effect of mating potential on the number surviving eight years (see Table 1 for model summary), outperformed all others (Table 2). The effect of mating potential on seedling emergence was positive and significantly differed from zero (Emergence:Mating

Potential,  $\beta = 0.26$ ,  $p < 0.0001$ , Appendix E Figure S2). Maternal plants' number of offspring at emergence was positively correlated with their number of offspring surviving to age eight (Kendall's Tau-b,  $\tau = 0.40$ ,  $p < 0.0001$ , Appendix E Figure S3). Our model comparisons indicate, however, that after accounting for the relationship between mating potential and seedling emergence, there was no evidence of a direct relationship between mating potential and seedlings' survival to eight years (Figure 2, Table 2).

Based on the best-performing model ("Null + Emergence"), our model covariate analysis indicated that head count, cohort, site, and mating potential all influenced the number of seedlings that emerged. The full model (including covariates for head count, cohort, site, and mating potential) outperformed all other models (AIC = 5504.7,  $w(\text{AIC}) = 1$ ) (Appendix E Table S1). The second-best model in this analysis included all covariates except mating potential (head count, cohort, site), but the Akaike weight analysis indicated no support for it compared to the full model ( $\Delta\text{AIC} = 57.6$ ;  $w(\text{AIC}) = 0$ ; Appendix E Table S1).

Final offspring count varied among offspring cohorts (Figure 3A) and sites (Figure 3B), but as with mating potential, initial differences in offspring count by cohort and site were far larger than final differences (effect sizes shown in Supplemental Figure 2). Maternal plants producing offspring in certain years (e.g., 2011) saw larger numbers of offspring emerge and maintained their advantage over maternal plants in lower-emergence years through eight years (Figure 3A, Appendix E Figure S4). However, the difference in the number of surviving offspring by year eight among cohort years was small and the rank order of cohort years in terms of offspring count changed (i.e., the lines cross in Figure 3A). Similarly, certain sites had detectably high (e.g., site 'eelr') or low offspring (e.g., site 'ngc') emergence and survival through eight years (Figure 3B, Appendix E Figure S5). Again, however, maintenance of rank across sites was not uniform (i.e., the lines cross in Figure 3B) and by year eight, variation in the number of offspring among all sites was small, with predicted values for all less than 0.4 seedlings.

## DISCUSSION

The number of offspring that emerged following a reproductive bout increased with the mating potential of the maternal plant (Table 2). These results are consistent with previous findings that mate availability limits seed set in these populations (Wagenius et al. 2020) and support the hypothesis that mating potential enhances early fitness components. In contrast, we found no evidence of a direct relationship between mating potential and offspring survival, or the number of offspring eight years after a reproductive bout (Table 2). Notably, we observed many fewer offspring per maternal plant than the number of seeds a typical individual with adequate pollination could produce. Based on the average number of fruits per individual in our study area (mean = 164 achenes, unpublished data) and average seed set (mean = 0.38 seeds/achene, unpublished data), a typical individual might produce approximately 60 seeds in a mating bout. In contrast, we found a mean of 0.71 seedlings around maternal plants in the spring following a mating bout, and zero seedlings around 973 (76%) of the maternal plants. Furthermore, only 11% of offspring were still alive after eight years (98 of 914 found initially). Only two offspring reached reproductive maturity during the study period and more will likely die before flowering. Thus, at least in considering the outcomes of single mating bouts, factors that reduce seedling emergence and juvenile survival, rather than those governing seed fertilization, limit maternal plants' fitness.

A maternal plant's maintenance of an initial fitness advantage over others depends on the size of its initial advantage—in our case, how many more seedlings a maternal plant with high mating potential produces than do others with low mating potential—and juvenile survival (Figure 4). Consider the analogy of a lottery, in which one ticket represents a seedling, e.g., a ticket holder with two tickets represents a maternal plant that produces two seedlings. How much of a difference does it make to buy two tickets, rather than one, when the odds of winning are very low? We might expect the same result: no winning tickets. Similarly, given that we observed a small range of seedling counts (95% of mating bouts produced four or fewer seedlings) and low



juvenile survival (11% survived to age eight), it is unsurprising that high mortality obscured initial differences: most offspring died, including those that formed the small margin between high- and low-emergence maternal plants.

A simple binomial model illustrates how our results are consistent with demographic stochasticity at the maternal plant level resulting from low survival and offspring counts. If the final difference in offspring count between two maternal plants ( $X$ ) is a binomially distributed random variable that depends on the difference in offspring count at emergence ('trials'),  $E$ , and probability of survival of each of these offspring,  $S$ , then the expected final difference in offspring count is  $ES$  (i.e.,  $X \sim \text{Bin}(E,S)$ ;  $E[X] = ES$ ) (Figure 4A). When  $ES > 1$  (or alternatively, when  $E > 1/S$ ), we expect the individual with the fitness advantage at emergence would also have more offspring after survival. The probability of  $ES$  being greater than or equal to 1 is  $1 - (1-S)^E$ . Based on a survival rate of 11% ( $S = 0.11$ ), as we observed, a maternal plant would need to have nine seedlings initially emerge to maintain, in expectation, a fitness advantage over a maternal plant that produced none. Because maternal plants produced nine or more seedlings following only 1.5% of mating bouts (20 of 1278) in our study, based on this reasoning, the erosion of initial fitness advantages that we observed was predictable.

At the same time, the stochastic nature of survival means that the range of possible outcomes is wide. We developed a simulation based on our binomial model (code and details provided in Appendix G) demonstrating that even at low rates of juvenile survival, individuals may maintain their emergence advantages by chance (e.g., points above the dashed line in Figure 4B). In our study, the highest fitness maternal plants at year eight were indeed the plants that had high fitness assessed at emergence. We note that we focus here on the outcome of single reproductive bouts; iteroparous plants could "enter the lottery" multiple times through repeated reproductive episodes. Our model also assumes that the probability of survival is the same for all seedlings. The data from this study suggests that variation in survival does not depend, at least, on maternal mating potential. Unexplained variance in our data could result from myriad

sources that we did not measure or adequately specify in our models. However, the erosion of mating potential effects that we observed was consistent with stochastic variation in maternal fitness (i.e., offspring counts) given low seedling emergence and juvenile survival probabilities.

Do initial fitness proxies provide an accurate representation of relative fitness differences? Our results showed that differences in offspring count at emergence (e.g., among sites and cohorts) largely eroded before offspring reached reproductive maturity and rank order was not uniformly maintained (Figure 3). Thus, early fitness proxies offered an unreliable representation of the relative fitness differences we ultimately observed. This conclusion is consistent with previous studies of long-lived plants, which find that population growth is often disproportionately sensitive to survival rates (Franco and Silvertown 2004). For instance, using a subset of the data presented in this study, Dykstra (2013) found that population growth rate was sensitive to both recruitment and juvenile survival, and Nordstrom et al. (2021) found that differences among populations' demographic responses to burning hinged on whether juvenile survival was high or low. Our results here demonstrate the same dynamic at the level of reproductive individuals: individuals having more offspring in the year after flowering due to large mating potential may not have correspondingly high fitness if juvenile survival is low. Altogether, these findings caution against deriving inferences, for instance, of relative fitness or population growth rate, from early fitness proxies (e.g., seed set) without investigating their correspondence with later reproductive outcomes.

Population persistence and ongoing evolutionary change depend on recruitment of successive generations of reproductively mature plants from seeds. To put our results into a lifetime context for *E. angustifolia*, an iteroparous and hermaphroditic species, we must consider multiple bouts of mating and fitness components. Our findings suggest that, per mating bout, many *E. angustifolia* in our study area fail to produce any offspring that survive to adulthood. The same may be true for individuals across their lifetimes. As offspring survival decreases, a maternal plant's production of at least one successful

offspring depends on an increasing number of reproductive episodes over its lifetime. With an average of one seedling per year and 11% offspring survival to reproductive maturity, maternal plants would have to undergo approximately nine reproductive bouts to produce (in expectation) a single offspring that survives to age eight. Many *E. angustifolia* individuals fail to reach this threshold of reproductive bouts (Waananen et al. 2018). We emphasize that a complete accounting of an individual's fitness would also include the success of its offspring generated through pollen export (e.g., male fitness, Kulbaba and Shaw 2021), which, at the individual level, may respond differently to mating potential. Thus, the extent to which the outcome of one reproductive bout will reflect lifetime fitness depends on the relationship between mating potential, frequency of reproduction, and fitness components across an individual's lifespan. Taking these relationships and their variability into account would improve estimates of properties often derived from fitness proxies, such as mean population fitness or population growth rates.

## CONCLUSIONS

Initial measures of fecundity, or proxies for the quantity of offspring produced, often represent the terminal component in estimates of individual fitness. By “bridging the generation gap” between parental reproduction and offspring survival (Price et al. 2008), we revealed that the apparent fitness disparities in offspring emergence related to mating potential were transitory. This finding is consistent with findings of Snyder and Ellner (2018) that luck can obscure the relationship between fitness and individual differences, especially in plants, and that luck in early life history stages can be decisive for fitness outcomes (Snyder et al. 2020). We suspect similar dynamics may be common in other long-lived plant species and other taxa that experience low reproductive output and high juvenile mortality. However, mating potential could be more likely to affect later fitness components in systems where population sizes are smaller or exhibit greater spatial genetic structure, and thus inbreeding effects on juvenile survival might be more severe. The insights of our study help to clarify the interpretation of analyses using initial

measures of reproductive success as the basis for derived measures such as mean population fitness and population growth rates. Future studies that quantify how iteroparity reinforces or diminishes the patterns we observed here would further advance accounting of lifetime fitness.

#### ACKNOWLEDGEMENTS

A. Waananen helped collect and compile the data, designed the analysis, and wrote the manuscript. A. Dykstra, R. Shaw, and S. Wagenius conceived of and initiated the survey design. G. Kiefer, E. Eichenberger, R. Thoen, S. Nordstrom, and L. Richardson all helped compile the dataset. All authors helped to revise the manuscript, especially R. Shaw, S. Nordstrom, and L. Richardson. Numerous other members of Team Echinacea contributed to data collection in the field, led in recent years by M. Stevens and A. Carroll. This work was funded by NSF awards 2051562, 2050455, 1557075, 1555997, 1052165, 1051791, 0545072, and 0544970 and the Dayton Bell Museum Fund.

## ILLUSTRATIONS

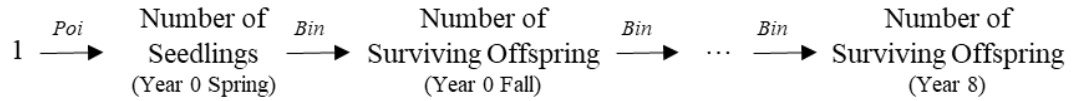


Figure 1. Graphical model for aster analysis of offspring emergence and survival. Arrows point from prior to later nodes. Labels above the arrows indicate the distribution we used to represent that transition: Poi = Poisson, Bin = binomial. “Number of Seedlings” indicates the count of seedlings found in the initial search (Year 0 Spring), while ‘Number of Surviving Offspring’ nodes represent the progeny count in the fall after emergence and subsequent annual surveys.

Table 1. Description of aster models. “Graph nodes” refer to the fitness components within the aster model (see Figure 1). “Layer” is a variable indicating the correspondence of observations to nodes representing either seedling emergence or subsequent progeny counts. “Emergence” and “Yr8Survival” refer to an indicator variable for nodes corresponding to the initial or final counts of progeny, respectively. Terms separated by colons indicate a predictor influencing a node or set of nodes. Terms that distinguish these models from each other are bolded.

Model Name	Model Formula	Model Df	Model Deviance
Null	Graph Nodes + Emergence : Search Radius + Layer : (Cohort + Site + Head Count)	51	-5460.4
Null + Emergence	Graph Nodes + Emergence : Search Radius + Layer : (Cohort + Site + Head Count) + <b>Emergence : Mating Potential</b>	52	-5399.9
Null + Survival	Graph Nodes + Emergence : Search Radius + Layer : (Cohort + Site + Head Count) + <b>Yr8Survival : Mating Potential</b>	52	-5457.8
Null + Emergence + Survival	Graph Nodes + Emergence : Search Radius + Layer : (Cohort + Site + Head Count) + <b>Emergence : Mating Potential + Yr8Survival : Mating Potential</b>	53	-5399.5

Table 2. Comparisons of nested models based on likelihood ratio tests. Comparisons test the null hypothesis that a reduced model performs as well as a more complex one by comparing the difference in deviance (a goodness-of-fit measure) between nested models (Test Deviance) to a  $\chi^2$  distribution with degrees of freedom equal to the difference in degrees of freedom between the two models ('Df'). 'Test *P*-value' indicates the probability of a value from  $\chi^2_{Df}$  greater than the difference in deviance. These tests evaluate hypotheses that mating potential affects progeny emergence, survival, or both. The specific terms in each model are detailed in Table 1. We consider *P*-values < 0.05 statistically significant.

Model Comparison	Test Df	Test deviance	Test <i>P</i> -value
Null vs. Null + Emergence	1	60.468	< 0.0001
Null + Emergence vs. Null + Emergence + Survival	1	0.399	0.53
Null vs. Null + Survival	1	2.558	0.11
Null + Survival vs. Null + Emergence + Survival	1	58.31	< 0.0001

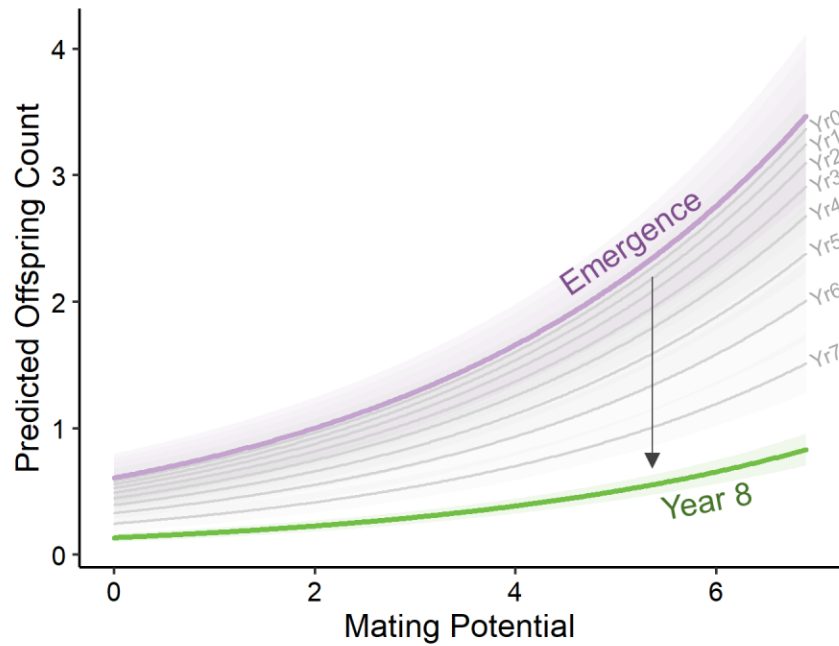


Figure 2. Predicted offspring count per mating bout at emergence (shown in purple) and in year eight (shown in green) based on the full model ('Null + Emergence + Survival'). Predictions here represent hypothetical individuals with one head that had seedlings emerge in 2012 in the site 'sap', a small remnant with intermediate seedling emergence and survival (Figure 3). Shaded bands indicate one standard error on each side of the mean. Mating potential represents a weighted sum of distance between a maternal plant and its 1<sup>st</sup> - 7<sup>th</sup> nearest conspecific neighbors in the year before seedling searches.

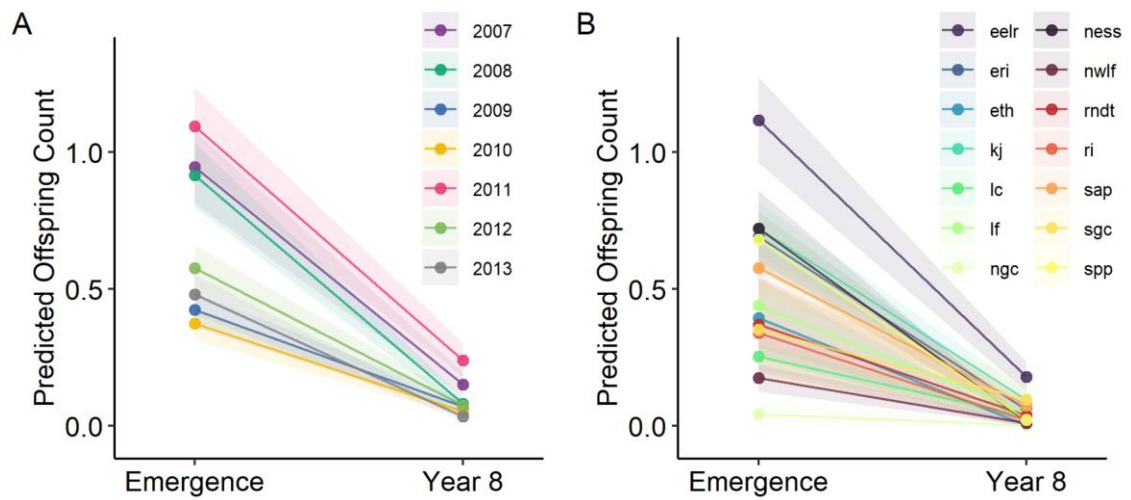


Figure 3. Predicted offspring count per mating bout at emergence and after eight years by (A) cohort and (B) site. Predictions here are derived from the ‘Null + Emergence’ model for hypothetical individuals with one head; in (A) the hypothetical individuals are from site ‘sap’ and in (B) the cohort is 2012. The shaded areas indicate one standard error on each side of the mean.



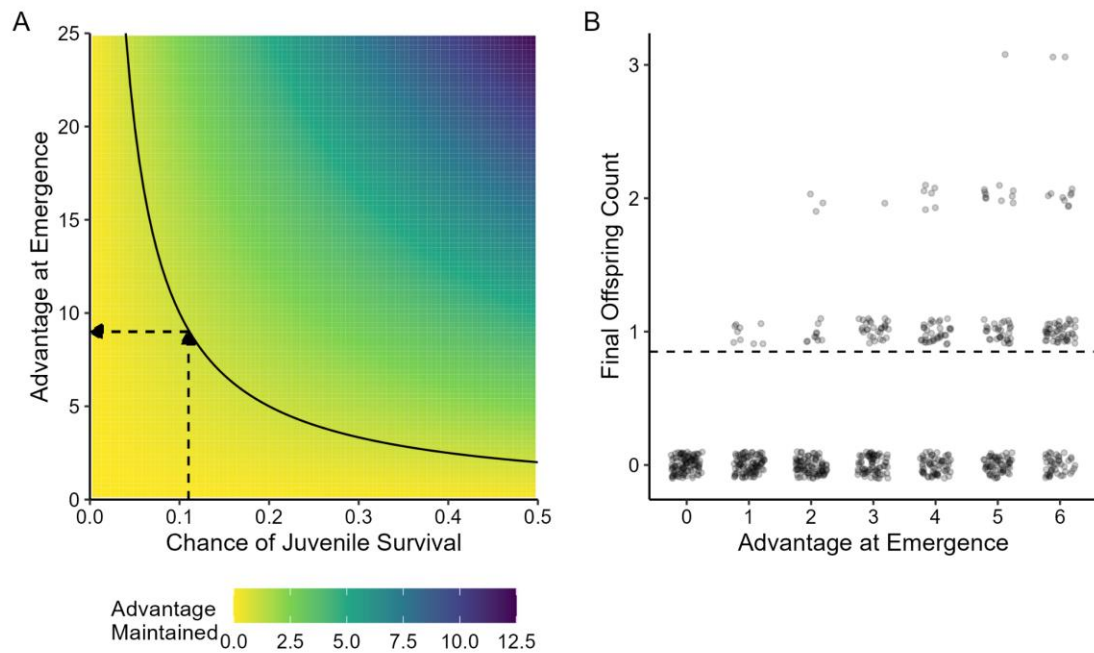


Figure 4. (A) Output from simulation model investigating final offspring count as a function of a maternal plant's emergence advantage and the chance of juvenile survival. The solid curve represents  $E = 1/S$ ; above the curve, we expect initial advantages to persist while below the curve, we expect the emergence advantage to be obviated by low survival. The vertical dashed line indicates the observed juvenile survival rate (11%) and the horizontal line indicates the number of seedlings a maternal plant would have needed to produce to maintain its fitness advantage. (B) Results from simulations investigating final offspring advantage following survival given different sizes of emergence advantages where the juvenile survival rate is 0.11 (what was observed empirically in this study). Points are jittered to avoid overplotting at integer values of offspring counts. Points above the dashed line indicate simulations in which the emergence advantage was maintained (at least one of the offspring in the emergence advantage survived; the line is lowered below one to account for vertical jitter). Below the line, all offspring in the emergence advantage died.

## BIBLIOGRAPHY

Aguilar, R., E. J. Cristóbal-Pérez, F. J. Balvino-Olvera, M. de Jesús Aguilar-Aguilar, N. Aguirre-Acosta, L. Ashworth, J. A. Lobo, S. Martén-Rodríguez, E. J. Fuchs, and G. Sanchez-Montoya. 2019. Habitat fragmentation reduces plant progeny quality: a global synthesis. *Ecol. Lett.* 22:1163–1173.

Akaike, H. 1974. A new look at the statistical model identification. *IEEE Trans. on Auto. Cont.*, 19:716–723.

Campbell, D. R., A. K. Brody, M. V. Price, N. M. Waser, and G. Aldridge. 2017. Is plant fitness proportional to seed set? An experiment and a spatial model. *Am. Nat.* 190:818–827.

Dykstra, A. B. 2013. Seedling recruitment in fragmented populations of *Echinacea angustifolia*. University of Minnesota.

Franco, M. and J. Silvertown. 1996. Life history variation in plants: an exploration of the fast-slow continuum hypothesis. *Phil. Trans. Bio. Sci.* 351:1341–1348.

Gascoigne, J., L. Berec, S. Gregory, and F. Courchamp. 2009. Dangerously few liaisons: a review of mate-finding Allee effects. *Popul. Ecol.* 51:355–372.

Geyer, C. J., S. Wagenius, and R. G. Shaw. 2007. Aster models for life history analysis. *Biometrika* 94:415–426.

Geyer, C.J. 2021. R package aster version 1.1-2. <https://cran.r-project.org/web/packages/aster>

Ison, J. L., and S. Wagenius. 2014. Both flowering time and distance to conspecific plants affect reproduction in *Echinacea angustifolia*, a common prairie perennial. *J. Ecol.* 102:920–929.

Kulbaba, M. W., and R. G. Shaw. 2021. Lifetime fitness through female and male function: Influences of genetically effective population size and density. *Am. Nat.* 197:434–447.

Nordstrom, S. W., A. B. Dykstra, and S. Wagenius. 2021. Fires slow population declines of a long-lived prairie plant through multiple vital rates. *Oecologia* 196:679–691.

Price, M. V., D. R. Campbell, N. M. Waser, and A. K. Brody. 2008. Bridging the generation gap in plants: Pollination, parental fecundity, and offspring demography. *Ecology* 89:1596–1604.

Richardson, L. K., K. M. Gallagher, T. E. Hayes, A. S. Gallinat, A. S., G. Kiefer, K. Manion, M. Jenkins, G. Diersen, and S. Wagenius. 2021. Competition for pollination and isolation from mates differentially impact four stages of pollination in a model grassland perennial. *J. Ecol.* 109:1356–1369.

Schmitt, J., and D. W. Ehrhardt. 1990. Enhancement of inbreeding depression by dominance and suppression in *Impatiens capensis*. *Evolution* 44:269–278.

Shaw, R. G., C. J. Geyer, S. Wagenius, H. H. Hangelbroek, and J. R. Etterson. 2008. Unifying life-history analyses for inference of fitness and population growth. *Am. Nat.* 172:35–47.

Smith, C. C. and S.D. Fretwell. 1974. The optimal balance between size and number of offspring. *Am. Nat.* 108:499–506.

Snyder, R. E., and S. P. Ellner. 2018. Pluck or Luck: Does trait variation or chance drive variation in lifetime reproductive success? *Am. Nat.* 191:90–107.

Snyder, R. E., S. P. Ellner, and G. Hooker. 2020. Time and chance: Using age partitioning to understand how luck drives variation in reproductive success. *Am. Nat.* 197:110–128.

Waser, N. M., D. R. Campbell, M. V. Price, and A. K. Brody. 2010. Density-dependent demographic responses of a semelparous plant to natural variation in seed rain. *Oikos*, 119:1929–1935.

Waananen, A., G. Kiefer, J. L. Ison, and S. Wagenius. 2018. Mating opportunity increases with synchrony of flowering among years more than synchrony within years in a nonmasting perennial. *Am. Nat.* 192:379–388.

Wagenius, S. 2004. Style persistence, pollen limitation, and seed set in the common prairie plant *Echinacea angustifolia* (Asteraceae). *Int. J. Plant Sci.* 165:595–603.

Wagenius, S. 2006. Scale dependence of reproductive failure in fragmented *Echinacea* populations. *Ecology* 87:931–941.

Wagenius, S., E. Lonsdorf, and C. Neuhauser. 2007. Patch aging and the S-Allee effect: breeding system effects on the demographic response of plants to habitat fragmentation. *Am. Nat.* 169:383–397.

Wagenius, S. and S. P. Lyon. 2010. Reproduction of *Echinacea angustifolia* in fragmented prairie is pollen-limited but not pollinator-limited. *Ecology* 91:733–742.

Wagenius, S., A. B. Dykstra, C. E. Ridley, and R. G. Shaw. 2012. Seedling recruitment in the long-lived perennial, *Echinacea angustifolia*: a 10-year experiment. *Rest. Ecol.* 20:352-359

Wagenius, S., J. Beck, and G. Kiefer. 2020. Fire synchronizes flowering and boosts reproduction in a widespread but declining prairie species. *PNAS* 117:3000-3005.

Wright, S. 1943. Isolation by distance. *Genetics* 28:114–138.

## APPENDICES

### Appendix A. Flowering Asynchrony Mediates Trade-Offs between Reproductive Success and Dispersal: A Conceptual Model

#### INTRODUCTION

Flowering asynchrony within a population reduces the density of flowering compared to if all individuals flowered at the same time. Furthermore, individuals that flower at different times within the season experience different densities of potential mates. Reductions in mate density have two common consequences for individual reproductive success. First, as I discuss in Chapter 1, low mate density reduces an individual's quantity of mating opportunities and consequent reproductive success (i.e., a mate-finding Allee effect). Second, reduced mate density can result in mating between individuals that are more distant. As I discuss in Chapter 2, distance between mates often corresponds with the quality of mating and the fitness of subsequent offspring. For instance, in populations where there is spatial genetic structure, greater distance between parental plants can correspond with higher offspring fitness, due to alleviating inbreeding depression.

Based on these observations, I hypothesized that flowering asynchrony might be favored when the fitness benefits of long-distance mating outweigh the costs of isolation from mates. Further, when individuals' reproductive fitness peaks at lower densities, populations may evolve to flower more asynchronously. However, the optimal density will depend on how pollinators forage with respect to density, such as how far they are willing to go between isolated plants, and the shape of the relationship between interparent distance and offspring fitness. My goal here is to outline my assumptions underlying these hypotheses, discuss conditions that could shape the trade-off between the costs and benefits of reproductive asynchrony and lead to its maintenance over generations, and develop a set of expectations for reproductive asynchrony under different biological scenarios.

## KEY RELATIONSHIPS

### 1. TIME, FLOWERING, AND ISOLATION

First, I assume that individuals that flower on days of season when many other individuals are flowering will be less spatially isolated from other flowers than individuals that flower early or late in the season, when few individuals are flowering. It is certainly possible to contrive a population in which this is not true; for instance, flowering across the season could be spatially stratified such that individuals flower synchronously within smaller patches. However, if flowering time is distributed randomly across space, then, on average, we should expect that individuals that flower early or late will be further from potential mates than those that flower at peak.

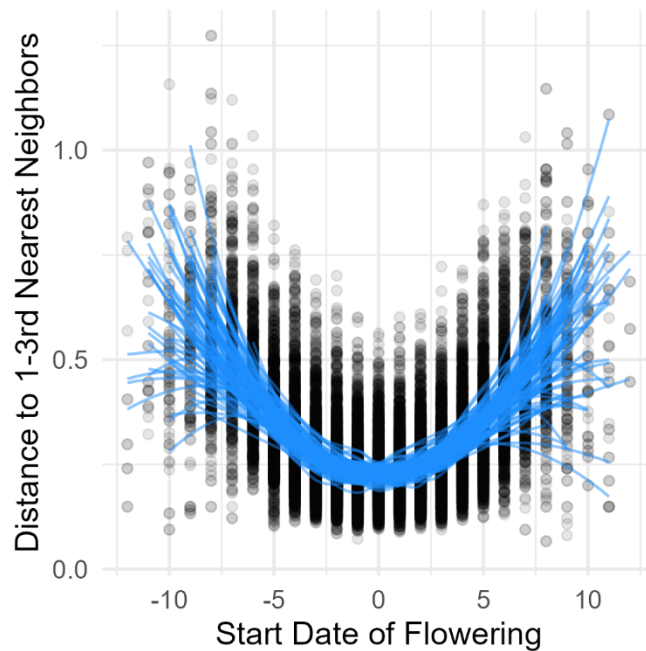


Figure 1. Distance to individuals 1-3<sup>rd</sup> nearest co-flowering neighbors based on date of flowering when individual coordinates are assigned to a 15 x 15 grid and flowering dates are drawn from a normal distribution with a mean of 0 and standard deviation of 4.

Individuals flower for one day. Each blue line shows a local polynomial regression for a single simulation.

For simplicity, we begin by assuming that a population's flowering has a single peak in time. Such a distribution of flowering is common among plants and represents a null expectation under the “temporal mid-domain hypothesis”—the expectation that there will be most individuals flowering in the middle of the flowering season if individuals with some duration of flowering are distributed randomly through time within the bounds of seasonal abiotic constraints.

## 2. REPRODUCTION AND DISTANCE BETWEEN PLANTS

Next, I assume that the likelihood of two plants mating depends on their proximity, or their isolation. This relationship can be described as a pollen dispersal kernel, or the probability distribution that dispersal occurs over distance. Many plants show sharp declines in mating between plants with increasing distance, reflected in leptokurtic pollen dispersal kernels. For bee-pollinated plants, this is because bees may be less likely to travel farther distances between flowers or patches of floral resources.

## 3. DISTANCE BETWEEN PLANTS AND OFFSPRING FITNESS

Pollen movement or “outcrossing” distance corresponds with fitness when mating occurs between genetically differentiated plants. One mechanism that can lead to differentiation is spatial isolation (isolation-by-distance); patterns of genetic structure arising at fine scales are common in plants due to their limited dispersal abilities. A consequence of isolation is genetic drift and mating between related individuals (inbreeding), which can lead to reduced fitness. Cross breeding between genetically differentiated populations will ameliorate the expression of deleterious recessive alleles and lead to increased offspring fitness, a process known as ‘heterosis.’ If genetic differentiation increases with distance, then we might expect mating between more distant individuals to alleviate inbreeding depression and lead to higher offspring fitness.

On the other hand, offspring fitness might decline with distance between parents if distance corresponds with adaptation to distinct environments. Mating between plants adapted to different environments could dilute adaptation to either environment or disrupt co-adapted gene complexes through recombination. If the likelihood that two individuals are adapted to different conditions increases with the distance between them, then we might expect offspring fitness to decline as distance between parental plants increases. Finally, offspring fitness might be greatest when parents are isolated by intermediate distance (“intermediate optimum”). This would occur when populations are both inbred and adapted to local conditions. Intermediate distances might achieve the benefits of outcrossing while minimizing the costs of disrupting local adaptation.

## EXPECTATIONS

What we care about is the distance between plants that maximizes product of the reproductive-distance function (which I will refer to as  $R$ ) and fitness-distance function (which I refer to as  $W$ ). Because the  $R$  yields the relative number of offspring expected based on distance and  $W$ , the fitness of each offspring depending on the distance between their parents, we can think of  $R*W$  as the fitness of a maternal plant considering both its reproductive output and fitness of its progeny. The distance between plants what maximizes  $R*W$  will be inversely related to the “optimal” density for individuals to flower; that is, low distances between plants correspond to high density. Given that density corresponds to time of flowering, this will indicate on which days flowering will lead to the highest fitness.

Assuming that the distribution is at least roughly symmetric, then anytime that the optimal density does not occur on the peak day of flowering, there will be two occurrences of optimal density on opposite shoulders of the flowering curve, that is, once before peak and once after. This leads to several expectations: (1) when the shape of the  $R$  and  $W$  lead to lower optimal densities, we expect the occurrences of optimal density to occur further apart in time, and (2) when the times at which optimal density occurs are



further apart, populations will be more asynchronous, or have greater variance in flowering time. Below, I discuss expectations under this conceptual model for different biological scenarios. In particular, I focus on how scenarios correspond to the key relationships described above leading to shifts in the optimal density and subsequent asynchrony. Please note that the optimal ‘time from peak flowering’ indicated on the graphs below are approximate and depend on the precise shapes of R and W.

## 1. HETEROSIS VS. LOCAL ADAPTATION VS. INTERMEDIATE OPTIMUM

The shape of W will influence its intersection with R and the distance that maximizes the product of the two functions,  $R*W$ . For each scenario below, assume that R shows the same generally exponential decline with distance and that beyond large distances, R is 0. If it were not, increasing W could lead to infinite distances maximizing  $R*W$ .

*Heterosis* - If fitness increases with distance (“heterosis,” as discussed above), the shape of increase may depend on the pattern of how genetic similarity is structured across space. For instance, if populations are structured at a very fine scale, then relatedness may decline rapidly with distance and change little over greater distances, leading to a saturating function for W. Alternatively, individuals may be genetically uniform within patches of individuals and then highly dissimilar beyond a distance threshold. Such a scenario might be common, for instance, when strong barriers to gene flow exist between two populations, but movement within populations is not limited by distance. This could lead to strong increases in W beyond a certain distance threshold, or may be approximated by W having an accelerating form over distance. Finally, genetic dissimilarly might scale in a linear fashion with distance.

Whether W displays a linear, accelerating, or saturating increase will influence the trade-off of fitness and reproductive opportunity. Assuming that a saturating W function increases faster than a linear W function at low distances between plants, a saturating function lead to maximization of  $R*W$  at lower distances between plants

(higher densities) than the linear function. Conversely, an accelerating function will maximize  $R \cdot W$  at greater mean distances between plants than a linear function. So, the optimal distances for these shapes of  $W$ , that is, the distances between plants that maximizes  $R \cdot W$ , will rank largest to smallest as accelerating, linear, then saturating. The inverse will be true for density: an accelerating  $W$  function will favor flowering at lower density than a linear or saturating  $W$  function. Based on the reasoning that lower optimal densities will increase variance in flowering time through disruptive selection, then, where  $W$  is accelerating, populations would be expected to be more asynchronous than where  $W$  is linear or saturating.

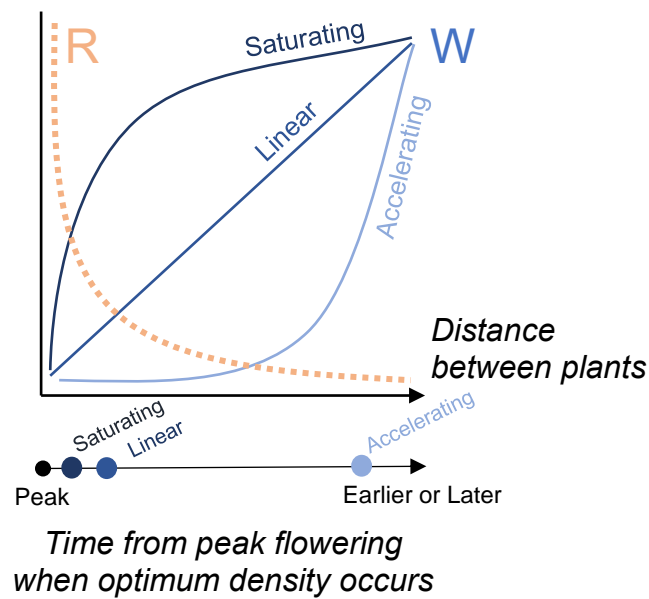


Figure 2. Heterosis scenarios.

*Local adaptation* – If R and W both show monotonic declines with increasing distance, then  $R \cdot W$  will be maximized at the minimum distance between plants, or the maximum density. Individuals that flower on the peak day of flowering will have the most and highest fitness offspring. Variation in flowering time should quickly deplete; over generations, we would expect a population to maintain maximal flowering synchrony, constrained only by degree to which flowering time is heritable. This assumes, however, that the variation in flowering time is highly heritable, with genetic variation attributable to a single or very few loci.

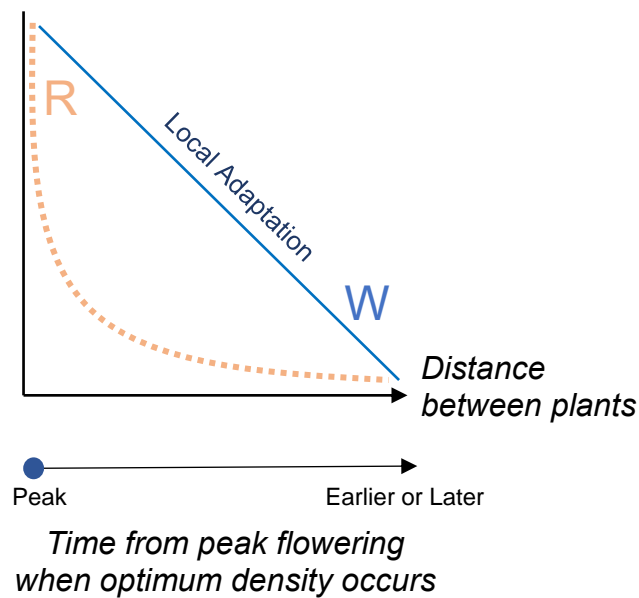


Figure 3. Local adaptation scenario.

*Intermediate Optimum* - If  $W$  has a shape that peaks at intermediate distances, the distance that maximizes  $R*W$  will vary depending on the degree to which  $W$  varies across distance. In particular, if fitness is very low at small distances in comparison to intermediate distances, due to a strong effect of inbreeding over fine scales, then  $R*W$  will be greater at larger distances than if fitness showed a subtle peak at intermediate distances, but was not very low at small distances. As a result, more extreme variation in fitness with distance could lead to greater flowering asynchrony than more subtle variation.

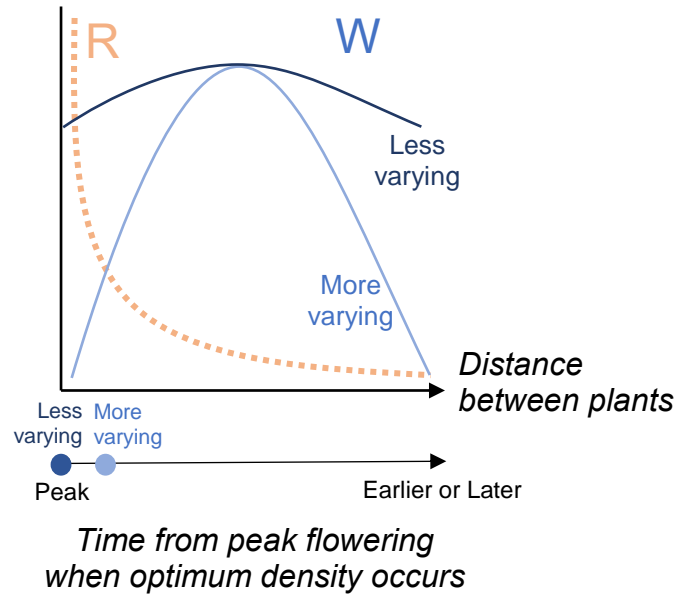


Figure 4. "Intermediate outcrossing optimum" scenarios.

## 2. POLLEN DISPERSAL PATTERNS

The pollen dispersal function,  $R$ , might also vary in shape, with implications for the optimal density of flowering and subsequent advantage of flowering asynchrony.

*Exponential Decline* – The reasoning that reduced mate density will improve overall reproductive outcomes by increasing the frequency of long-distance mating assumes that pollination will still occur, though less often, between distant plants. Certain pollinators do have high fidelity to a particular type of flower or floral morphology, either across seasons or within a single foraging bout, but the response of different pollinators to distance may vary. Assuming function for  $W$ , if  $R$  declines more quickly with distance, then  $R*W$  will peak at lower distances, or higher densities. High fitness when flowering density is high would then lead to higher flowering synchrony. Conversely, slower declines in probability of mating with distance, perhaps indicating flexibility in pollinator foraging distances or higher pollinator fidelity, could lead to greater reproductive asynchrony.

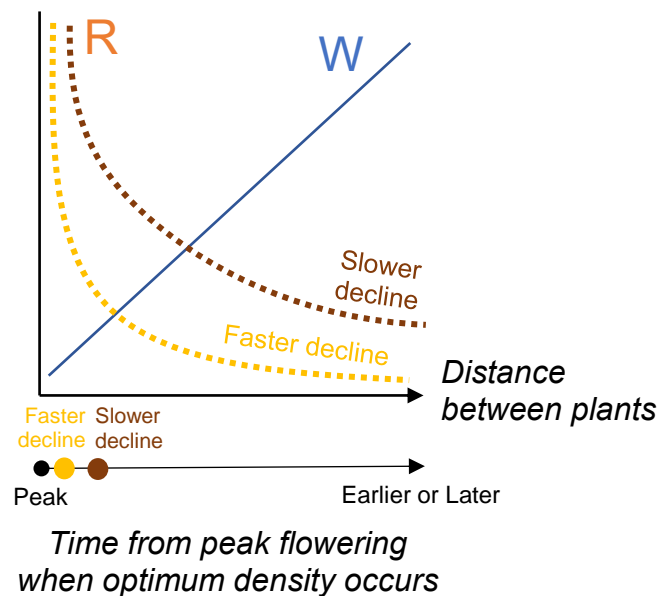


Figure 5. Pollen dispersal declining more or less quickly with distance scenarios.

*Foraging Thresholds* – Generalist pollinators may switch to other flowering resources when flowering density falls below a threshold. Furthermore, limitations to long-distance pollen movements due to physical constraints could render the fitness advantages of long-distance mating, and thus of flowering asynchrony, irrelevant beyond certain thresholds of isolation. The outcome of foraging thresholds for  $R \cdot W$ , and expected flowering asynchrony, will depend on whether fitness benefits of long-distance mating are mainly accrued beyond the maximum distance for which  $R$  is non-zero, that is, beyond the foraging threshold. For instance, if  $W$  is consistent across the range of distances for which  $R$  is non-zero, then the maximum of  $R \cdot W$  will be determined by the maximum value of  $R$ , i.e., at small distances. If  $W$  increases with distance appreciably before the foraging threshold, then it would be possible to have  $R \cdot W$  peak at greater distances, leading to greater flowering asynchrony.

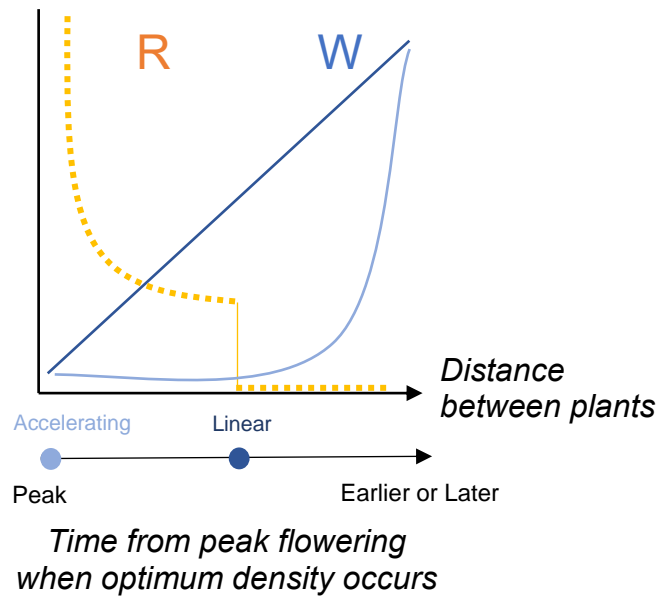


Figure 6. Threshold in mating over distance scenarios.

*Non-Monotonic Patterns* – For plants, the reproductive consequences of proximity to mates can be complex, particularly if individuals compete for pollinator visits. In this case, reproductive potential might be low when distances between plants are very small, peak at intermediate distances between plants, and then decline with distance between plants. In this case, the density of individuals that would maximize  $R \cdot W$  is harder to predict as it will depend on the precise shape of the functions.

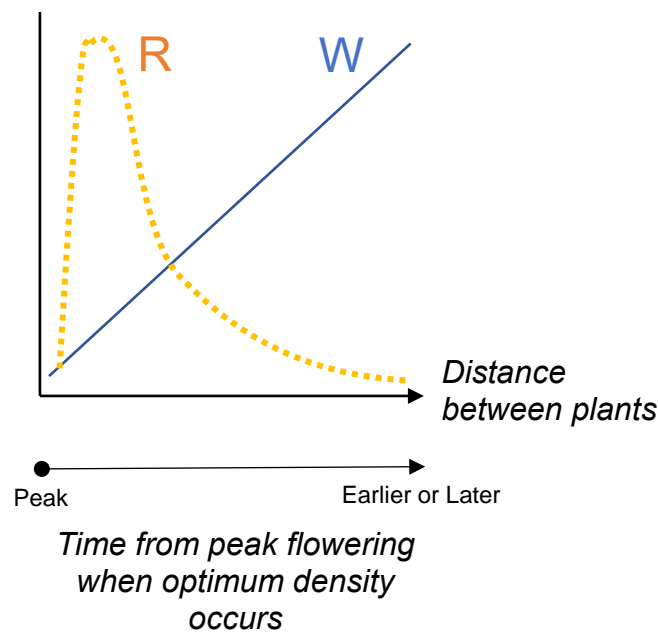


Figure 7. Non-monotonic patterns of mating with distance scenario.

### 3. CLUMPED VS. RANDOM SPATIAL DISTRIBUTIONS

The spatial configuration and seed dispersal of plants could also shape the trade-off between the costs and benefits of reproductive asynchrony. In populations with an even distribution of individuals across a landscape, few plants will be very close together and therefore have the potential of producing highly inbred offspring. Flowering asynchrony might reduce mating opportunities more than it increases mating quality. In contrast, in spatially clumped populations, individuals that are close together are most likely to mate—and to be close relatives. Flowering asynchrony between highly

proximate plants could prevent inbreeding depression in offspring. Thus, we might expect to see asynchrony favored in clumped populations, but less so in more evenly distributed ones.

## DISCUSSION

Reproductive asynchrony is widespread across sexually reproductive taxa, including flowering plants, despite its potential to reduce opportunities to mate. The conceptual model presented here outlines one mechanism that may maintain asynchrony in flowering plant populations. It may be that trade-offs between reproductive opportunity and mate quality is but one of many mechanisms that contribute to asynchrony; other explanations include reducing competition with co-flowering, predator satiation. However, this mechanism may be relevant for plants in fragmented environments because mate quality could depend strongly on parental distance in fragmented environments, which may have high degrees of inbreeding within small populations and/or environmental heterogeneity to which individuals may adapt.

While I focused here on discussing asynchrony as populations that had more or less of unimodal peak in flowering, the same reasoning could apply to a population with a bimodal distribution of flowering. In fact, it is possible that a bimodal distribution of flowering is a possible outcome of balancing selection on flowering time. If selection for flowering time is negative frequency dependent, such that individuals that flower at periods of intermediate density are favored, we might expect that there will not be any consistent optimal date of flowering and instead it might fluctuate over generations. In real populations, environmental heterogeneity over space and time will also surely lead to variation in both timing of flowering and its fitness consequences. Nevertheless, this hypothesis offers a new potential mechanism by which we can understand reproductive asynchrony and its consequences for plant fitness.



## Appendix B: Chapter 1 Supplemental Materials

### *Seed Set Model Selection Details*

We first modeled seed set using a binomial model, to predict the odds that a fruit contains a seed, given our set of terms. Many individuals had zero seeds in their sample of fruits (96 of 983 observations) and the ratio of sum of squared residuals to residual degrees of freedom in our initial binomial model of seed set was 7.2, indicating overdispersion. Simulations of the fitted model from the ‘DHARMA’ R package indicated 3.7x more zeros in the data than expected under the binomial model ( $p < 0.001$ ), indicating strong zero-inflation. To attempt to address the overdispersion and zero-inflation, we also considered a zero-inflated binomial model, a betabinomial model, and a zero-inflated betabinomial model. We used the R package ‘glmmTMB’ (Brooks et al. 2017) to implement the beta-binomial model and the a zero-inflated beta-binomial model. The zero-inflated binomial model performed better than the binomial model ( $\chi^2 = 1211.5$ ,  $df_{ZI-Bin} - df_{Bin} = 9$ ,  $p < 0.001$ ,  $AIC_{ZI-Bin} - AIC_{Bin} = -1193$ ), but did not perform as well as the less-complex betabinomial model ( $\chi^2 = 0$ ,  $df_{ZI-Bin} - df_{Betabin} = 8$ ,  $p = 1$ ,  $AIC_{ZI-Bin} - AIC_{Betabin} = 3441$ ). In contrast, a zero-inflated beta-binomial model outperformed the betabinomial model ( $\chi^2 = 61.59$ ,  $df_{ZI-Betabin} - df_{Betabin} = 9$ ,  $p < 0.001$ ,  $AIC_{ZI-Betabin} - AIC_{Betabin} = -102$ ). Model fit also improved based on visual inspection of model diagnostics (qq-plots and DHARMA simulated residuals vs. model fitted values). Thus, we used a zero-inflated betabinomial model for our subsequent analyses of seed set.

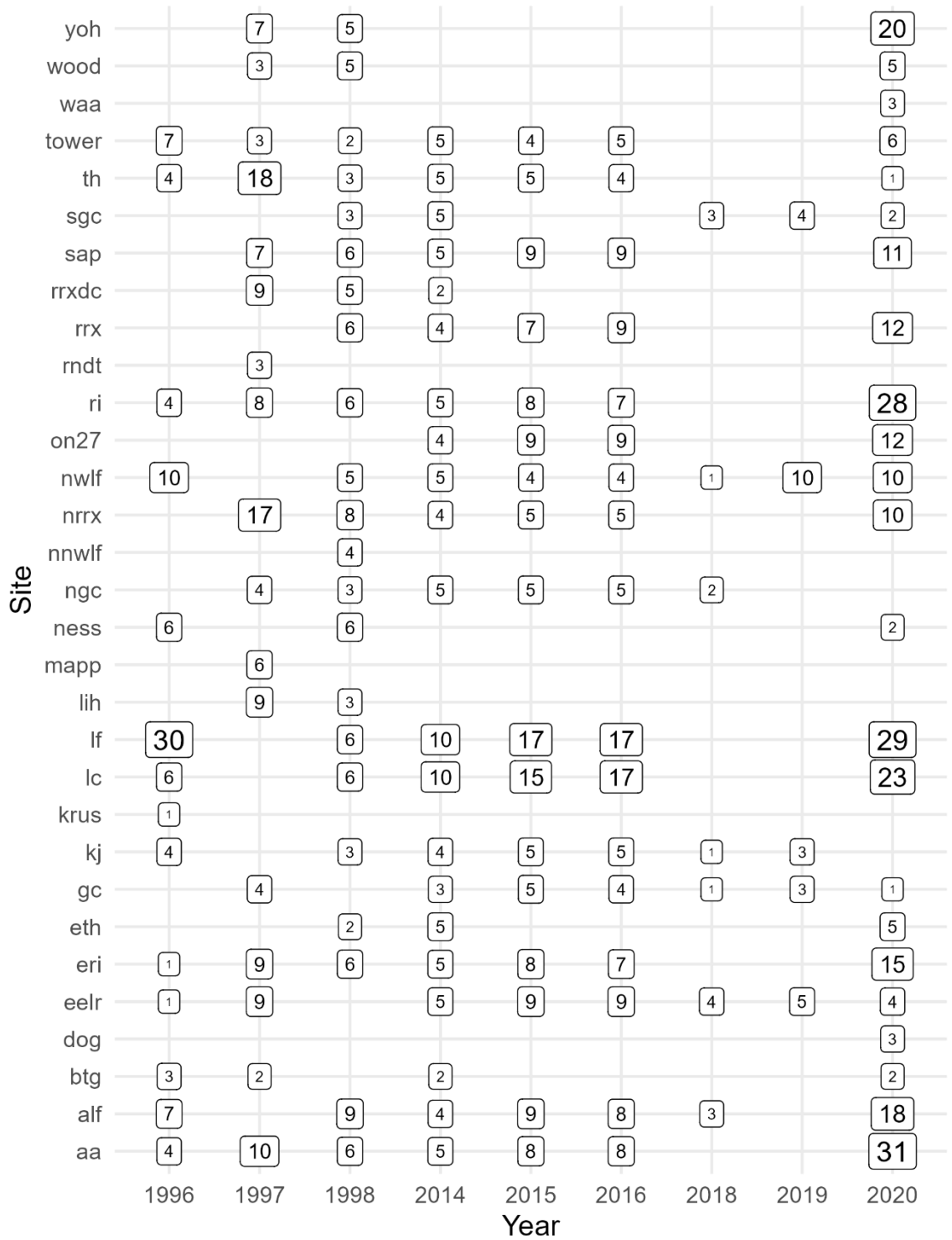


Figure S1. Number of seed set observations by population and year.

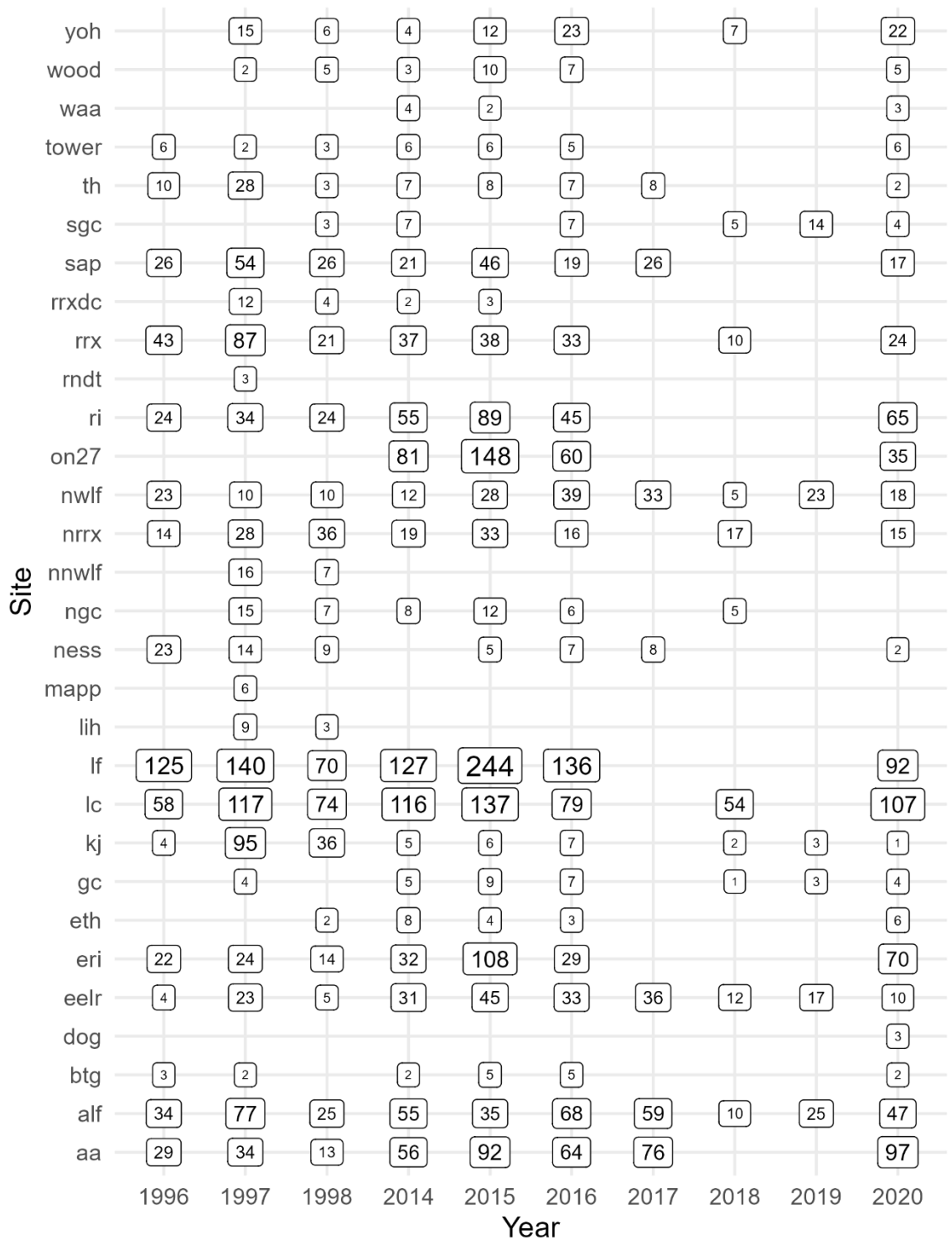


Figure S2. Number of observations per site and year for style persistence.

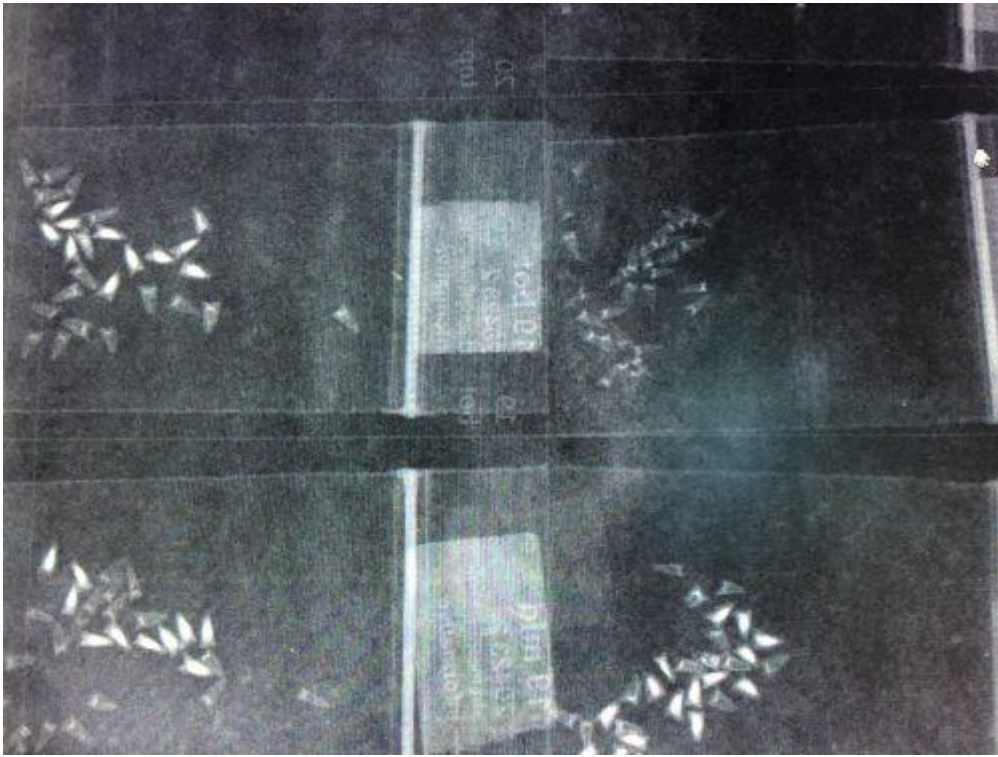


Figure S3. Example of x-ray image of achenes used to assess seed set.

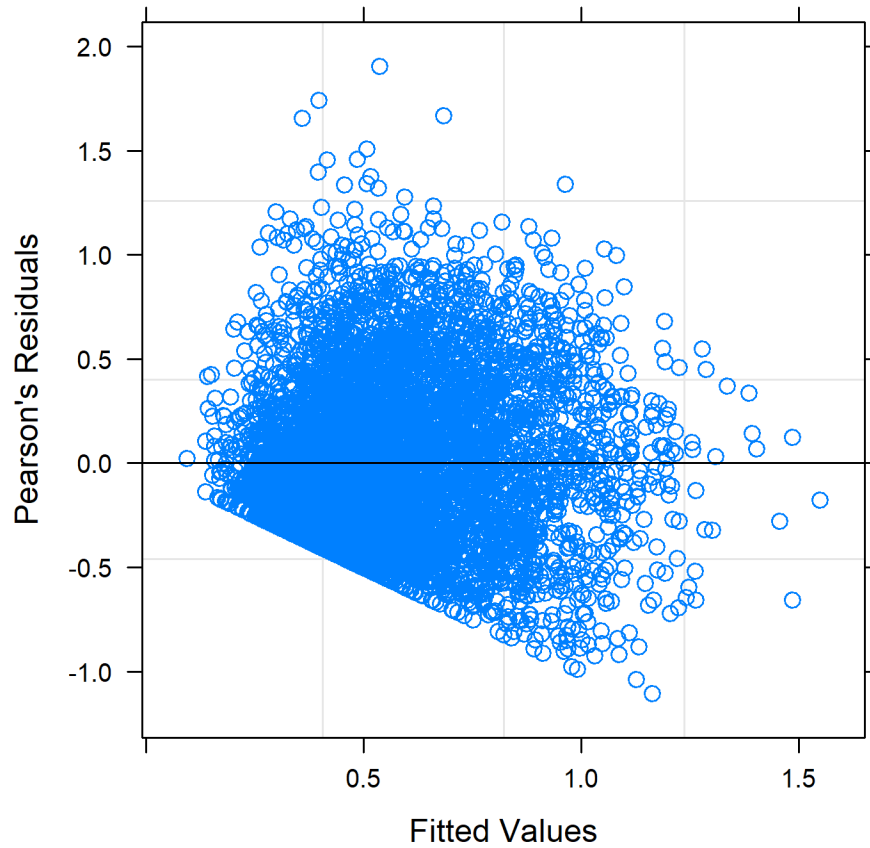


Figure S4. Residuals vs. fitted values of the full model for style persistence  $\text{Log}(\text{Style Persistence}) \sim \text{Sync.} + \log(\text{Dist. to 4}^{\text{th}} \text{ Nearest Neighbor}) + \text{Date of Flowering} + \log(\text{Census Size}) + \text{Date of Flowering} * \log(\text{Dist. to 4}^{\text{th}} \text{ Nearest Neighbor}) + \log(\text{Census Size}) * \log(\text{Dist. to 4}^{\text{th}} \text{ Nearest Neighbor}) + \log(\text{Census Size}) * \text{Sync.} + \log(\text{Dist. to 4}^{\text{th}} \text{ Nearest Neighbor}) * \text{Sync.}$ , plus random effects for site and year.

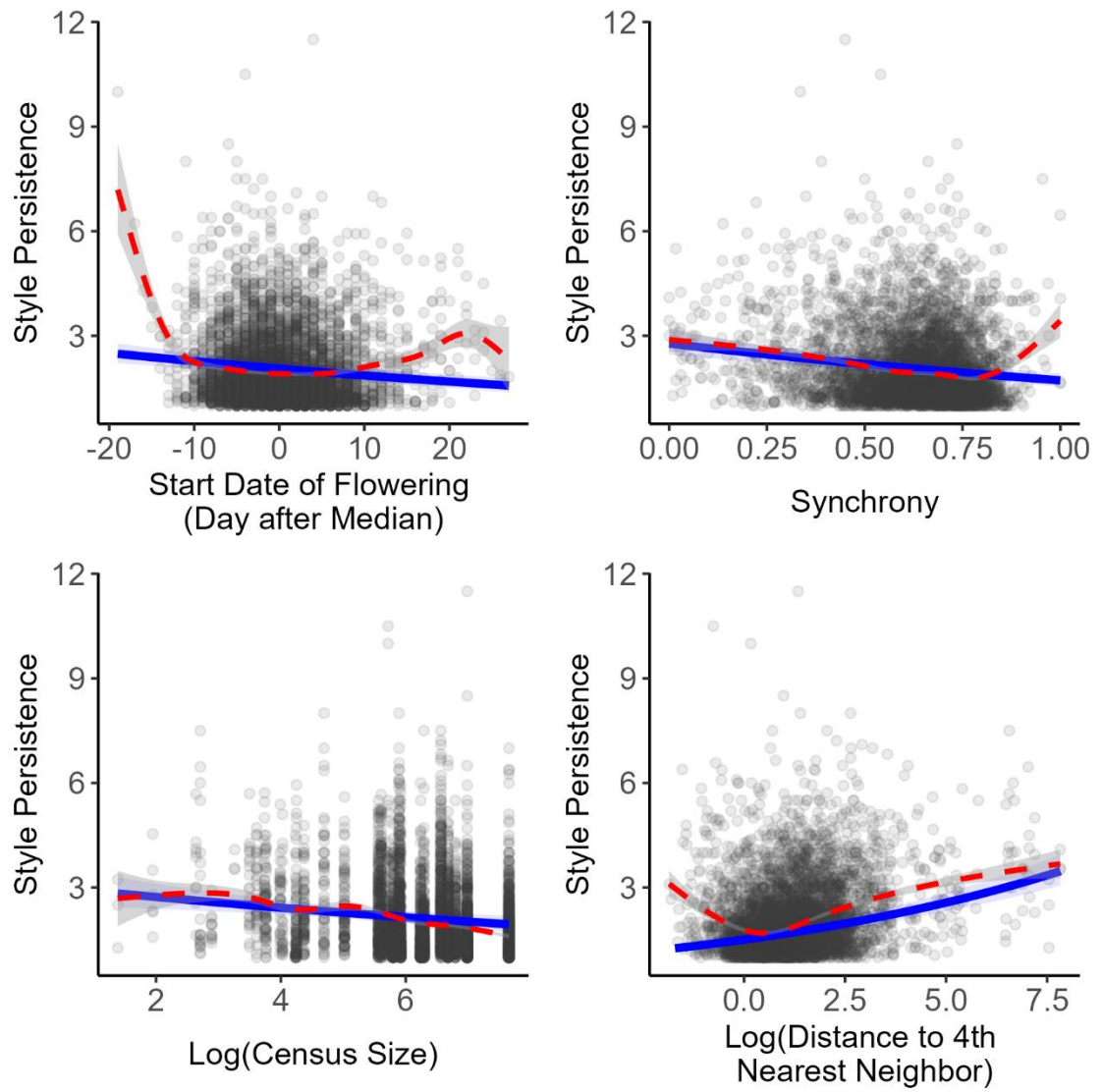


Figure S5. Generalized additive models (dashed) compared to fit from the full model for style persistence indicate no strong non-linearities. Deviations between the generalized additive models and the linear model predictions are greatest in areas where there are few observations and so do not appear to indicate meaningful trends.

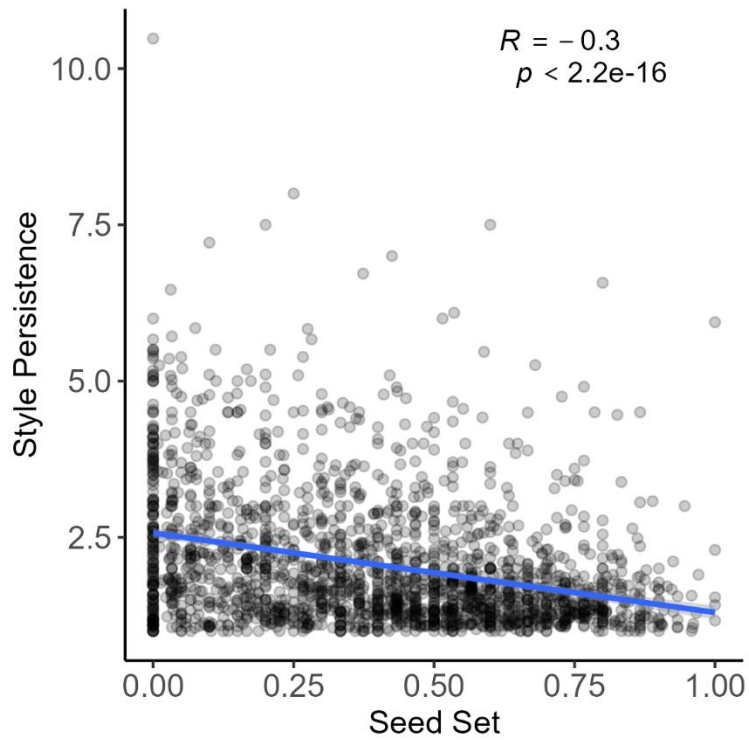


Figure S6. The correlation between seed set and style persistence.

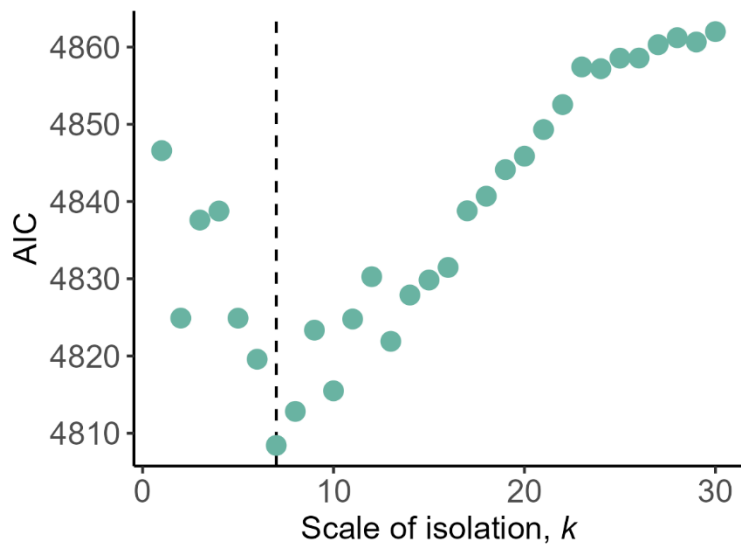


Figure S7. Variation in model performance, as measured by AIC, considering models that measured isolation to individuals'  $k$ th nearest neighbor as a predictor of style persistence.

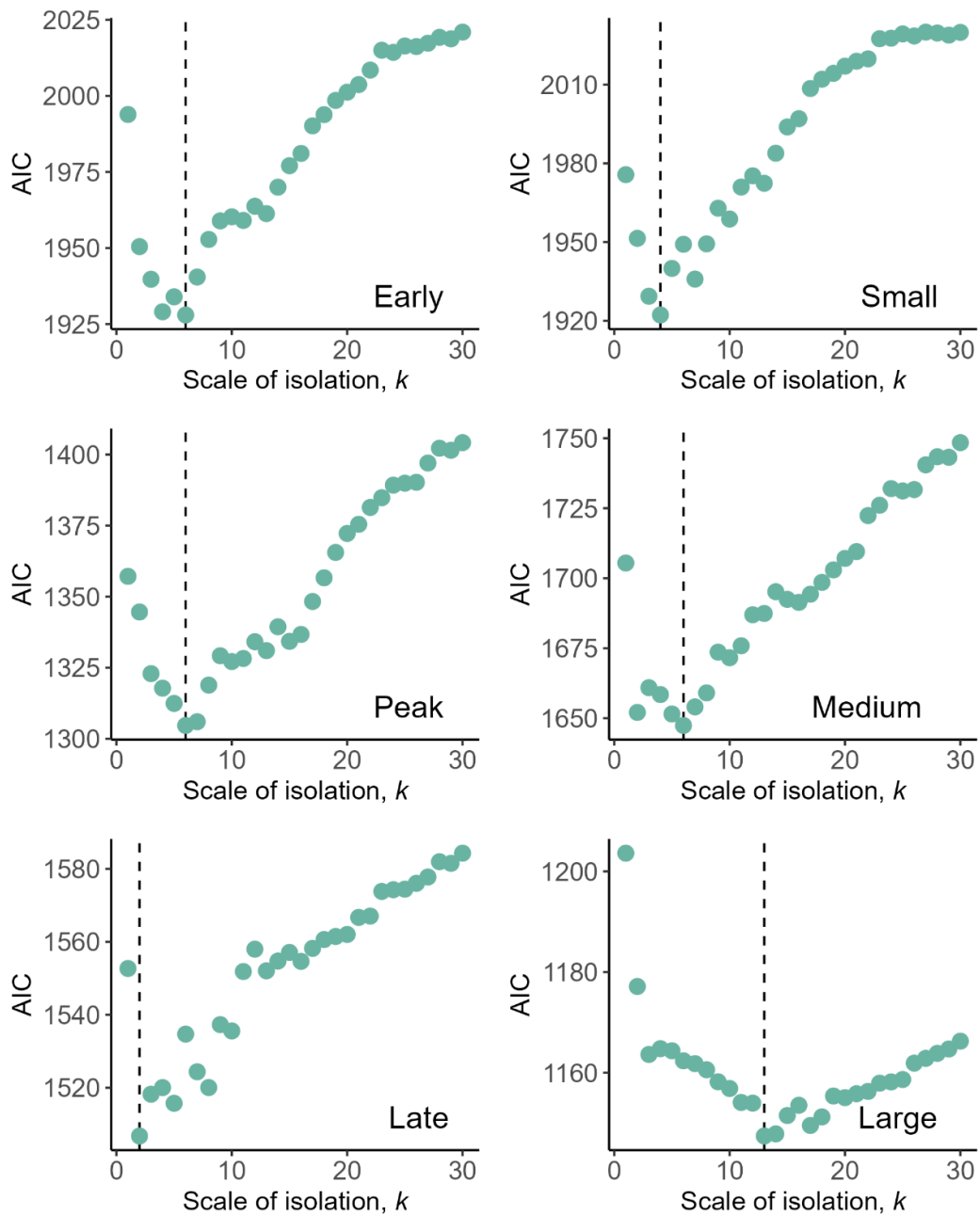


Figure S8. Variation in model performance, as measured by AIC, considering models that measured isolation to individuals'  $k$ th nearest neighbor as a predictor of style persistence when considering different subsets of the data. From top to bottom, the first column represents thirds of the dataset for early, peak, late and the relationship of  $k$  and model performance for that portion of the data. The second column, top to bottom, represents small, medium, and large populations relationships between the value of  $k$  and model performance.



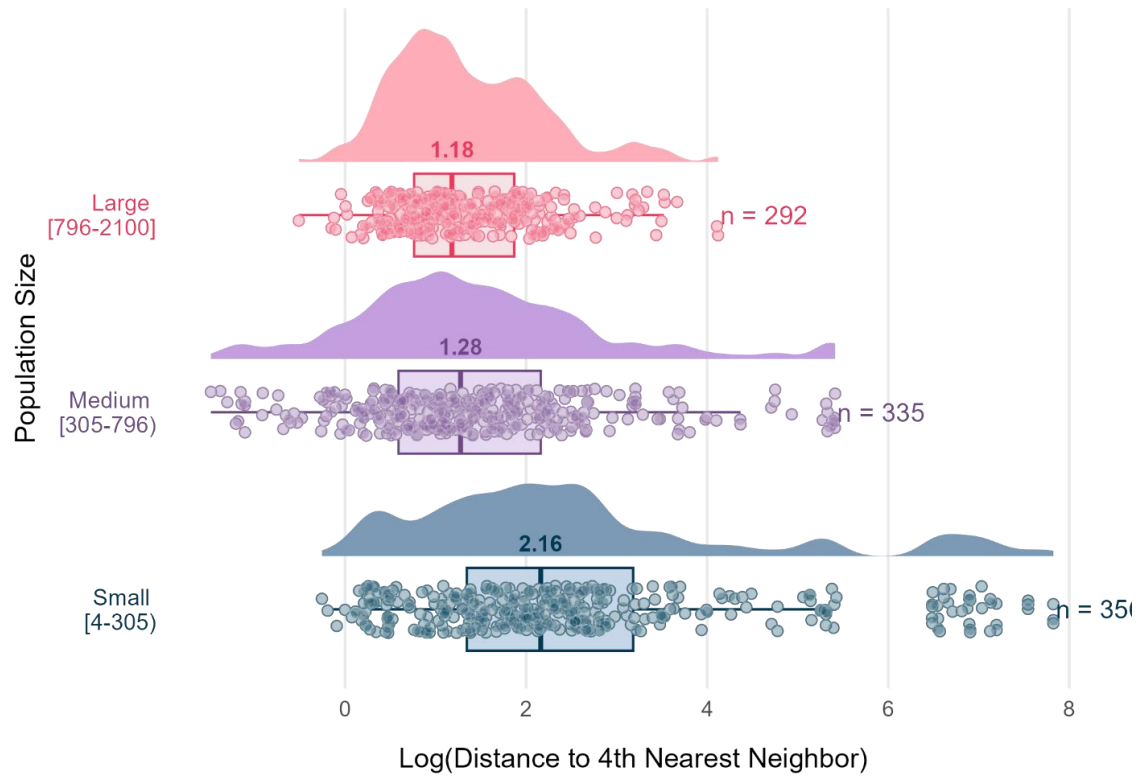
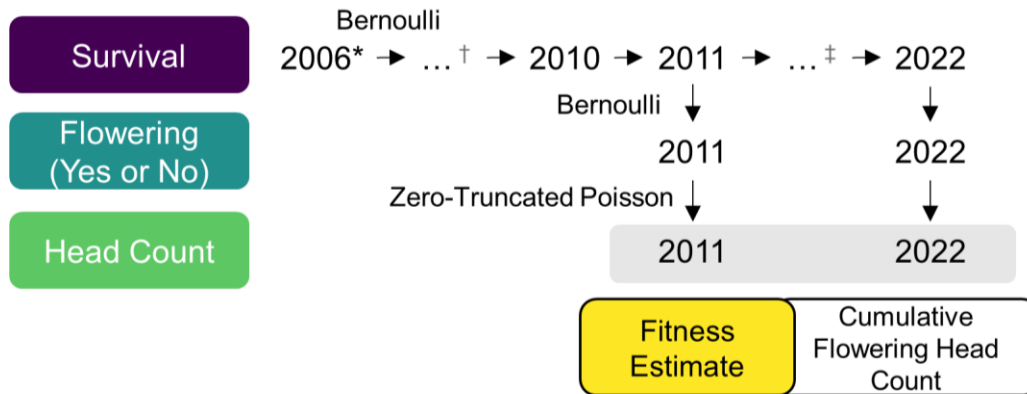


Figure S9. Distribution Log (Distance to 4th Nearest Neighbor) by population size category, as used in the scale dependence analyses.

Appendix C: Chapter 2 Supplemental Tables and Figures



\* Nodes omitted due to lack of variation: Flowering (Y/N) 2006-2010, Head Count 2006-2009 (all zero), Flowering (Y/N) 2012

† Same pattern for each intervening year, except for the omitted nodes, listed above.

‡ Nodes omitted due to experimental manipulation: All 2018 Nodes

Figure S1. Graphical model for the aster analysis of fitness. The statistical distribution used for transitions between nodes is indicated adjacent to arrows denoting the transition. All transitions between ‘Survival’ nodes are Bernoulli, transitions from a ‘Survival’ node to a ‘Flowering (Yes or No)’ node are Bernoulli, and transitions from a ‘Flowering (Yes or No)’ node are zero-truncated Poisson. Note that transition from one stage to the next are contingent upon the previous stage (e.g., a non-zero head count is contingent upon an individual flowering, and flowering is contingent upon survival through that year).

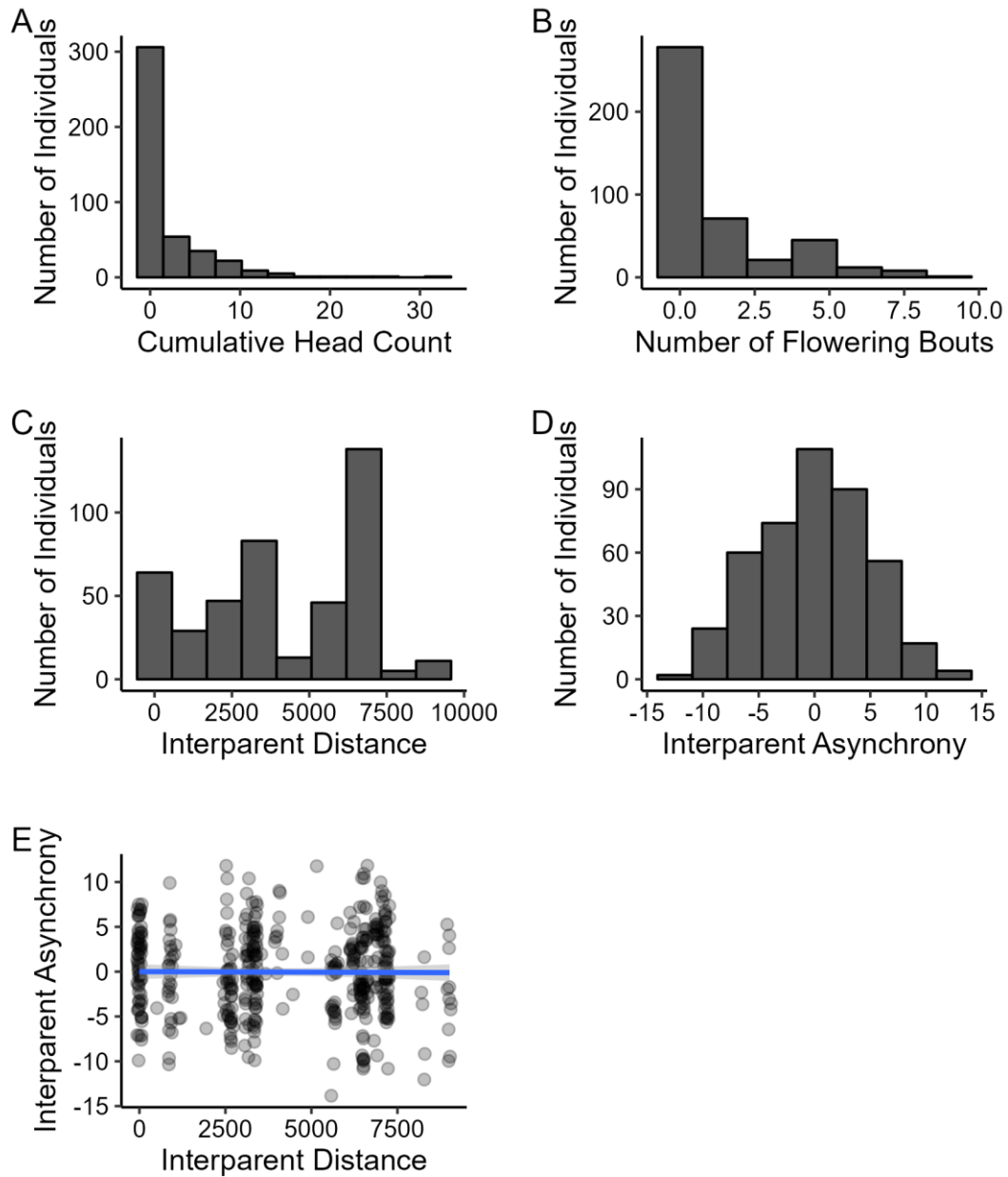


Figure S2. Distribution of the (A) the number of flowering bouts, (B) the cumulative number of flowering heads produced by individuals during the study period (including those that died before flowering), (C) interparent distance (m), the geographic distance between source populations of parental individuals in meters, and (D) interparent asynchrony, the difference in parents start date of flowering in 2005. (E) The joint distribution of interparent distance and interparent asynchrony, which are not correlated. The line shows a linear model of interparent asynchrony  $\sim$  interparent distance.

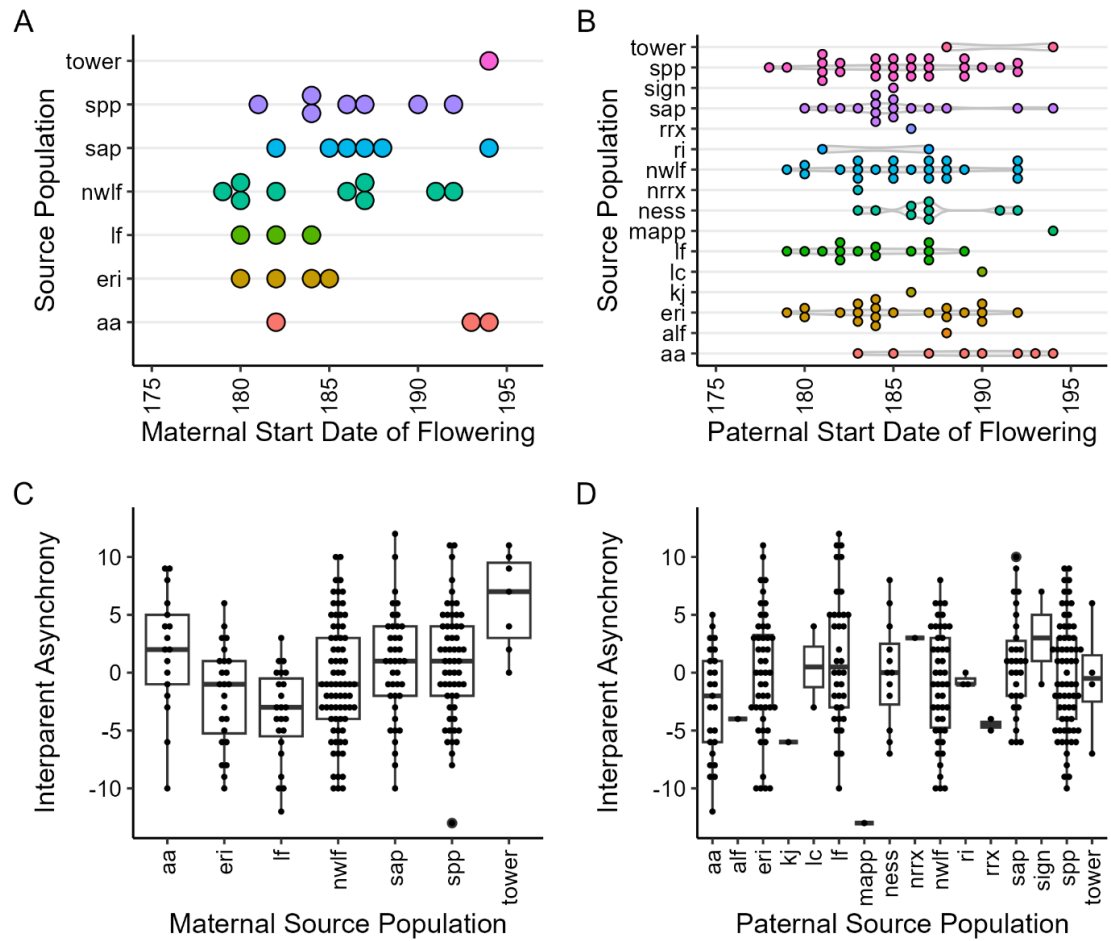


Figure S3. Variation in start date (A, B) and interparental asynchrony (C, D) among source populations of the maternal (A, C) and paternal (B, D) plants.

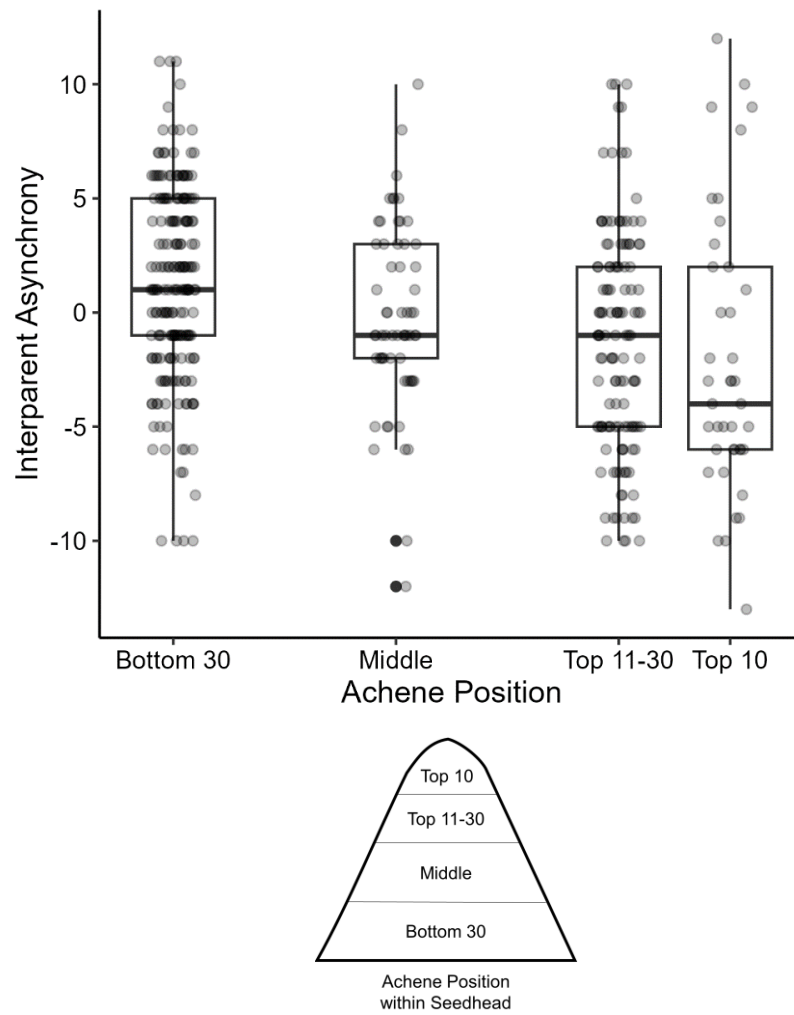


Figure S4. Achene position (an ordinal measure indicating whether the offspring seed originated from the 10 topmost achenes, the 11<sup>th</sup>-30<sup>th</sup> topmost achenes, the bottom 30 achenes, or selected randomly from the remaining ‘middle’ achenes) and interparent asynchrony are weakly correlated.

Appendix D: Analysis including all genotyped plants based on fitness in years 2014-2022

An additional 279 plants were genotyped after flowering between 2014 and 2018; we performed an analysis of fitness based on flowering between 2014 and 2022 included these individuals, as well as any of the AJB plants that survived through 2014 (291 individuals), for a total of 570 individuals. We performed the same analyses as described in the main text for this subset of the data

Table S1. Model selection results for models of interparent asynchrony and interparent distance separately. Each row represents a candidate model: its predictors (in addition to the null model, as described below), AIC, difference between AIC and the lowest AIC of all candidate models ( $\Delta$ AIC), the Akaike weight ('Weight'), which is proportional to the probability that the model is the best of the set of candidate models, and proportional Akaike model weights (Prop. Weight). All models included predictors for location within the plot (row and position) on the different types of fitness components (or 'layers': ld, fl, hdCt) and had the structure:  $\text{resp} \sim \text{varb} + \text{layer} : (\text{row} + \text{position}) + \text{fit} : (\dots)$ , where ' $\dots$ ' is indicated by the covariates in the 'Predictors' column. The bolded row indicates the best-performing model.

Hypothesis	Predictors	No. Par	AIC	$\Delta$ AIC	Weight	Prop. Weight
<i>Asynchrony</i>						
Null	None	19	8461.23	0	1	0.51
Directional Effects (H4)	+ Asynchrony	20	8462.89	1.65	0.44	0.22
Heterosis (H1) or Outbreeding Depression (H2)	+  Asynchrony	20	8463.19	1.95	0.38	0.19
Intermediate Optimum (H3)	+  Asynchrony  + Asynchrony <sup>2</sup>	21	8465.01	3.78	0.15	0.08
<i>Distance</i>						
Null	None	19	8461.23	41.58	0	0
<b>Heterosis (H1) or Outbreeding Depression (H2)</b>	+ Distance	20	8419.65	0	1	1
Intermediate Optimum (H3)	+ Distance <sup>2</sup>	20	8463.08	43.43	0	0

Table 2. Results from likelihood ratio tests comparing nested models that included the final terms selected for interparent asynchrony and interparent distance, as indicated by AIC analysis (Table 1), and their interaction. Comparisons test the null hypothesis that a reduced model performs as well as a more complex one by comparing the difference in deviance (a goodness-of-fit measure) between nested models ( $\Delta$  Deviance) to a  $\chi^2$  distribution with degrees of freedom equal to the difference in degrees of freedom between the two models ('Df'). ' $P(\chi^2_{Df} > \Delta \text{ Deviance})$ ' indicates the probability of a value from  $\chi^2_{Df}$  greater than  $\Delta$  Deviance.

Pairwise Model Comparison	Df	$\Delta$ Deviance	$P(\chi^2_{Df} > \Delta \text{ Deviance})$
Interactive vs. Additive	1	3.08	0.07
Additive vs. Asynchrony Only	1	0.06	0.81
Additive vs. Distance Only	1	43.29	< 0.001

Table S3. Summary of best model ('Interactive') of offspring fitness, which included an interaction between interparent distance and asynchrony. The graphical model also includes terms for each life-history node (Supplemental Figure 1); for simplicity, we omit those terms here. The model terms of primary interest are bolded.

	Estimate	Std. Error	z value	Pr(> z )	Signif.
Row: Survival	0.008	0.001	5.50	< 0.001	***
Position: Survival	-0.015	0.002	-6.22	< 0.001	***
Row: Head Count	-0.011	0.001	-12.12	< 0.001	***
Position: Head Count	0.004	0.001	2.98	0.003	**
<b>Distance</b>	0.112	0.017	6.65	< 0.001	***
<b>Asynchrony</b>	0.001	0.003	0.22	0.82	
<b>Distance : Asynchrony</b>	0.005	0.003	1.76	0.08	*

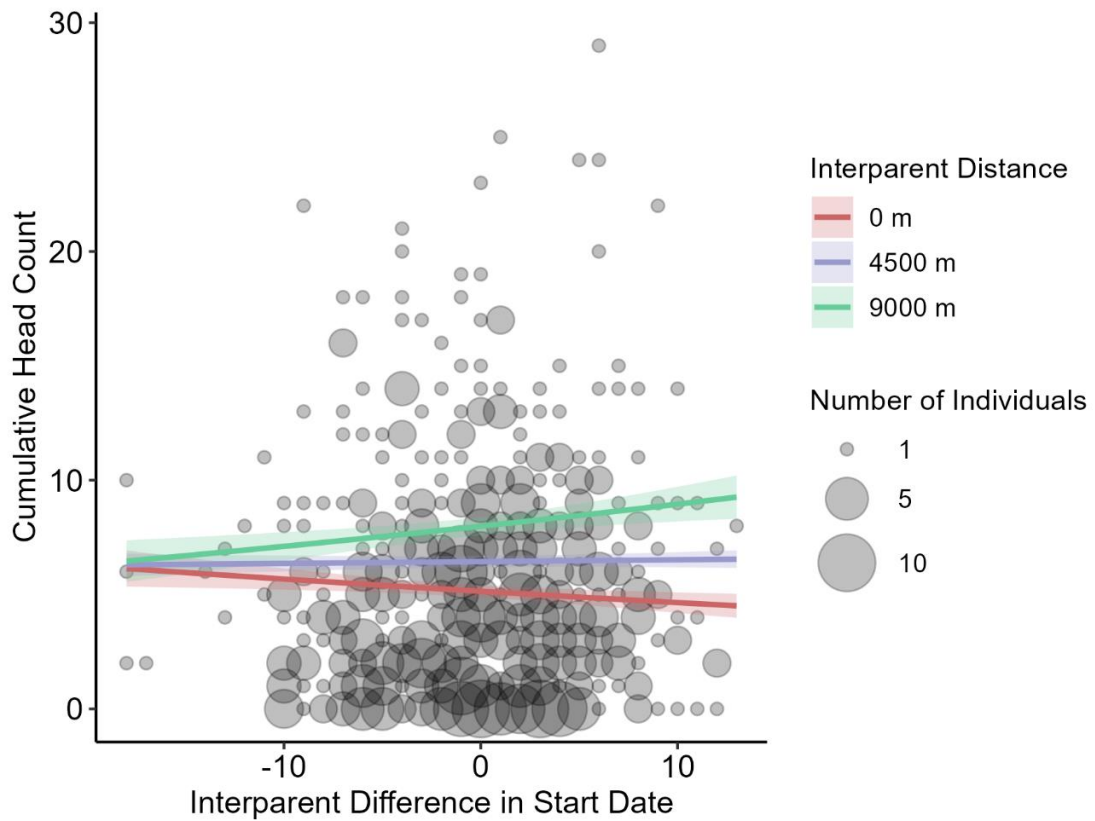


Figure S1. Predicted cumulative head count as a function of the interaction between interparent distance and interparent asynchrony in 2014-2022. Predictions are for hypothetical individuals located at Row 5 and Position 5 and with three levels of interparent distances: within the same population (0 m), intermediate (4500 m), and far (9000 m). Points indicate the cumulative head counts of offspring with corresponding interparent asynchrony observed in our study and are scaled with the number of individuals at the respective combination of values.



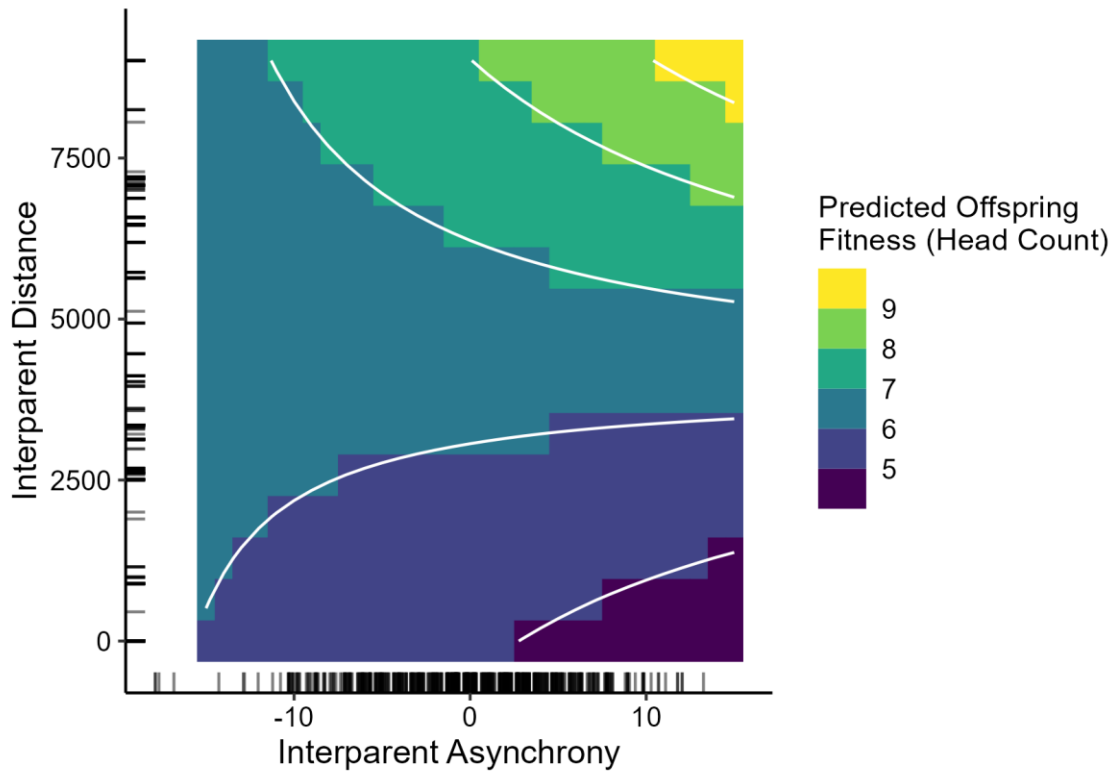


Figure S2. Predicted fitness contours across the range of observed interparent distances and asynchronies for 2014-2017. Specifically, offspring fitness is an individuals predicted cumulative head count.

Appendix E: Chapter 3 Supplemental Tables and Figures.

Table S1. Results of AIC analysis for competing models using Akaike weights. No. Par indicates the number of estimated parameters in the model; AIC is the Akaike Information Criterion;  $\Delta$ AIC is the difference between AIC and the minimum AIC in the set of competing models;  $w(\text{AIC})$  is the Akaike weight for the model. All models also contained all graph nodes and the effect of search radius on initial emergence. That is, we generated the set of models by iteratively dropping all combinations head count, cohort, site, and mating potential from the “Emergence” model.

Covariates Included in Model	No. Par <sub><i>i</i></sub>	AIC <sub><i>i</i></sub>	$\Delta$ <sub><i>i</i></sub> AIC	$w_i(\text{AIC})$
HdCt + Cohort + Site + Mating Potential	52	5503.9	0	1
Cohort + Site + Mating Potential	50	5593.3	89.4	0
HdCt + Site + Mating Potential	40	5638.9	135.0	0
HdCt + Cohort + Mating Potential	26	5687.1	183.1	0
HdCt + Cohort + Site	51	5562.4	58.4	0
Site + Mating Potential	38	5741.8	237.9	0
HdCt + Mating Potential	14	5831.9	328.0	0
HdCt + Cohort	25	5807.0	303.1	0
HdCt + Site	39	5713.6	209.7	0
Cohort + Site	49	5674.7	143.8	0
HdCt	13	5970.9	466.97	0
Cohort	23	5952.9	449.0	0
Site	37	5821.7	317.8	0
Mating Potential	12	6026.6	522.7	0

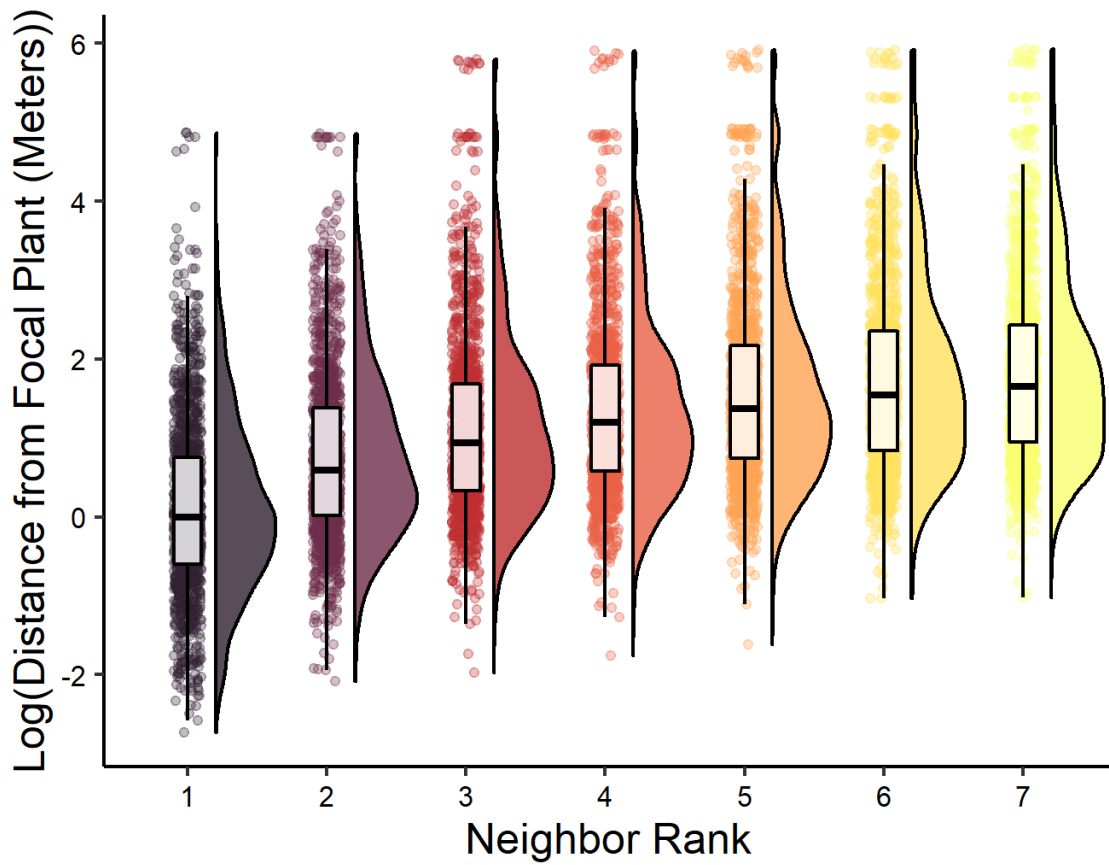


Figure S1.  $\text{Log}_{10}$  of distances (m) between a maternal plant and its 1<sup>st</sup> through 7<sup>th</sup> nearest neighbors across all sites and years in the study.

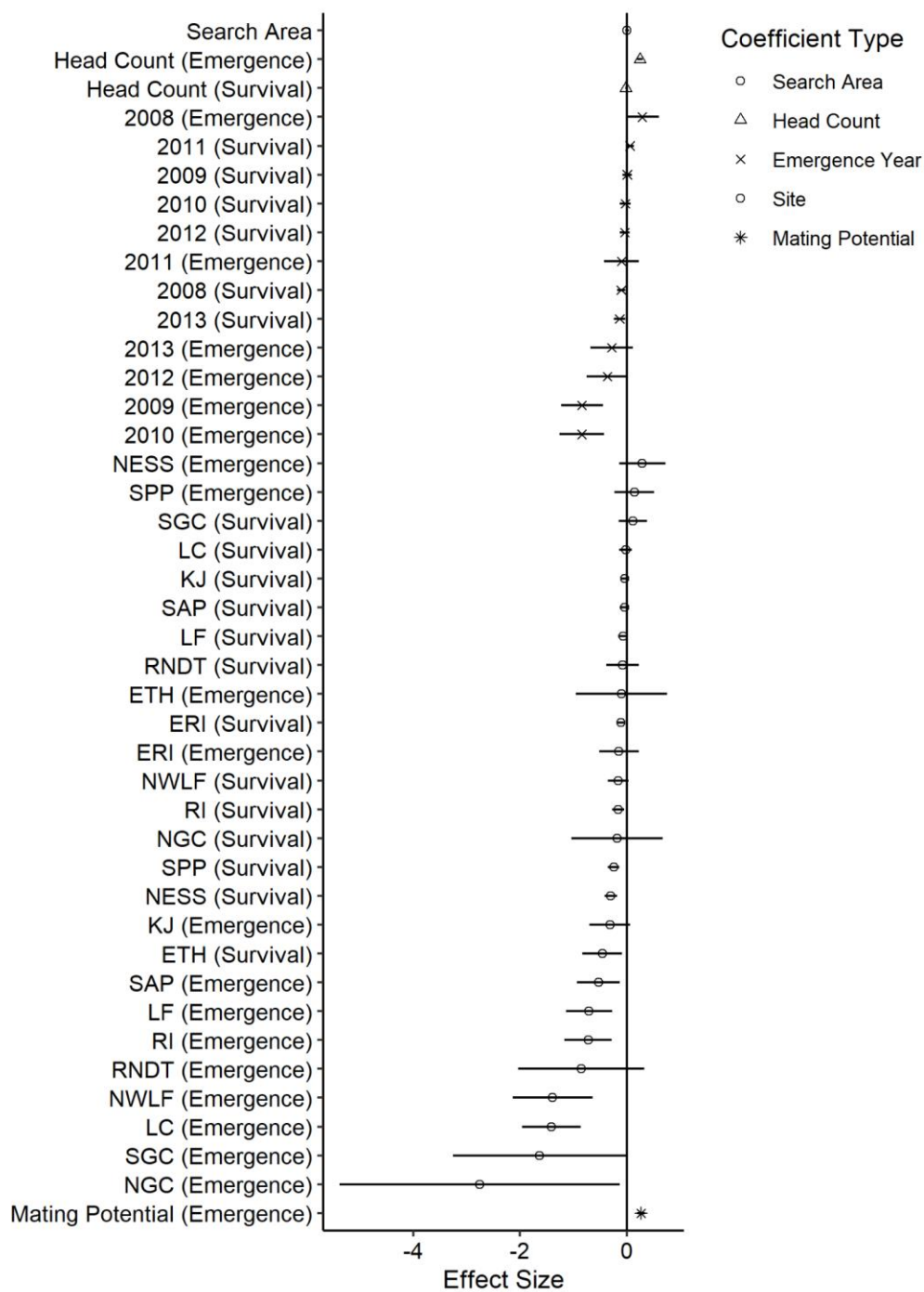


Figure S2. Effect sizes of model coefficients from the best performing aster model, which included effects of mating potential on maternal plant’s number of seedlings emerging, but not on the number of offspring persisting at year eight. Points indicate model estimates while line ranges denote +/- one standard error. In parentheses, “Emergence”

and “Survival” indicate which layer of the graph the covariates affected: the emergence layer consisted of the “Seedling Emergence” node, while the “Survival” layer consisted of all nodes following emergence. The effect sizes for categorical variables (site and cohort) are presented in reference to site EELR and the 2007 cohort. Aster models also estimate coefficients for each node of the graph; for simplicity, we have omitted these estimates here.

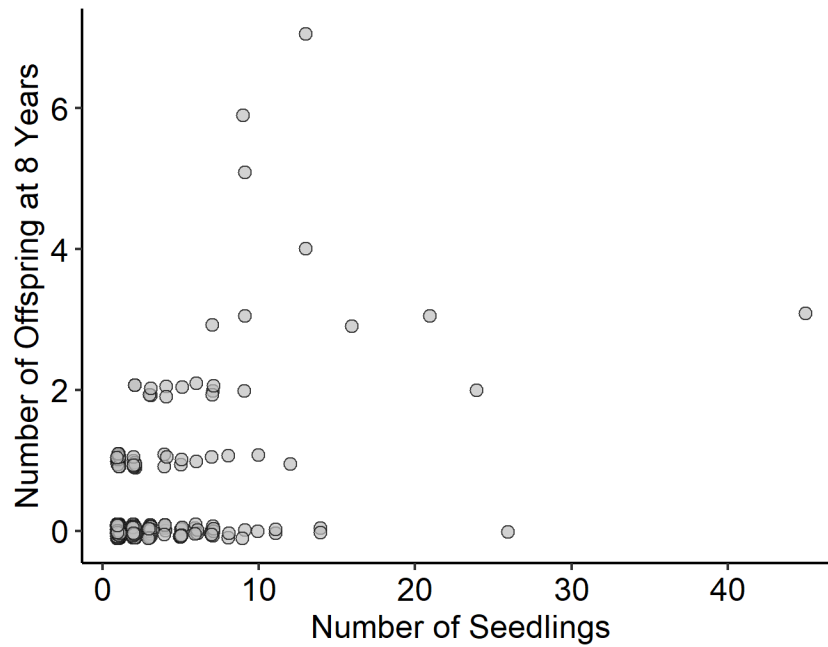


Figure S3. Correlation between a maternal plant’s number of seedlings and its number of offspring at eight years. Points are slightly transparent and jittered to reduce overplotting.

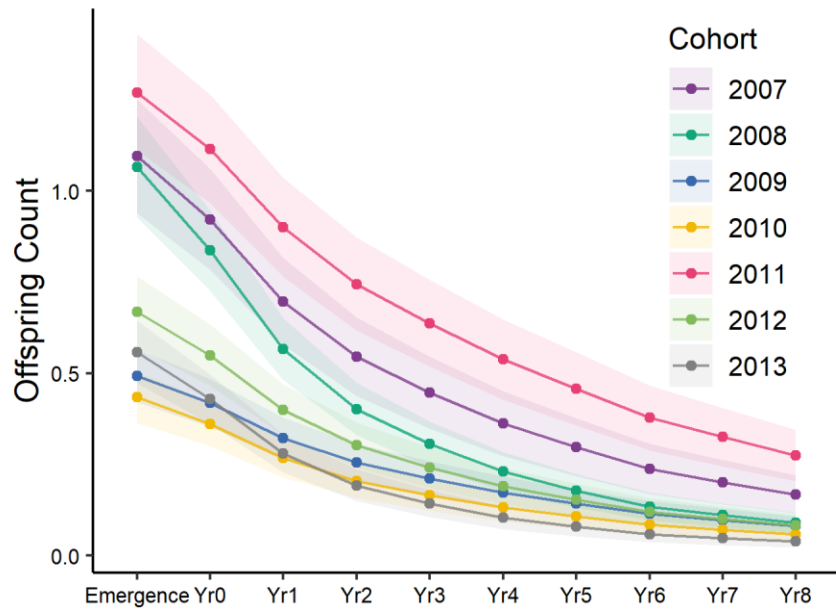


Figure S4. Predicted offspring count at emergence and after eight years by year of emergence. Predictions here are for a one-headed hypothetical individual at the site ‘sap’, a small remnant with intermediate seedling emergence and survival (Figure 3b). Shaded bands indicate one standard error on each side of the mean.

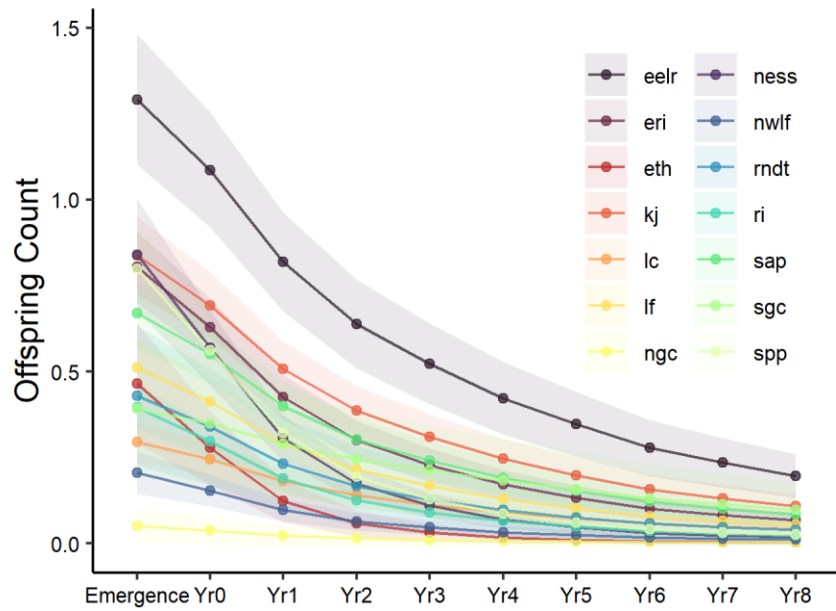


Figure S5. Predicted offspring count at emergence and after eight years by site. Predictions here are for a one-headed hypothetical individual with an offspring cohort emerging in 2012, a year that had intermediate emergence (Figure 3a). Shaded bands indicate one standard error on each side of the mean.

## Appendix F: Mating Potential Calculations

As described in the main text of Chapter 3, we calculated mating potential (MP) as an inverse-weighted sum of the distances ( $d$ ) between a focal plant  $i$  and its 1- $k$ th nearest conspecific neighbors,  $j$  (Wagenius et al. 2007):

$$MP_i = \sum_1^k e^{d_{ij}^{-\gamma}}$$

Specifically, we calculated mating potential with  $k = 7$  and  $\gamma = 1/13.3$ . The value of the exponential decay parameter  $\gamma$  determines how quickly a neighbor's contribution to a focal plant's mating potential decays with distance. The relationship between distance and contribution to mating potential is  $e^{d^{-\gamma}}$  and is displayed for  $\gamma = 1/13.3$  in Figure 1. Given the form of this function, the difference in contribution to mating potential of highly proximate neighbors and intermediately proximate neighbors is much greater than the difference between intermediately proximate neighbors and distant neighbors. We did not have phenology data to include a within-season temporal component to our mating potential metric, as we have done in previous studies (Wagenius et al. 2020). However, our previous analyses have found that mating potential depends more on annual flowering rates than within-season timing (Waananen et al. 2018).

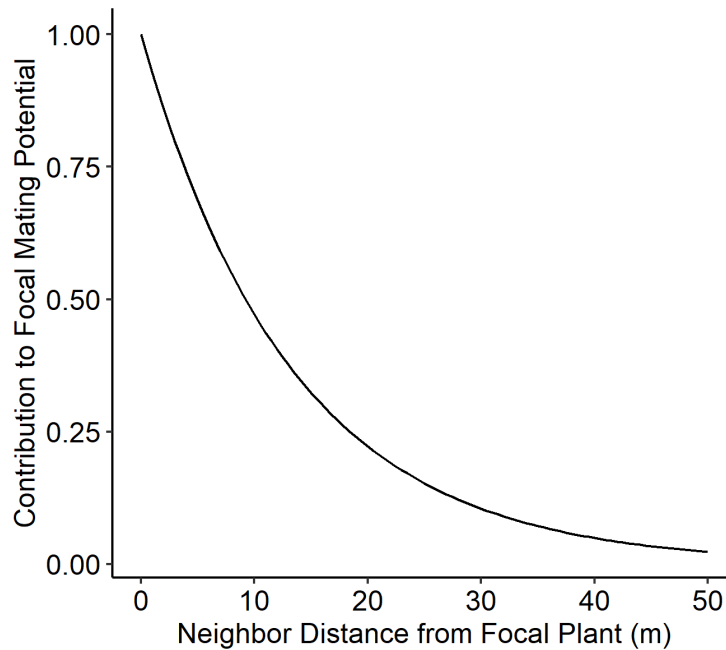


Figure S1. Relationship between a neighbor's distance to a focal plant and its contribution to the focal plant's mating potential for  $\gamma = 1/13.3$ .



These values are summed across  $k$  neighbors. To illustrate, calculations for several examples with  $k = 7$  and  $\gamma = 1/13$  for focal plants in our dataset are below.

### Example 1

Focal plant with 1-7th neighbors 4.75, 6.64, 13.97, 19.97, 31.68, 44.65, and 60.61 m away.

$$MP = e^{4.75 \cdot \frac{1}{13.3}} + e^{6.64 \cdot \frac{1}{13.3}} + e^{13.97 \cdot \frac{1}{13.3}} + e^{19.97 \cdot \frac{1}{13.3}} + e^{31.68 \cdot \frac{1}{13.3}} + e^{44.65 \cdot \frac{1}{13.3}} + e^{60.61 \cdot \frac{1}{13.3}} = 0.70 + 0.61 + 0.35 + 0.22 + 0.09 + 0.03 + 0.01 = 2.01$$

R Code:

```
# Distances from 1-7th neighbors to focal plant
distances <- c(4.75, 6.64, 13.97, 19.97, 31.68, 44.65, 60.61)

# Contribution of each neighbor to focal plant mating potential
sapply(distances, FUN = function(x) exp(x*(-1/13.3)))

# Sum individual neighbor contributions for focal plant mating potential
sum(sapply(distances, FUN = function(x) exp(x*(-1/13.3))))
```

### Example 2

Focal plant with 1-7th neighbors 7.55, 10.31, 11.05, 11.66, 11.94, 12.95, and 14.94 m away.

$$MP = e^{7.55 \cdot \frac{1}{13.3}} + e^{10.31 \cdot \frac{1}{13.3}} + e^{11.05 \cdot \frac{1}{13.3}} + e^{11.66 \cdot \frac{1}{13.3}} + e^{11.94 \cdot \frac{1}{13.3}} + e^{12.95 \cdot \frac{1}{13.3}} + e^{14.94 \cdot \frac{1}{13.3}} = 0.57 + 0.46 + 0.44 + 0.42 + 0.41 + 0.38 + 0.33 = 2.99$$

R Code:

```
# Distances from 1-7th neighbors to focal plant
distances <- c(7.55, 10.31, 11.05, 11.66, 11.94, 12.95, 14.94)

# Contribution of each neighbor to focal plant mating potential
sapply(distances, FUN = function(x) exp(x*(-1/13.3)))

# Sum individual neighbor contributions for focal plant mating potential
sum(sapply(distances, FUN = function(x) exp(x*(-1/13.3))))
```

### Example 3

Focal plant with 1-7th neighbors 1.39, 2.18, 4.41, 4.91, 5.16, 6.33, and 7.71 m away.

$$MP = e^{1.39 \cdot \frac{1}{13.3}} + e^{2.18 \cdot \frac{1}{13.3}} + e^{4.41 \cdot \frac{1}{13.3}} + e^{4.91 \cdot \frac{1}{13.3}} + e^{5.16 \cdot \frac{1}{13.3}} + e^{6.33 \cdot \frac{1}{13.3}} + e^{7.71 \cdot \frac{1}{13.3}} = 0.90 + 0.85 + 0.72 + 0.69 + 0.68 + 0.62 + 0.56 = 5.02$$

R Code:

```
# Distances from 1-7th neighbors to focal plant
distances <- c(1.39, 2.18, 4.41, 4.91, 5.16, 6.33, 7.71)

# Contribution of each neighbor to focal plant mating potential
sapply(distances, FUN = function(x) exp(x*(-1/13.3)))

# Sum individual neighbor contributions for focal plant mating potential
sum(sapply(distances, FUN = function(x) exp(x*(-1/13.3))))
```

### BIBLIOGRAPHY

Wagenius, S., E. Lonsdorf, and C. Neuhauser. 2007. Patch aging and the S-Allee effect: breeding system effects on the demographic response of plants to habitat fragmentation. *Am. Nat.* 169:383–397.

## Appendix G: Demographic Stochasticity Simulations.

We developed a simulation model to explore when differences between maternal plants' fitness due to seedling emergence would persist if there is no relationship between mating potential and survival. This corresponds to the hypothesis that mating potential influences the quantity of offspring that emerge, as is supported by evidence about how mating potential influences seed set, but has no relationship with mating quality, which would be the case when there is not a strong association between mate abundance and offspring fitness, e.g., a population without strong spatial genetic structure. For each simulation, we represented fitness differences as one plant's advantage over another in its number of offspring at emergence. We simulated emergence advantages ( $E$ ) at each integer between 1 and 50 seedlings and juvenile survival rates ( $S$ ) between 0 and 1 in twenty evenly spaced increments. For each seedling comprising the advantage in 1 to  $E$ , we drew at random whether or not it survived where chance of survival was equal to  $S$ . Then, we tallied how many offspring were still alive, i.e., how much of the advantage observed at emergence persisted. We repeated the simulation for each combination of  $E$  and  $S$  100 times and calculated the average number of surviving offspring across all replicates of each combination. To gain insight specific to the survival rate and range of number of seedlings per maternal plant we observed in our system, we repeated the simulation with the survival rate observed from emergence to age 8 in our data and  $E$  at each integer between 1 and 10.

### RESULTS

Our simulations illustrated that when survival rates were lower, maternal plants needed a greater advantage in number of offspring at emergence (i.e., a greater emergence advantage) to maintain a fitness advantage after eight years (Figure 4A). When the survival rate was high, emergence advantages were persistent and even a small advantage in offspring count at emergence translated to more offspring at a later life stage. In contrast, at low survival rates, even an emergence advantage of 50 seedlings (the maternal plant with the largest number of seedlings that we observed had 45) did not reliably secure an advantage following survival. When we considered this model with a survival rate of 0.11 we found similar patterns; across the range of emergence advantages we most commonly observed, between 0 and 6 offspring difference between high- and low-emergence maternal plants, the final advantage of an high-emergence maternal plant was still typically 0 (Figure 4B). However, our simulation also illustrated exceptions to this expectation; even at low emergence advantages (e.g.,  $E = 1$ ), our simulation showed instances where the advantage was maintained.